MUTATION OF A KATANIN-LIKE MICROTUBULE-SEVERING PROTEIN AFFECTS PLANT CELL ELONGATION

by

DAVID HUGHES BURK

(Under the Direction of Zheng-Hua Ye)

ABSTRACT

Plant cells are able to elongate anisotropically due to a constraining network of cellulose microfibrils in their cell walls and cortical microtubules underneath the plasma membrane. As it is believed that the cortical microtubules (CMTs) somehow direct the organized deposition of cellulose microfibrils (CMFs) identification of proteins involved in controlling microtubule (MT) dynamics or organization will help us better understand the cellular processes of anisotropic growth.

Mutation of the Arabidopsis katanin-like MT-severing protein, *FRA2*, hereafter called *AtKTN1*, an ortholog of the animal p60 subunit of katanin, caused a dwarf phenotype with reductions in the anisotropic growth of cells in all organs. Transmission electron microscopic examination of cells in the interfascicular region of wild-type and AtKTN1 mutant stems showed a reduction in the thickness of secondary wall in mutant cells and revealed differences in secondary wall structure. Defects in AtKTN1 function caused a defect in MT dynamics in cells as determined by confocal microscopy and appeared to involve a delay in the disassembly of the perinuclear MT array after cytokinesis. This defect results in a disorganized CMT array in cells of elongating roots, stems, and petioles. Visualization of CMFs in the primary and secondary cell walls of these cell types using field emission scanning electron microscopy showed a correlation between disruption of the CMTs and CMFs. CMFs in wild-type cells were typically arranged transverse to the axis of elongation while those of AtKTN1 mutants were disorganized and appear to form bands of microfibrils that changed their orientation over short distances. Overexpression of AtKTN1 cDNA in transgenic Arabidopsis did not result in the fragmentation of CMTs but affected CMT organization, the deposition pattern of CMFs, and anisotropic growth.

Analysis of the AtKTN1 mutant revealed the importance of the katanin-like MT-severing protein in the proper formation of the CMT array in elongating Arabidopsis cells. Lack of katanin function is implicated in the delay of the disassembly of the

perinuclear MT array which leads to aberrantly organized CMTs and a reduction of anisotropic growth.

INDEX WORDS: Cortical microtubules, Cellulose microfibrils, katanin, AtKTN1, *fragile fiber 2,* Cell elongation

MUTATION OF AN ARABIDOPSIS KATANIN-LIKE MICROTUBULE SEVERING PROTEIN AFFECTS PLANT CELL ELONGATION

by

DAVID HUGHES BURK

B.S., The University of Alabama, 1994

M.S., The University of Alabama, 1997

A Dissertation Submitted to the Graduate Faculty of The University of Georgia in Partial Fulfillment of the Requirements for the Degree

DOCTOR OF BOTANY

ATHENS, GEORGIA

2003

MUTATION OF AN ARABIDOPSIS KATANIN-LIKE MICROTUBULE SEVERING PROTEIN AFFECTS PLANT CELL ELONGATION

by

DAVID HUGHES BURK

Major Professor: Zheng-Hua Ye

Committee: Kelly Dawe
Mark Farmer
Russell Malmberg
Lee Pratt
Mike Scanlon

Electronic Version Approved:

Maureen Grasso
Dean of the Graduate School
The University of Georgia
May 2003

ACKNOWLEDGEMENTS

This moment has been a long time in the making and I'd like to thank those that helped me reach the end of my journey. First, I'd like to thank my committee members, Kelly Dawe, Mark Farmer, Russell Mallmberg, Lee Pratt, and Mike Scanlon for their input, assistance, and reminders of what's feasible and what isn't. Each of them was always willing to answer any questions I had and many taught me a great deal through classes or seminars. I owe much and am indebted to my major professor, Zheng-Hua Ye. No one could ask for a better mentor or friend. Zheng-Hua was always willing to help out and always did so with a smile. He is perhaps one of the nicest people I know and I want to thank him for his (limitless) patience and assistance. I would like to thank Ruiqin Zhong for all her help, her conversations about anything, and her friendship throughout my stay in Zheng-Hua's lab. Many thanks go to Beth Richardson, Glenn Freshour, John Shields, and Mark Farmer for all of their assistance in learning how to perform a multitude of microscopic examinations and how to use the fancy equipment that I have come to love. Thanks to you I was able to complete the bulk of my work as it deals primarily with microscopy. I want to thank some of my fellow students, some of which are no longer here, but all made graduate school bearable and even fun. Becky Mroczek and Carolyn Lawrence in Kelly's lab have been here for as long as I have and both are good friends and have helped me out immeasurably. Misa Ward and Sara Crockett have been gone for several years but they also made this experience worthwhile and I wish them all the best of luck in whatever they choose to do. Finally I want to thank my

family, especially my parents, for their never-ending support and love throughout my scholastic endeavors. They never questioned my goals and were always willing to help me when I needed it and for that I love them all the more.

TABLE OF CONTENTS

CHAPTER 1

INTRODUCTION AND LITERATURE REVIEW

The proper formation of plant organs from hypocotyls to leaves to roots is highly dependent upon the ability of cells to elongate rapidly and in a particular orientation. This anisotropic growth, or directed growth, is known to be regulated by many internal and external factors such as hormone levels within the plant, turgor pressure, cell wall structure and proteins associated with the cell wall, light, and stress (reviewed in Shibaoka, 1994; McQueen-Mason, 1995; Kende and Zeevaart, 1997; Van Volkenburgh, 1999). Directed growth is contrasted with isotropic growth where cells expand more or less equally in all directions and tend to produce swollen spherical cells (Figure 1.1).

Development of leaves requires the proper expansion of cells within the lamina and epidermis to produce tissues involved in photosynthesis (palisade or columnar mesophyll), gas exchange (spongy mesophyll and guard cells), water/nutrient transport (xylem and phloem) or protection (trichomes) (see Carland and McHale, 1996; Oppenheimer, 1998; Pyke and Lopez-Juez, 1999; Scanlon, 2000). Root growth relies on the proper elongation of cells in the so called “elongation zone” and the proper elongation of root hair cells for water and mineral uptake. The directional elongation of cells may occur in many cells of a particular organ (epidermis and cortex of roots) or may be primarily localized to particular cell types as in vessel elements, phloem, and fiber cells within stems.

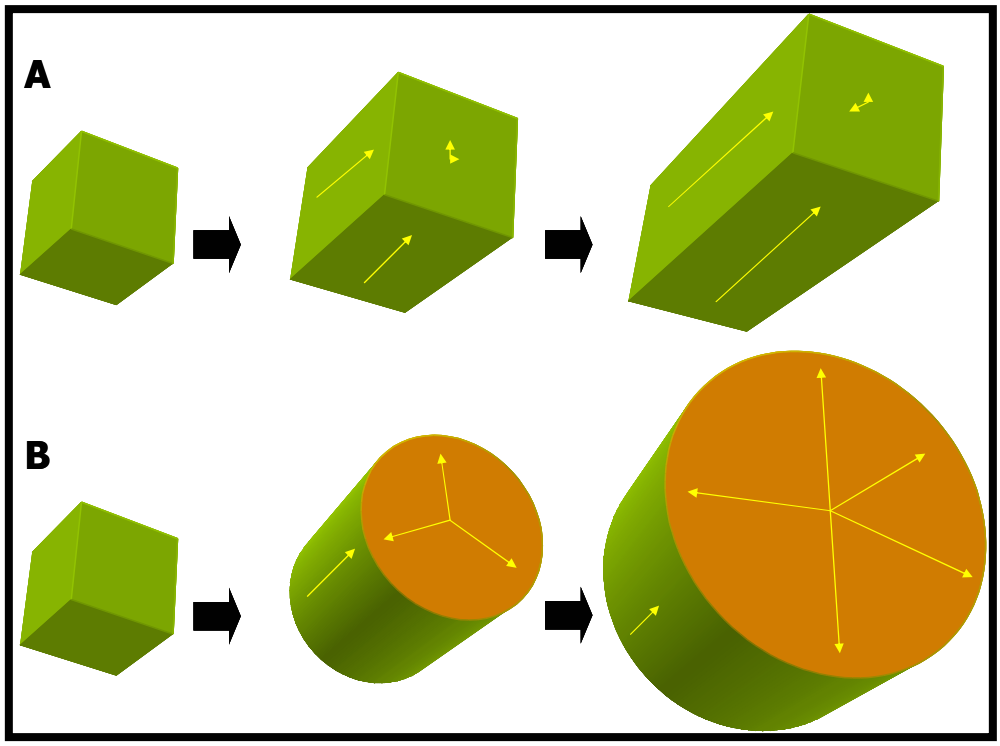

Figure 1.1 Comparison of anisotropic (a) and isotropic or radial growth (b).

Anisotropic growth of many cell types appears to rely heavily on the organization of cellulose microfibrils in the primary cell wall as well as the cortical microtubules (MT) that are believed to be associated with plant plasma membranes. Disruption of cellulose synthesis or disruption/stabilization MT arrangement by addition of certain compounds can inhibit directional elongation of certain cell types and result in isotropic or abnormal growth (Shibaoka, 1994; Fisher and Cyr, 1998; Mathur and Chua, 2000; Szymanski, 2001; Mathur and Hülskamp, 2002). Mutants of Arabidopsis that have defects in certain hormone biosynthesis genes have shown the importance of compounds such as auxins, brassinosteroids, and gibberellic acid in proper cell elongation and possible roles of these molecules in the regulation of MT and cellulose microfibril arrangement (Shibaoka, 1994; Li and Chory, 1999; Schumacher and Chory, 2000; Catterou et al., 2001b; Hong et al., 2002).

MUTATIONS IN GENES ENCODING PUTATIVE CELLULOSE SYNTHASE SUBUNITS CAN AFFECT CELL ELONGATION AND THE ORGANIZATION OF CELLULOSE MICROFIBRILS IN THE CELL WALL

It is generally accepted that the organization of the cellulose microfibrils (CMFs) in plant cell walls constrains cell growth perpendicular to the orientation of microfibrils. The CMFs act much like the hoops around a barrel or the wire of a slinky and only allow diffuse growth in one (or more) directions using internal turgor pressure as a driving force for expansion. In rapidly elongating cells in internodes or cells of the cortex and epidermis of Arabidopsis roots the CMFs are arranged transversally to the axis of maximum elongation. The disruption of the arrangement of CMFs either by mutation of genes involved in cellulose synthesis or by the addition of specific inhibitors to cellulose synthesis disrupt this organization and lead to cellular expansion in a more isotropic manner.

Our understanding of how cellulose microfibrils, composed of β-1,4-D-glucan, are synthesized has advanced considerably (for review see Delmer, 1999) and the isolation of mutants with defects in cellulose synthase-like genes has aided our understanding of the importance of the role CMF play in controlling plant and cell morphology. Presently, over 12 genes have been discovered in plants that either play a putative role in cellulose synthesis or that affect the organization of primary or secondary cell wall structure (Table 1.1). Of primary importance appear to be a group of putative glycosyltransferases and cellulose synthase-like genes (*CesA* and *Csl*, respectively) that are relatively abundant in the Arabidopsis genome as well as in other plant species examined and comprise the cellulose synthase superfamily (Richmond, 2000; Dhugga, 2001; Burn et al., 2002; Williamson, 2002). Analysis of the Arabidopsis genome reveals that there are 10 *CesA* and approximately 30 *Csl* genes present in this organism. To date, seven of the AtCesA genes have been examined using mutants in Arabidopsis or by using anti-sense technology to determine putative phenotypes of reduced expression plants while only one

Csl gene, *CslD3*/*KOJAK*, has been studied extensively in plants and was shown to be involved in proper root-hair formation (Dhugga, 2001).

Table 1.1 Partial list of genes involved in cellulose biosynthesis or cell wall structure

Gene	Gene product	References
Rsw1/*AtCesA1*	Glycosyl transferase	(Arioli et al.,1988)
Irx1/*AtCesA8*	Cellulose synthase subunit	(Scheible et al., 2001)
Irx3/*AtCesA7*	Cellulose synthase subunit	(Taylor et al., 1999)
Irx5/*AtCesA4*	Cellulose synthase subunit	(Taylor et al., 2003)
Ixr1/*Cev1*/*AtCesA3*	Cellulose synthase subunit	(Ellis et al., 2002) (Richmond, 2000)
Procuste/*Ixr2*/*AtCesA6*	Cellulose synthase subunit	(Desnos et al., 1996)
CslD3	Cellulose synthase subunit	(Dhugga 2001)
Kor	Endo-1,4-β-glucanase	(Nicol et al., 1998)
Kob1	Novel, plant-specific with N-terminal membrane anchor	(Pagant et al., 2002)
Cob	GPI-anchored protein	(Martin et al., 2001)

The temperature sensitive mutant *rsw1* was shown to encode a putative cellulose synthase gene and under the proper growth conditions showed aberrant cell expansion in epidermal cells of young seedlings. This phenotype is believed to be due to the reduction of crystalline cellulose in primary cell walls to approximately 44% of wild type levels with an increase in non- crystalline β-1,4-glucan to over three times that of wild type (Arioli et al., 1998). Mutant plants grown at the restrictive temperature were also shown to have increases in width and decreases in length in roots and dark grown hypocotyls. Trichomes of *rsw1* plants showed a swollen phenotype accompanied with a decrease in branch number as compared to wild type and leaf epidermal cells showed aberrations in their shape. In accordance with the expression profile of *Rsw1* mRNA which localized in roots, rosette leaves, and inflorescences, the length of mutant petals and filaments was

shorter than wild type (Williamson et al., 2001). Researchers later determined that the swollen phenotype of *rsw1* plants could be mimicked by the addition of 2,6-dichlorobenzonitrile (DCB), a specific inhibitor of cellulose synthesis. Interestingly, it was shown via field-emission scanning electron microscopy that the CMFs in mutant primary cell walls of root epidermal cells were wavy and crooked and after longer exposures to restrictive temperature, became difficult to visualize and had no clear order. Observation of CMTs in rapidly elongating root epidermal cells showed no difference in their arrangement when compared to control wild type plants. That randomization of the CMFs in root epidermal cells was phenocopied by addition of DCB led the researchers to conclude that the disruption of cellulose synthesis by mutation of *Rsw1* (also known as the *AtCesA1* gene) causes a randomization of CMFs in the primary wall without a concomitant disruption of CMTs and leads to isotropic growth of cells (Sugimoto et al., 2001).

Three other members of the AtCesA family have been cloned and their phenotypes in mutant plants examined. The *Irx* (IRREGULAR XYLEM) genes *Irx1*, *Irx3*, and *Irx5* correspond to *AtCesA8*, *AtCesA7*, and *AtCesA4*, respectively, and all share similar phenotypes including weakened stems, dark green leaves and stem sections show collapsed xylem elements and irregular appearances of the secondary cell walls in xylem and cells of the interfascicular region (Dhugga, 2001; Taylor, 2003). Measurements of the cellulose content of *irx5* mutant plants revealed that these plants contained only about 30% of the wild type levels of crystalline cellulose. By utilizing antibodies to the three known IRX proteins on tissue prints of wild type Arabidopsis stem sections researchers showed co-localization of each antibody to the same cell types in the stem, specifically in xylem and interfascicular cells. To determine what, if any, type of protein association may occur between the three IRX proteins, immobilized metal affinity chromatograpyhy was conducted using detergent solubilized extracts containing epitope tagged IRX3. The researchers determined that IRX5 and IRX1 bind to IRX3. Immunoprecipitation studies

revealed that IRX3 coimmunoprecipates IRX1 and vice-versa. If detergent solubilized extracts from *irx5-1* mutants were used in these experiments, IRX1 no longer precipated with anti-IRX3 antibody and anti-IRX1 could no longer precipitate IRX3. These results strongly support the hypothesis that the three IRX proteins are assembled in a highly ordered manner to make a full sized complex. This complex is believed to be essential for the proper formation of secondary cell walls in Arabidopsis (Taylor, 2003).

The ISOXABEN RESISTANCE (IXR) genes, *Ixr1* and *Ixr2*, were initially identified by their resistance to the potent cellulose synthase inhibiting compound, isoxaben. Recently it has been shown that the Arabidopsis PROCUSTE and CEV1 proteins are identical to the IXR2 and IXR1 proteins, respectively, and these mutants show phenotypes typical of other mutants with *CesA* defects. Specifically, the *procuste* and *Cev1* mutants are impaired in their ability to elongate hypocotyls normally and instead expand radially while mutants in *Cev1* also show defects in root elongation (Desnos, 1996; Ellis, 2002). Interestingly, the *cev1* mutant was isolated in a screen for plants that constitutively expressed a jasmonate (JA) responsive gene, *VSP1*, and these mutant plants were shown to have higher levels of JA and ethelyne than wild type plants. As JA is known to inhibit whole plant growth and can be induced by wounding, water deficit, and pathogen attack, the overall phenotype of the mutants could be due to this increase in the two plant hormones JA and ethylene. It is thought that perhaps defects in cellulose synthesis somehow upregulate these stress response phytohormones and may lead to the stunted phenotypes seen in many of the cellulose deficient *CesA* mutants (Ellis, 2002).

In addition to the *CesA* and *Csl* genes, there are several that are known to affect cellulose organization or deposition in Arabidopsis, notably KORRIGAN (KOR), KOBITO1 (KOB1), and COBRA (COB). The *KORRIGAN* gene of Arabidopsis encodes an endo-1,4-β-D-glucanase and has been shown to be involved in the proper cell elongation and division of cells. *kor* mutants are characterized as having a smaller stature than wild type at the seedling stage but begin to produce white-colored calli from the

shoot apical meristem before the production of the first true leaves. In addition, epidermal hypocotyls cells of *kor* plants were irregularly arranged and misshapen and seemed to be composed of many cells that had undergone incomplete cell plate formation. Localization studies using a KOR1-GFP fusion protein showed that the KOR-GFP was predominantly localized to the region of cell plate formation after the onset of cytokinesis. The authors theorize that KOR1 is involved in the maturation of the cell plate and acts to aid in the cell elongation process after mitosis as KOR1 is also localized to the plasma membrane (Nicol et al., 1998; Zuo et al., 2000). More recently another *KOR* allele was discovered by Sato et al, 2001. *acw1* was identified in a screen for swollen root phenotypes under restrictive (31°C) temperature and shown to be allelic to *KOR1*. The researchers determined that the glucose content of TFA-soluble wall fractions from the *acw1* mutant were 44% that of wild type and also showed, via field-emission scanning electron microscopy, that the CMF bundles in petiole mesophyll cells were slightly altered and appeared to be covered by larger amounts of pectic material. Additionally, under restrictive temperatures, mutant protoplasts exhibited a delay in the formation of CMFs which may indicate a possible role of KOR1 in contributing directly to cellulose synthesis by mediating the transfer of glucose residues to the growing β-glucan chain during this process (Sato et al., 2001).

The KOBITO1 (KOB1) gene was identified in a screen for reduced growth anisotrophy in dark grown hypocotyls and appears to encode a novel, highly conserved, plant-specific protein that carries a putative N-terminal membrane anchor. Mature *kob1* plants exhibited a strong dwarf phenotype, were sterile but had normal root hair initiation and extension. The cells of *kob1* hypocotyls were larger in diameter than wild type while roots showed no increase in width but were shorter than wild type. In addition, it was noted that incomplete cell walls existed in epidermal, cortical, and endodermal cell layers of the kob1 hypocotyls, ectopic lignin was present in roots, and *kob1* hypocotyls accumulated callose. Measurements of the cellulose levels in *kob1* revealed a 33%

reduction of this polymer when compared to wild type plants and direct visualization of CMFs in elongating cells of *kob1* roots showed no transverse CMFs but an "amorphous mass." Utilizing a GFP::KOB1 fusion protein, the researchers were able to determine that KOB1 appears to be localized to the plasma membrane of all cells in the root except for those of the meristamatic region and the root cap (Pagant et al., 2002).

The putative glucosylphosphatidyl (GPI)-anchored protein, COBRA (COB), when mutated, causes reduced levels of crystalline cellulose microfibrils in Arabidopsis and appears to reduce the elongation of roots by allowing them to expand radially while maintaining cell volume (Martin et al., 2001; Roudier et al., 2002). This protein has a cellular localization at discrete regions along the longitudinal cell surfaces in roots and may define regions within elongating cells resistant to expansion thereby defining the polarity of expansive growth (Martin et al., 2001).

MUTATIONS IN GENES ENCODING PROTEINS THAT INTERACT WITH THE PLANT CYTOSKELETON CAN CAUSE ABERRATIONS IN PLANT GROWTH BOTH AT THE WHOLE-PLANT AND CELLULAR LEVEL

It is known that the cortical microtubules (CMTs) and microfilaments (MFs) in plant cells are necessary for proper growth and expansion (Cyr and Palevitz, 1995; Azimzadeh et al., 2001; Martin et al., 2001; Smith, 2003). A cell's ability to respond to external stimuli such as light and gravity as well as phytohormones relies on the rapid reorientation of CMTs (Shibaoka, 1994; Wasteneys, 2000; Blancaflor, 2001). It has also been observed that immediately after cytokinesis in tobacco BY-2 cells, the microtubules follow a well defined sequence to finally reach their usual orientation perpendicular to the axis of cell elongation at the plasma membrane (Hasezawa and Kumagai, 2002). Studies using potent stabilizers or depolymerizers of MTs and MFs have shown that in the presence of these drugs, diffuse growth is affected, root hair and pollen tube growth is altered, and trichome morphogenesis and branching is inhibited (Mathur and Hülskamp, 2002; Smith, 2003). It appears that by disrupting the normal organization and timing of

reorganization of MTs, proper anisotropic growth cannot occur. Exactly how these ubiquitous members of the plant cell accomplish the act of regulating proper cell elongation is still a mystery but it is believed that the CMTs, and perhaps MFs, probably play a very important role in regulating the deposition pattern and organization of cellulose microfibrils (CMFs) which then constrain the cells growth to a particular direction. Luckily, research has advanced significantly in discovering genes and gene products that appear to play crucial roles in the organization, polymerization, and localization of CMTs in plant cells, some of which are discussed below (Table 1.2).

Recently a very interesting mutant, *mor1*, was isolated in Arabidopsis and was found to be temperature-sensitive. Mutants grown under the restrictive temperature exhibit left-handed twisting of organs, isotropic cell expansion, and impaired root hair polarity. In addition, direct visualization of CMTs in *mor1* plants showed that under the restrictive temperature, CMTs were quickly disorganized and shortened dramatically. This disruption of CMTs was completely reversible, however, and upon growth at the non-restrictive temperature, the CMTs regained their wild type length and orientation (Martin, 2001; Whittington et al., 2001). A MOR1 homolog, TMBP200 exists in tobacco and has been shown to form inter-microtubule bridges about 10nm in length (Lloyd and Chan, 2002). MOR1, then, may function to bundle microtubules together and may act to stabilize them from rapid dissociation into tubulin heterodimers.

The Arabidopsis mutants *lefty1* and *lefty2* were isolated as suppressors of the *spiral1* and *spiral2* mutants, respectively. The mutations in each of these genes were quite specific and caused single amino-acid changes in the genes encoding α-tubulin4 and α-tubulin6, respectively. As their name implies, mutants grew in left-handed helices while observations of the CMT in these plants revealed that they were organized in right-handed helices (Thitamadee et al., 2002). The isolation of these mutants with specific defects in the α-tubulin monomers lends more evidence to that obtained by using

antisense α-tubulin gene expression experiments which showed that reduced α-tubulin mRNA levels and protein mimicked the phenotypes of plants treated with oryzalin, a MT

Table 1.2. Partial list of plant mutants that appear to have MT and cell elongation defects

Mutant	Phenotype	Gene product	References
angustifolia	Leaves narrow, 2-branched trichomes	CtBP/BARS	(Kim et al., 2002)
brick1, brick2, *brick3*	Unlobed epidermal Novel pavement cells		(Smith, 2003)
botero1/ ectopic root hair 3/ fragile fiber2/lue1	Dwarf stature, swollen cells, reduced stem strength	Katanin p60	(Burk et al., 2001) (Bouquin et al., 2003) (Webb et al., 2002) (Bichet et al., 2001)
tonneau2/fass	Dwarf plant	PP2A subunit	(Camilleri et al., 2002)
lefty1/lefty2	Left-handed plant twisting	α-tubulin4/α-tubulin6	(Lloyd and Chan, 2002)
microtubule organization 1	Temp-sensitive, short plant, swollen cells	XMAP215 homolog	(Whittington et al., 2001)
pilz group	Callus-like growth	Tubulin-folding cofactors	(Mathur and Hülskamp, 2002)
porcino	Trichome defect	TFC-C	(Smith, 2003)
kiesel	Trichome defect, plants reduced in size	TFC-A	(Kirik et al., 2002)
spike1	Reduced trichome branching	CDM family protein	(Qiu et al., 2002)
spiral1/spiral2	Right-handed growth	Unknown	(Furutani et al., 2000)
zwichel	Reduced trichome branching	KCBP	(Oppenheimer et al., 1997)
tangled	Aberrant cell files	Similarity to animal APC proteins	(Smith et al., 2001)

depolymerizing drug (Smith, 2003). Just as specific mutations in the genes which encode α-tubulin, mutations in tubulin folding cofactor (TFC) genes can produce strong phenotypes in plants. Defects in the KIESEL (KIS) protein resulted in plants that were reduced in size when compared to wild type and also showed defects in meiotic events, cell division, and caused trichomes to become bulged and less branched. The *Kis* gene encodes the *microtubule- folding cofactor A* gene (*TFC-A*) and a mutation in this gene is

believed to reduce the availability of assembly-competent α/β-tubulin heterodimers thereby resulting in an inability to polymerize new microtubules in expanding cells (Kirik et al., 2002).

The functions of the maize TANGLED1 (TAN1) and Arabidopsis TONNEAU2 (TON2) proteins are somewhat similar in that mutation of each result in the misdirection of division plane formation and subsequently cause aberrant cell files and arrangements. In *tan1* mutants all of the necessary cytoskeletal structures appear to be present and are structurally normal, however the preprophase band (PPB) and phragmoplast fail to orient properly. In *ton2* mutant plants CMTs appear to align properly perpendicular to the long axis of hypocotyls cells but are randomized in interphase cells of roots. Perhaps most important is the total lack of the PPB in these mutant cells during the onset of mitosis. Cloning of both of these genes have shown that *Tan1* encodes a highly basic protein that is distantly related to a basic MT-binding protein domain of vertebrate APC proteins and *Ton2* encodes a putative regulatory subunit of type 2A protein phosphatase (PP2A). Based upon the morphological phenotypes of these mutants and their similarity to other proteins it is hypothesized that TAN1 may play a role in aiding in the orientation of the cytoskeletal structures involved in dividing cells perhaps by directing microtubules to proper positions at the cell cortex (Smith et al., 2001). Based on the phenotypes of weak alleles of *Ton2* mutants, it is proposed that TON2 may play a direct role in organizing the CMTs (Camilleri et al., 2002).

A screen of Arabidopsis T-DNA insertion lines for trichome defects allowed the isolation of the *spike1* mutant. *spk1* trichomes had a reduction in the number of branches and a reduction in stalk elongation when compared to wild type and were similar to those of *zwi* mutants. In addition to the trichome phenotype, the mutant plants displayed a dwarf phenotype with narrow leaves that were comprised of epidermal cells that appeared to lose their normal 'lobed' appearance. The cotyledons of *spk1* mutants were more severely affected than mature leaves and seemed to show defects in cell adhesion. *Spk1*

transcripts were determined to be found in all organs examined and are predicted to encode a protein with similarity at its carboxy-terminus to a CDM-family protein implicated in the reorganization of the cytoskeleton in animal cells in response to extracellular stimuli. Confocal observation of CMTs and MFs in epidermal pavement cells revealed that in *spk1* mutants the spatial arrangement of these cytoskeletal elements is altered and may be the cause of the cell morphologies seen in epidermal cells of leaves and cotyledons (Qiu et al., 2002).

ZWICHEL (ZWI), like SPK1, was found in a screen for trichome morphogenesis mutants (Oppenheimer 1997) and the *Zwi* gene encodes a KCBP (KINESIN-LIKE CALMODULIN-BINDING PROTEIN) with Ca^{2+}/calmodulin-regulated minus end-directed MT motor activity (Song, 1997). ZWI is able to bundle MTs and may be involved in the directed transport of vesicles to regions of localized growth or in the maintenance of MT arrays during cell division (Martin et al., 2001; Smith, 2003). Defects in trichome branching in the *zwi* mutant can be alleviated by addition of MT stabilizing drugs such as taxol and the *zwi* mutant phenotype can be mimicked by addition of MT depolymerizing agents if added after initial stalk formation (Mathur and Chua, 2000). Recently it has been discovered that ZWI may interact with another protein involved in cell expansion, ANGUSTIFOLIA (AN) which displays an aberrant CMT network in mutant trichomes and is a CtBP/BARS-like protein (Folkers et al., 2002).

Katanin is an ATP-dependent microtubule-severing protein present in both animal and plant cells. Katanin was initially discovered by its MT-severing activity in mitotic cell extracts in *Xenopus laevis* eggs (Vale, 1991) and subsequently was identified as a heterodimer of p60 and p80 subunits after purification of sea urchin (*Strongylocentrotus purpuratus*) egg supernatants. The p60-p80 heterodimer was shown to have in vitro MT binding and severing activity that was dependant on the availability of ATP (McNally and Vale, 1993). Antibodies to sea urchin p80 and p60 katanin subunits were used to show that the localization of these subunits was highly concentrated at the centrosomes

during the complete cell cycle. This subcellular localization was found to be dependent on the presence of intact MTs as depolymerization of MTs by use of nocodazole caused the dispersal of katanin-specific staining (McNally et al., 1996). Further research determined that it is the p60 subunit of katanin that possesses microtubule-stimulated ATPase and MT-severing activity and the p80 subunit is responsible for the targeting of p60 to the centrosome via WD40 repeats and also may negatively regulate the activity of p60 (Hartman et al., 1998; McNally et al., 2000). Since its initial isolation, katanin has been shown to be involved in the deflagellation process of *Chlamydomonas*, the release of MT from neuronal centrosomes and the regulation of MT length in neurons, and to play a role in the meiotic spindle organization in *Caenorhabditis elegans* (Lohret et al., 1998; Ahmad et al., 1999; Quarmby and Lohret, 1999; Srayko et al., 2000).

The identification of Arabidopsis katanin was accomplished using both forward and reverse genetics. Screens for mutants with defects in hypocotyl length (BOTERO1), aberrant root morphology (ECTOPIC ROOT HAIR 3), reduced stem strength (FRAGILE FIBER 2), and inappropriate regulation of a gene involved in gibberellin response (LUC super expressing) all eventually resulted in the isolation of the Arabidopsis katanin p60 ortholog which was shown to have in vitro microtubule-severing activity (Bichet et al., 2001; Burk et al., 2001; Stoppin-Mellet et al., 2002; Webb et al., 2002; Bouquin et al., 2003). Defects in the Arabidopsis katanin p60 subunit cause mutant plants to display a semi-dwarf phenotype in which all organs are apparently affected in proper anisotropic growth. Roots, internodes, leaves, and floral organs are all shorter than wild type and many organs show a dramatic increase in width. Microscopic observations reveal that the reduction in organ length can be attributed to a decrease in anisotropic growth of cells along with an increase in their radial dimension. It also appeared that in certain tissues such as the pith of petioles and elongating stems there are apparent disruptions of the normally ordered cell files of parenchyma cells possibly due to incorrect placement of cell plates during cytokinesis. Tip growth is apparently not affected in any of the mutants

examined although ectopic root hairs were reported in one mutant, *ectopic root hair 3* (*erh3*) (Webb et al., 2002). Observation of microtubules in rapidly elongating regions of *fra2* plants including root, petiole, and stem pith revealed that the CMT array was not organized in parallel arrays perpendicular to the growth axis of the cells. In addition, direct observation of the primary and secondary walls using field-emission scanning electron microscopy revealed that the innermost layer of CMFs was aberrantly arranged. In wild type cells undergoing rapid anisotropic growth the CMFs are usually arranged in a manner reflecting that of the underlying CMTs. They typically run in tight parallel arrangement around the cell transverse to the axis of elongation with very slight deviations that form a slight right- or left-handed helix. The CMFs found in the innermost layer of the cell wall in mutant plants, however, showed a large distribution of angles with obvious bands of approximately 6 to 12 individual cellulose microfibrils traveling together. These bands of microfibrils sometimes completely reversed their direction within the cell wall and appeared to make turns of 180 degrees. Transmission electron microscopy analysis of stem sections from wild type and *fra2* mutants showed a reduction in the thickness of both primary walls of pith and secondary walls in interfasicicular fibers of mutant plants. It also appeared that the secondary walls of the *fra2* mutants were abnormal as they lacked visible layers normally seen in wild type and also had inner surfaces that were wavy and seemed to have an uneven distribution of wall material along their length (Burk et al., 2001; Burk and Ye, 2002).

THE CORTICAL MICROTUBULE/CELLULOSE MICROFIBRIL PARADIGM: THE ORIENTATION OF THE CMT ARRAY CAN AFFECT THE ARRANGEMENTS OF THE CMFS WITHIN PLANT CELL WALLS

Through the observation of effects of specific mutations in cellulose biosynthesis genes, genes involved in regulation of the plant cytoskeleton, and that of inhibitors of cellulose biosynthesis and proper cytoskeleton polymerization researchers have concluded that the CMT array plays a significant role in the proper orientation of the

CMF in the primary and secondary cell walls — the MT/CMF paradigm (Shibaoka, 1994; Fisher and Cyr, 1998; Baskin, 2001; Burk and Ye, 2002; Hasezawa and Kumagai, 2002; Mathur and Hülskamp, 2002). How these two structural elements, the CMTs and the CMFs, interact to produce an organized framework that acts to constrict cell elongation to specific regions or promote growth anisotropically is still a matter of debate in the scientific community. Not surprisingly there are several models that are currently being examined and each, perhaps, may play a part in particular situations depending on the cell types examined and their current expansion conditions.

First proposed by Heath (1974), the 'monorail' hypothesis posits that cellulose synthesizing terminal rosettes interact directly with CMTs via plasma membrane spanning linking proteins, and through this interaction CMF synthesis can be directed by the CMT array (Figure 1.2 A.). This model gained significant support through experiments using taxol-treated tobacco BY-2 protoplasts. The production of protoplasts involves the removal of their cell walls and results in spherical 'naked' cells whose CMT arrays become disorganized. The removal of the cell wall is only temporary, however, as new cellulose microfibrils are generated and eventually a new cell wall is formed. If tobacco BY-2 cells are treated with the microtubule stabilizing drug taxol before the removal of the cell wall, microtubules in the middle portion of the cells retain their normal orientation (parallel and perpendicular to the axis of maximum cell elongation). When these taxol-treated protoplasts are allowed to recover in medium, it was observed that the newly formed CMFs appeared to lie almost exactly over the stabilized CMTs. Transmission electron observation of sectioned protoplasts cut obliquely to the cell membrane/cell wall interface showed that bundles of CMFs appeared directly over CMTs. In addition, in sections of protoplasts cut at right angles to the cell wall/plasma membrane interface, CMFs appeared directly over CMTs (Hasezawa and Nozaki, 1999).

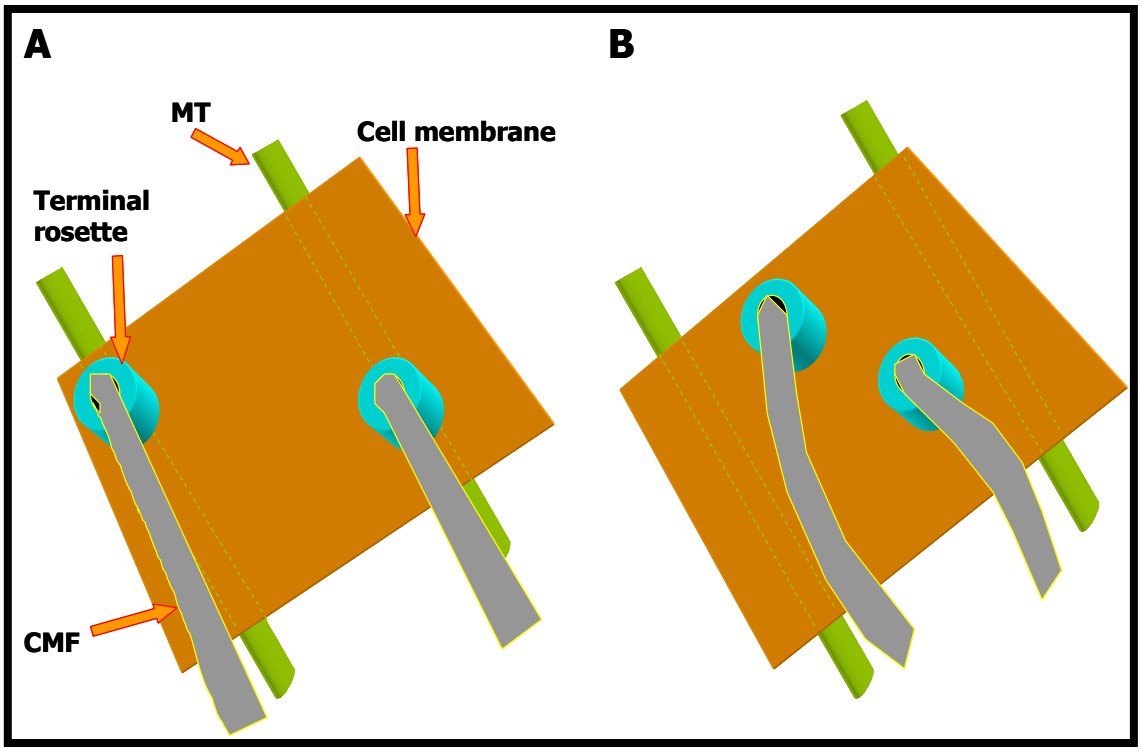

Figure 1.2. Schematic diagram of the monorail hypothesis proposed by Heath (1974) (A) and the membrane channel hypothesis of Giddings and Staehelin (1991) (B).

In contrast to the 'monorail' hypothesis is the 'guard-rail' hypothesis (Figure 1.2 B.). In the unicellular green alga, *Closterium*, the addition of MT depolymerizing agents have been shown to disrupt the normal organization of CMFs. Examination of freeze-fractured cell replicas revealed rows of two to five terminal rosettes in the plasma membrane which were apparently arranged parallel to CMFs perpendicular to the long axis of the cell. Further examination of these cells showed that the terminal rosettes appeared to lie between MTs adjacent to the inner surface of the plasma membrane and not directly over the MTs (Giddings and Staehelin, 1991). Further evidence supporting the idea that the cellulose synthesizing rosettes do not directly associate with MTs comes from studies of xylem vessels during the formation of the secondary cell wall. During this process it appears that the terminal rosettes are arranged more randomly than would

be expected if they followed the straight paths delineated by CMTs (Schneider and Herth, 1986). Based on these facts, Giddings and Staehelin (1991) propose that the cellulose synthase complexes travel in paths formed in the plasma membrane by the close association of MTs to the membrane. The rosettes can travel between these 'guard rails' using the force generated by the crystallization of cellulose to propel them.

More recently two other models of how the CMFs are deposited in an organized fashion have been proposed. Even though much evidence exists that shows that disruption of the CMT array causes isotropic growth in plant cells, usually accompanied by a disruption in the CMF, it is a fact that cellulose biosynthesis does not rely on the presence of MTs. Additionally, there are many examples of seemingly ordered CMFs at a whole-cell level in several plant species and in certain cell types in which MTs have been shown to play little role in the overall organization of the CMFs. Typically in these cell types or under experimental conditions which disrupt MTs, the CMFs have been shown to maintain their ordered structure or adopt a helicoidal arrangement (Giddings and Staehelin, 1991; Emons and Mulder, 1998; Baskin, 2001). A mathematical model proposed by Emons and Mulder (1998), is based on cell geometry and makes assumptions of how the terminal rosettes interact in the plasma membrane, how long they are actively producing cellulose (based on time before they are degraded or removed from the membrane), the density of these particles in the membrane, and cell geometry. Computer projections of the putative CMF orientations in this model closely resemble many of the recognized patterns seen in the lamellae of real plant cells (Emons et al., 2002). This model, however, fails to take into account the importance CMTs appear to play in the rapid reorientation of CMFs in the cell wall as well as fails to tackle the problem generated when dealing with a living cell that can alter its overall geometry significantly while maintaining apparent order in the cellulose matrix. The other model that is gaining attention relies on the idea that a scaffold of some sort exists between individual or bundles of cellulose microfibrils in the cell wall as well as between newly

polymerized cellulose and microtubules located in the CMT array. This 'templated incorporation' hypothesis is based on observations of cells that can form helicoidal arrangements of CMFs independently of CMTs as well as experiments that showed that even in the absence of MT polymers, CMFs can maintain a 'localized' order and may remain parallel to each other even if their orientation with respect to cell growth polarity is aberrant (Baskin, 2001). Research conducted using tobacco BY-2 protoplasts cells indicated that the synthesis of CMFs is necessary for proper CMT orientation as cells treated with a cellulose synthase inhibitor prevented MTs from organizing into transverse arrays. In addition, treatment of walled suspension culture BY-2 cells with isoxaben eventually led to swollen portions of the cells which corresponded to areas lacking cellulose. In these swollen areas the arrangement of CMTs was randomized while areas of the same cell that still retained cell wall material had CMTs organized in transverse arrays perpendicular to the growth axis of the cell. It therefore seems that information about the proper orientation of polymers at the cell wall/plasma membrane interface can travel from previously synthesized CMFs to MTs and vice versa. The 'templated incorporation' model is apparently a blend of the other models presented and, with the caveat that the CMT/CMF scaffolding has a higher affinity for newly laid cellulose in the cell wall than that between two CMFs, this model allows for the rapid reorientation of the CMFs in the cell wall in response to changes in the CMT organization (Baskin, 2001; Smith, 2003).

The recent characterization of the *fragile fiber 1* mutant of Arabidopsis and the cloning of the gene responsible for the mutant phenotype may aid in the development of more detailed models of how CMTs interact with CMFs. The *fra1* mutant was isolated in a screen for plants with a reduction in their stem strength and was shown to have a reduction in the height of mature stems, dark grown hypocotyls, and roots. Microscopic examination of fibers in mutant and wild type stems revealed no difference in the length of these cells. Additionally, TEM analysis showed that there was no difference in the

thickness of primary or secondary cell walls in the mutant when compared to wild type. However, FESEM studies of the innermost layer of CMFs in wild type and *fra1* fiber cells revealed that the mutants had a disruption of the normal CMF pattern. Instead of tightly packed parallel microfibrils, the mutant fibers' walls had CMFs that appeared to be less densely packed and had an altered arrangement. Primary walls of pith cells showed no difference in the CMF orientation or organization. The *fra1* gene was cloned and encodes a kinesin-like protein with high similarity to a group of animal kinesin-like proteins in the KIF4 family. As kinesins are motor proteins that are known to bind to MTs, it is thought that perhaps FRA1 is involved in the MT control of CMF orientation (Zhong et al., 2002). Many of the current models attempting to explain how CMTs control CMF orientation are based on the premise that linking proteins exist between CMTs and the plasma membrane where they interact with newly synthesized CMFs (Giddings and Staehelin, 1991). That the *fra1* mutant shows defects in the organization of CMFs in secondary cell walls without changes in the CMT array is exciting in that it may be one of the first examples of a gene product that links MTs and CMF organization.

HIGHER PLANT PHYTOHORMONES ARE KNOWN TO BE INVOLVED IN CELL ELONGATION AND CAN AFFECT THE ORGANIZATION OF CMTS

Alterations in cell expansion are also seen in mutants that disrupt the synthesis of certain plant hormones. Many brassinosteroid (BR) biosynthesis mutants are known and have been shown to affect certain steps in the biosynthesis of BR. All of the BR mutants have severe dwarf phenotypes with a reduction in cell elongation in most plant cell types. The *det2* mutant, when grown in the dark, is much shorter than wild type, accumulates anthocyanins, has thick hypocotyls, and expanded cotyledons, and expresses light-regulated genes that should not be expressed. When these mutants are grown in the light the plants are dark green, have reduced male fertility and apical dominance, and have delayed chloroplast and leaf senescence (Li and Chory, 1999). Mutations at another 7 loci in Arabidopsis disrupt the biosynthesis of BRs and share the dwarf phenotype of *det2*

(Schumacher and Chory, 2000). The *boule* (*bul1-1*) mutant of Arabidopsis was initially isolated as a BR defective plant that had an extreme dwarf phenotype, short stems and petioles, and dark-green leaves. Cloning of the *bul1-1* gene revealed that it was allelic to *dwf7-3/ste1-4* and had a defect in the Δ^7-sterol-C5(6)-desaturation step necessary for brassinosteroid biosynthesis. Light and scanning electron microscopic analysis of petioles, hypocotyls, and leaves showed that there was a reduction in epidermal cell elongation, an increase in the number of stomata 5-6 times that of wild type, a reduction in the size of the stomata and that *bul1-1* leaves were thicker than wild type owning to an increase in the size of parenchyma cells in the leaf (Catterou et al., 2001a). Using immunocytochemical methods to directly visualize CMT in mutant petiole and hypocotyls cells, the researchers observed that the CMTs were randomly organized and appeared to be fainter than wild type perhaps due to a decrease in the number of CMTs. Northern analysis of wild type and the *bul1-1* mutant indicated that there was a considerable reduction in the amount of β-tubulin mRNA corresponding to the *TUB1* gene transcript. These results are significant in that they suggest that the CMT phenotype may be a result of inadequate levels of β-tubulin for proper heterodimer formation with α-tubulin. The results presented by the authors are the first example in which a direct link between BR synthesis and a possible pathway in which BR may induce CMT organization and, subsequently, anisotropic cell expansion (Catterou et al., 2001b).

Like BR mutants, disruption of the biosynthesis of gibberellin (GA) leads to a dwarf phenotype, reduced apical dominance, narrow leaves, later flowering time, and a dark green appearance as seen in the *shi* (*short internodes*) mutant (Fridborg et al., 1999). Mutants that overexpress genes in the synthesis of GA have a "slender" phenotype as seen in the mutant *spindly* (*spy*). *spy* plants have pale green foliage, flower earlier than wild type, have partial male sterility, and parthenocarpic fruit development. This phenotype resembles that of Arabidopsis plants continually treated with exogenous GA. The *SPY* gene was cloned and had similarity to known tetratricopeptide repeat proteins

and probably functions as a negative regulator of the GA signal transduction pathway (Jacobsen et al., 1996). GA treatment is also known to cause an increase in transverse cortical MTs in azuki bean epicotyls, onion leaf-sheaths, dwarf maize mesocotyls, and cucumber hypocotyls and is believed to be responsible for regulation of the direction of cell expansion. However, some evidence implies that GA_3 reorganization of MTs may be separate from cell elongation. Reorientation of MTs in decapitated dwarf pea seedlings and onion leaf-sheaths does not appear to be correlated with an increase in cell expansion (Shibaoka, 1994).

The role of auxins in cell elongation has been known for some time and this hormone has been shown to be involved in photropism and gravitropism. One affect of auxin within cells is the activation of the plasma membrane H^+-ATPase and the subsequent reduction of apoplastic pH. This pH change is believed to activate proteins involved in cell wall expansion and may be due to the activation of a group of proteins called expansins (Cosgrove, 1997). Auxin can also cause the transverse orientation of MTs in wheat coleoptiles, oat mesocotyls, maize coleoptiles, and radish hypocotyls. This auxin-induced orientation of MTs does not seem to be involved in auxin-induced cell elongation as disruption of cortical MTs in maize coleoptiles did not affect cell elongation (Shibaoka, 1994). Recently it has been proposed that auxin-induced extension growth may rely on the production of hydroxyl radicals such as hydrogen peroxide (H_2O_2) and hydroxyl radicals (•OH). The use of methods to detect the production of reactive oxygen intermediates (mainly H_2O_2) in maize coleoptiles after the addition of IAA (indole-3-acetate) showed that the production of superoxide increased under these conditions. Measurements of wall extension after exogenous addition of H_2O_2 and inhibitors of reactive-oxygen production allowed researchers to determine that wall extension increases dramatically in the presence of hydroxyl radicals and that this extension is reduced in the presence of inhibitors. It is hypothesized that the production of reactive oxygen species in response to auxin can cause a weakening of the cell wall

structure which can ultimately lead to wall extension in the presence of turgor pressure (Schopfer et al., 2002).

The plant hormone ethylene seems to repress cell elongation and promote the lateral expansion of cells, which induces the classic triple-response phenotype in terrestrial plant seedlings (short roots, increase in root hairs, short hypocotyl, and exaggerated apical hook). In contrast, plant species that exist in aquatic habitats such as *Ranunculus sceleratus*, *Callitriche platycarpa*, and deepwater rice are known to respond to ethylene by increasing internode length and the promotion of lateral expansion. Ethylene is also known to cause a predominance of longitudinal MTs, but this MT reorientation appears to be independent of the subsequent change in cell expansion from longitudinal to lateral (Shibaoka, 1994).

Like ethylene, cytokinins are known to cause a longitudinal orientation of cortical MTs and inhibit longitudinal cell growth. Cytokinins are also known to suppress auxin-induced apical dominance, inhibit the senescence of organs, and induce the opening of stomata (Crozier et al., 2000). Research has shown that addition of colchicines and ethyl N-phenylcarbamate to azuki bean epicotyl segments partially rescues kinetin inhibition of auxin-induced cell elongation. In addition, this inhibition was shown to be dependant upon active cellulose synthesis (Shibaoka, 1994).

Enzymes Present in Plant Cell Walls are Necessary for Cell Wall Loosening and Subsequent Cell Expansion

As mentioned previously, cell elongation depends on the ability of the cell wall to undergo stress relaxation that causes a decrease in the cells osmotic potential. This osmotic potential decrease leads to the passive uptake of water and increases cell turgor. How cell walls accomplish this relaxation without rupturing from turgor pressures that approach 1000 atmospheres is still unknown, but several proteins appear to play a role in this process. Initial experiments using isolated growing cell walls that were clamped and put under constant tension revealed that under neutral pH conditions, the walls would

extend for a short while and quickly stop. If the cell walls were placed in acidic buffer with a pH of 5 or below, the clamped walls would extend rapidly and continue to expand for hours in some cases. This elongation under acidic pH is known as acid-induced creep and has been postulated to result in vitro after auxin induced proton ATPase activity and after treatment with fusicoccin (Cosgrove, 1997).

In addition to the above pH experiments, walls from growing cucumber hypocotyls that had been boiled and placed in either acidic pH or neutral pH showed almost no appreciable creep which indicates that the cell wall extension may be due to the action of enzymes. Using a reconstitution assay which involved adding proteins extracted from cucumber cell walls, McQueen-Mason et al. (1992) determined that only protein fractions from growing tissues contained proteins that would allow heat inactivated walls to undergo extension. This reconstitution assay was subsequently used to isolate two proteins from cucumber that induced cell wall expansion when added to heat-inactivated cell walls and were named expansins (McQueen-Mason and Cosgrove, 1994). Expansins have subsequently been isolated from several plant species such as Arabidopsis, tomato, tobacco, rice, and Zinnia and have been shown to be localized to regions of active cell expansion (Cosgrove, 2000). For example, two tomato expansins, *LeExp2* and *LeExp18*, were shown to be preferentially expressed in expanding tissues such as maturing flowers, expanding leaves, and leaf primordial or primarily in tissues with meristematic activity respectively (Reinhardt et al., 1998). The Arabidopsis α-expansin, AtEXP10 has been shown to be highly expressed in rapidly elongating leaves, petioles, and the bases of pedicles. Overexpression of the *AtEXP10* gene led to plants with longer petioles, larger leaves, and larger cells than wild type while reduction of AtEXP10 protein using antisense constructs produced plants with shorter petioles and leaf blades than wild type (Lee et al., 2001). Cho and Kende (1997) determined that deepwater rice expansins were preferentially expressed in specific organs where rapid cell elongation was occurring. Unfortunately, the exact biological activity of expansins is not known but several groups

believe that expansins function by loosening noncovalent associations between wall polysaccharides such as that between cellulose and hemicelluloses.

Another type of cell wall loosening protein is xyloglucan endotransglycosylase (XET). XET is capable of breaking xyloglucans and joining the newly formed end to another acceptor xyloglucan. While XET activity has been shown to correlate with high rates of cell growth, in vitro experiments show no increase in cell elongation or creep. XET may function to incorporate newly formed xyloglucans into the cell wall and, with expansins, allow cell walls to increase in size (Cosgrove, 1997; Cosgrove, 1999). The interactions of expansins and XET with hormones that promote or inhibit cell elongation are not known but future research may reveal a direct correlation between increased cell elongation, hormone levels, and expansin or XET transcript or protein levels.

RESEARCH GOALS AND BRIEF SUMMARY OF MY DISSERTATION WORK

The role of cortical microtubules in regulating and directing proper cell elongation has been inferred by many experiments that show that disruption or stabilization of MTs can have profound effects on cell expansion. In addition, several mutants of higher plants have been found that are known to carry lesions in proteins that appear necessary for proper microtubule maintenance, organization or assembly. Even with this knowledge, our understanding of how microtubule dynamics relate to cell growth is severely limited. How is the CMT array formed after cytokinesis? What is the importance of this array in elongating cells and how does a disruption of the CMT array affect CMF orientation directly? These are questions I attempted to answer.

A screen of ethyl methanesulfonate-mutagenized Arabidopsis populations for defects in stem strength led to the discovery of a mutant with a two- to threefold reduction in the force necessary to break their stems. This mutant was designated *fragile fiber 2* and is the basis of research done for Chapters 2, 3, and 4 of this volume. Chapter 2 deals with the gross morphological examination of mutant and wild type plants as well as the fine mapping of the *fra2* locus using CAPS-based markers. We determined that the dwarf

stature of mutant plants was due to a defect in proper cell elongation in diffuse-growing cells and this defect was due to a specific mutation in the *fra2* gene which encodes a homologue to animal p60 katanin subunit. As katanin is a member of the AAA (ATPase associated with diverse cellular activity) family of ATPases and is known to have ATP-dependant microtubule-severing activity in animal systems, we believe that this gene may be an excellent candidate for exploring the role of microtubule dynamics in plant cells. Unlike animal systems, the defect in Arabidopsis p60 katanin (renamed AtKTN1) caused no change in the mitotic spindle or preprophase band formation but appeared to cause a delay in the disassembly of the perinuclear microtubule array after cytokinesis. In addition, preliminary examinations of MTs in interphase mutant root cells appeared to show differences in the organization of the CMTs when compared to wild type.

Since it has been shown that pharmacological disruption of the CMTs of plant cells can disrupt the orientation of CMFs in the cell wall, I wished to determine if a specific genetic mutation in a microtubule-severing protein could also affect CMT organization or deposition. The characterization of the CMTs in wild type and mutant cells of elongating root, stem, and petiole as well as the direct visualization of the CMFs at the innermost surface of the cell wall in these cells is described in Chapter 3.

In order to increase our understanding of the function of AtKTN1 protein in Arabidopsis, I characterized the phenotype both at a gross morphological and cellular level of plants overexpressing wild type *AtKTN1* cDNA and these results are discussed in Chapter 4. I determined that overexpression of *AtKTN1* caused a similar cellular and morphological change to *fra2* mutant plants. Specifically, plants appeared much shorter than wild type with reductions in the lengths of all organs except roots. This change was due to an apparent inability of cells in these tissues to expand properly. In addition, the CMTs and CMFs of these overexpressing cells were disrupted in a similar manner to *fra2* mutants. Based on our examination of *fra2* mutants and transformants overexpressing

wild type *FRA2*, we developed a model of possible AtKTN1 function in Arabidopsis in regulating the proper MT dynamics necessary for the timely formation of the CMT array.

Based on the research done for my doctoral dissertation, I believe that we have greatly aided the plant scientific community in our understanding of the role CMT array formation and organization plays in the proper oriented deposition of CMF in plant cell walls. Our work is significant in that it is the first to show that a genetic mutation in a katanin-like microtubule-severing protein is involved in CMT arrangement at the plasma membrane and that defects in this protein can cause changes in cellulose deposition patterns and a subsequent disruption in anisotropic growth in rapidly elongating plant cells.

REFERENCES

Ahmad, F.J., Yu, W., McNally, F.J., and Baas, P.W. (1999). An essential role for katanin in severing microtubules in the neuron. J Cell Biology 145, 305-315.

Arioli, T., Peng, L., Betzner, A.S., Burn, J., Wittke, W., Herth, W., Camilleri, C., Hofte, H., Plazinski, J., Birch, R., Cork, A., Glover, J., Redmond, J., and Williamson, R.E. (1998). Molecular analysis of cellulose biosynthesis in Arabidopsis. Science 279, 717-720.

Azimzadeh, J., Traas, J., and Pastuglia, M. (2001). Molecular aspects of microtubule dynamics in plants. Current Opinion in Plant Biology 4, 513-519.

Baskin, T.I. (2001). On the alignment of cellulose microfibrils by cortical microtubules: a review and a model. Protoplasma 215, 150-171.

Bichet, A., Desnos, T., Turner, S., Grandjean, O., and Höfte, H. (2001). BOTERO1 is required for normal orientation of cortical microtubules and anisotropic cell expansion in Arabidopsis. Plant J 25, 137-148.

Blancaflor, E.B. (2002). The cytoskeleton and gravitropism in higher plants. J Plant Growth Regul 21, 120-136.

Bouquin, T., Mattsson, O., Næsted H., Foster, R., and Mundy, J. (2003). The Arabidopsis *lue1* mutant defines a katanin p60 ortholog involved in hormonal control of microtubule orientation during cell growth. Journal of Cell Science 116, 791-801.

Burk, D.H., and Ye, Z.-H. (2002). Alteration of oriented deposition of cellulose microfibrils by mutation of a katanin-like microtubule-severing protein. Plant Cell 14, 2145-2160.

Burk, D.H., Liu, B., Zhong, R., Morrison, W.H., and Ye, Z.-H. (2001). A katanin-like protein regulates normal cell wall biosynthesis and cell elongation. Plant Cell 13, 807-827.

Burn, J.E., Hocart, C.H., Birch, R.J., Cork, A.C., and Williamson, R.E. (2002). Functional analysis of the cellulose synthase genes *CesA1*, *CesA2*, and *CesA3* in Arabidopsis. Plant Physiol 129, 797-807.

Buster, D., McNally, K., and McNally, F.J. (2002). Katanin inhibition prevents the redistribution of γ-tubulin at mitosis. Journal of Cell Science 115, 1083-1092.

Camilleri, C., Azimzadeh, J., Pastuglia, M., Bellini, C., Grandjean, O., and Bouchez, D. (2002). The Arabidopsis *TONNEAU2* gene encodes a putative novel protein phosphatase 2A regulatory subunit essential for the control of the cortical cytoskeleton. Plant Cell 14, 833-345.

Carland, F.M., and McHale, N.A. (1996) *LOP1*: a gene involved in auxin transport and vascular patterning in Arabidopsis. Development 122, 1811-1819.

Catterou, M., Dubois, F., Schaller, H., Aubanelle, L., Vilcot, B., Sangwan-Norreel, B.S., and Sangwan, R.S. (2001b). Brassinosteroids, microtubules and cell elongation in Arabidopsis thaliana. II. Effects of brassinosteroids on microtubules and cell elongation in the bul1 mutant. Planta 212, 673-683.

Catterou, M., Dubois, F., Schaller, H., Aubanelle, L., Vilcot, B., Sangwan-Norreel, B.S., and Sangwan, R.S. (2001a). Brassinosteroids, microtubules and cell elongation in Arabidopsis thaliana. I. Molecular, cellular and physiological characterization of the

Arabidopsis bul1 mutant, defective in the Δ^7-sterol-C5-desaturation step leading to brassinosteroid biosynthesis. Planta 212, 659-672.

Cho, H.-T., and Kende, H. (1997). Expression of expansin genes is correlated with growth in deepwater rice. Plant Cell 9, 1661-1671.

Cosgrove, D.J. (1997). Relaxation in a high-stress environment: the molecular basis of extensible cell walls and enlargement. Plant Cell 9, 1031, 1041.

Cosgrove, D.J. (1999). Enzymes and other agents that enhance cell wall extensibility. Annu Rev Plant Physiol Plant Mol Biol 50, 391-417.

Cosgrove, D.J. (2000). New genes and new biological roles for expansins. Current Opinion in Plant Biology 3, 73-78.

Crozier, A., Kamiya, Y., Bishop, G., and Yokota, T. (2000). Biosynthesis of hormones and elicitor molecules. In Biochemistry and Molecular Biology of Plants, B.B. Buchanan, W. Gruissem, and R.L. Jones, eds (Rockville, MD: American Society of Plant Physiologists), pp. 850-929.

Cyr, R.J., and Palevitz, B.A. (1995). Organization of cortical microtubules in plant cells. Current Opinion in Cell Biology 7, 65-71.

Delmer, D.P. (1999). Cellulose biosynthesis: exciting times for a difficult field of study. Annu Rev Plant Physiol Plant Mol Biol 50, 245-276.

Desnos, T., Orbović, V., Bellini, C., Kronenberger, J., Caboche, M., Traas, J., and Höfte, H. (1996). *Procuste1* mutants identify two distinct genetic pathways controlling hypocotyl cell elongation, respectively in dark- and light-grown Arabidopsis seedlings. Development 122, 683-693.

Dhugga, K.S. (2001). Building the wall: genes and enzyme complex for polysaccharide synthases. Current Opinion in Plant Biology 4, 488-493.

Ellis, C., Karafyllidis, I., Wasternack, C., and Turner, J.G. (2002). The Arabidopsis mutant *cev1* links cell wall signaling to jasmonate and ethylene responses. Plant Cell 14, 1557-1566.

Emons, A.M.C. and Mulder, B.M. (1998). The making of the architecture of the plant cell wall: how cells exploit geometry. Proc Natl Acad Sci USA 95, 7215-7219.

Emons, A.M.C., Schel, J.H.N., and Mulder, B.M. (2002). The geometrical model for microfibril deposition and the influence of the cell wall matrix. Plant Biol 4, 22-26.

Fisher, D.D., and Cyr, R.J. (1998). Extending the microtubule/microfibril paradigm. Plant Physiol 116, 1043-1051.

Folkers, U., Kirik, V., Schöbinger, U., Falk, S., Krishnakumar, S., Pollock, M.A., Oppenheimer, D.G., Day, I., Reddy, A.R., Jürgens, G., and Hülskamp, M. (2002). The cell morphogenesis gene *ANGUSTIFOLIA* encodes a CtBP/BARS-like protein and is involved in the control of the microtubule cytoskeleton. EMBO J 21, 1280-1288.

Fridborg, I., Kuusk, S., Moritz, T., and Sundberg, E. (1999). The Arabidopsis dwarf mutant *shi* exhibits reduced gibberellin responses conferred by overexpression of a new putative zinc finger protein. Plant Cell 11, 1019-1031.

Furutani, I., Watanabe, Y., Prieto, R., Masukawa, M., Suzuki, K., Naoi, K., Thitamadee, S., Shikanai, T., and Hashimoto, T. (2000). The *SPIRAL* genes are required for directional control of cell elongation in Arabidopsis thaliana. Development 127, 4443-4453.

Giddings, T.H. Jr., and Staehelin, L.A. (1991). Microtubule-mediated control of microfibril deposition: a re-examination of the hypothesis. In The Cytoskeletal Basis of Plant Growth and Form. Edited by Lloyd C.W. London: Academic Press; 85-99.

Hartman, J.J., Mahr, J., McNally, K., Okawa, K., Iwamatsu, A., Thomas, S., Cheesman, S., Heuser, J., Vale, R.D., and McNally, F.J. (1998). Katanin, a microtubule-severing protein, is a novel AAA ATPase that targets to the centrosome using a WD40-containing subunit. Cell 93, 277-287.

Hasezawa, S., and Kumagai, F. (2002). Dynamic changes and the role of the cytoskeleton during the cell cycle in higher plant cells. International Rev Cytology 214, 161-191.

Hasezawa, S., and Nozaki, H. (1999). Role of cortical microtubules in the orientation of cellulose microfibril deposition in higher-plant cells. Protoplasma 209, 98-104.

Heath, I.B. (1974). A unified hypothesis for the role of membrane bound enzyme complexes and microtubules in plant cell wall synthesis. J Theor Biology 48, 445-449.

Hong, Z., Ueguchi-Tanaka, M., Shimizu-Sato, S., Inukai, Y., Fujioka, S., Shimada, Y., Takatsuto, S., Agetsuma, M., Yoshida, S., Wantanabe, Y., Uozu, S., Kitano, H., Ashikari, M., and Matsuoka, M. (2002). Loss-of-function of a rice brassinosteroid biosynthetic enzyme, C-6 oxidase, prevents the organized arrangement and polar elongation of cells in the leaves and stem. Plant Journal 32, 495-508.

Jacobsen, S.E., Binkowski, K.A., and Olszewski, N.E. (1996). SPINDLY, a tetratricopeptide repeat protein involved in gibberellin signal transduction in Arabidopsis. Proc Natl Acad Sci USA 93, 9292-9296.

Kende, H., and Zeevaart, A.D. (1997). The five “classical” plant hormones. Plant Cell 9, 1197-1210.

Kim, G.-T., Shoda, K., Tsuge, T., Cho, K.-H., Uchimiya, H., Yokoyama, R., Nishitani, K., and Tsukaya, H. (2002). The *ANGUSTIFOLIA* gene of Arabidopsis, a plant CtBP gene, regulates leaf-cell expansion, the arrangement of cortical microtubules in leaf cells and expression of a gene involved in cell-wall formation. EMBO J 21, 1267-1279.

Kirik, V., Grini, P.E., Mathur, J., Klinkhammer, I., Adler, K., Bechtold, N., Herzog, M., Bonneville, J.-M., and Hülskamp, M. (2002). The Arabidopsis *TUBULIN-FOLDING COFACTOR A* gene is involved in the control of the α/β-tubulin monomer balance. Plant Cell 14, 2265-2276.

Lee, Y., Choi, D., and Kende, H. (2001). Expansins: ever-expanding numbers and functions. Current Opinion in Plant Biology 4, 527-532.

Li, J., and Chory, J. (1999). Brassinosteroid actions in plants. Journal of Experimental Botany 50, 275-282.

Lloyd, C., and Chan, J. (2002). Helical microtubule arrays and spiral growth. Plant Cell 14, 2319-2324.

Lohret, T.A., Zhao, L., and Quarmby, L.M. (1999). Cloning of *Chlamydomonas* p60 katanin and localization to the site of outer doublet severing during deflagellation. Cell Motility and the Cytoskeleton 43, 221-231.

Martin, C., Bhatt, K., and Baumann, K. (2001). Shaping in plant cells. Current Opinion in Plant Biology 4, 540-549.

Mathur, J., and Chua, N.-H. (2000). Microtubule stabilization leads to growth reorientation in Arabidopsis trichomes. Plant Cell 12, 465-477.

Mathur, J., and Hülskamp, M. (2002). Microtubules and microfilaments in cell morphogenesis in higher plants. Current Biology 12, R669-R676.

McNally, F.J., and Vale, R.D. (1993). Identification of katanin, an ATPase that severs and disassembles stable microtubules. Cell 75, 419-429.

McNally, F.J., Okawa, K., Iwamatsu, A., and Vale, R.D. (1996). Katanin, the microtubule-severing ATPase, is concentrated at centrosomes. J Cell Science 109, 561-567.

McNally, K.P., Bazirgan, O.A., and McNally, F.J. (2000). Two domains of p80 katanin regulate microtubule severing and spindle pole targeting by p60 katanin. J Cell Science 113, 1623-1633.

McQueen-Mason, S., and Cosgrove, D.J. (1994). Disruption of hydrogen bonding between wall polymers by proteins that induce plant wall extension. Proc natl Acad Sci USA 91, 6574-6578.

McQueen-Mason, S., Durachko, D.M., Cosgrove, D.J. (1992). Two endogenous proteins that induce cell wall expansion in plants. Plant Cell 4, 1425-1433.

McQueen-Mason, S.J. (1995). Expansins and cell wall expansion. Journal of Experimental botany 46, 1639-1650.

Oppenheimer, D.G. (1998). Genetics of plant cell shape. Current Opinion in Plant Biology 1, 520-524.

Oppenheimer, D.G., Pollock, M.A., Vacik, J., Szymanski, D.B., Ericson, B., Feldman, K., and Marks, M.D. (1997). Essential role of a kinesin-like protein in Arabidopsis trichome morphogenesis. Proc Natl Acad Sci USA 94, 6261-6266.

Pagant, S., Bichet, A., Sugimoto, K., Lerouxel, O., Desprez, T., McCann, M., Lerouge, P., Vernhettes, S., and Höfte, H. (2002). *KOBITO1* encodes a novel plasma membrane protein necessary for normal synthesis of cellulose during cell expansion in Arabidopsis. Plant Cell 14, 2001-2013.

Pyke, K., and Lopez-Juez, E. (1999). Cellular differentiation and leaf morphogenesis in Arabidopsis. Critical Reviews in Plant Sciences 18, 527-546.

Qiu, J.-L., Jilk, R., Marks, M.D., and Szymanski, D.B. (2002). The Arabidopsis *SPIKE1* gene is required for normal cell shape control and tissue development. Plant Cell 14, 101-118.

Quarmby, L.M., and Lohret, T.A. (1999). Microtubule severing. Cell Motility and the Cytoskeleton 43, 1-9.

Reinhardt, D., Wittwer, F., Mandel, T., Kuhlemeier, C. (1998). Localized upregulation of a new expansin gene predicts the site of leaf formation in the tomato meristem. Plant Cell 10, 1427-1437.

Richmond, T. (2000). Higher plant cellulose synthases. Genome Biology 1, reviews3001.1-3001.6.

Richmond, T.A., and Somerville, C.R. (2000). The cellulose synthase superfamily. Plant Physiol 124, 495-498.

Roudier, F., Schindelman, G., DeSalle, R., and Benfey, P.N. (2002). The COBRA family of putative GPI-anchored proteins in Arabidopsis. A new fellowship in expansion. Plant Physiol 130, 538-548.

Sato, S., Kato, T., Kakagawa, K., Ishii, T., Liu, Y.-G., Awano, T., Takabe, K., Nishiyama, Y., Kuga, S., Sato., S., Nakamura, Y., Tabata, S., and Shibata, D. (2001). Role of the putative membrane-bound endo-1,4-β-glucanase KORRIGAN in cell elongation and cellulose synthesis in Arabidopsis thaliana. Plant Cell Physiol 42, 251-263.

Scanlon, M.J. (2000). Developmental complexities of simple leaves. Current Opinion in Plant Biology 3, 31-36.

Scheible, W.-R., Eshed, R., Richmond, T., Delmer, D., and Somerville, C. (2001). Modifications of cellulose synthase confer resistance to isoxaben and thiazolidinone herbicides in Arabidopsis *Ixr1* mutants. Proc Natl Acad Sci USA 98, 10079-10084.

Schneider, B., and Herth, W. (1986). Distribution of plasma membrane rosettes and kinetics of cellulose formation in xylem development of higher plants. Protoplasma 131, 142,-152.

Schopfer, P., Liszkay, A., Bechtold, M., Frahry, G., and Wagner, A. (2002). Evidence that hydroxyl radicals mediate auxin-induced extension growth. Planta 214, 821-828.

Schumacher K., and Chory, J. (2000). Brassinosteroid signal transduction: still casting the actors. Current Opinion in Plant Biology 3, 79-84.

Shibaoka, H. (1994). Plant hormone-induced changes in the orientation of cortical microtubules: alterations in the cross-linking between microtubules and the plasma membrane. Annu Rev Plant Physiol Plant Mol Biol 45, 527-544.

Smith, L.G. (2003). Cytoskeletal control of plant cell shape: getting the fine points. Current Opinion in Plant Biology 6, 63-73.

Smith, L.G., Gerttula, S.M., Han, S., and Levy, J. (2001). TANGLED1: A microtubule binding protein required for the spatial control of cytokinesis in maize. Journal of Cell Biology 152, 231-236.

Song, H., Golovkin, M., Reddy, A.S.N., and Endow, S.A. (1997). In vitro motility of AtKCBP, a calmodulin-binding kinesin protein of Arabidopsis. Proc Natl Acad Sci USA 94, 322-327.

Srayko, M., Buster, D.W., Bazirgan, O.A., McNally, F.J., and Mains, P.E. (2000). MEI-1/MEI-2 katanin-like microtubule severing activity is required for Caenorhabditis elegans meiosis. Genes Development 14, 1072-1084.

Stoppin-Mellet, V., Gaillard, J., and Vantard, M. (2002). Functional evidence for in vitro microtubule severing by the plant katanin homologue. Biochem J 365, 337-342.

Sugimoto, K., Williamson, R.E., and Wasteneys, G.O. (2001). Wall architecture in the cellulose-deficient *rsw1* mutant of *Arabidopsis thaliana*: microfibrils but not microtubules lose their transverse alignment before microfibrils become unrecognizable in the mitotic and elongation zones of roots. Protoplasma 215, 172-183.

Szymanski, D.B. (2001). Arabidopsis trichome morphogenesis: a genetic approach to studying cytoskeletal function. J Plant Growth Regul 20, 131-140.

Taylor, N.G., Howells, R.M., Huttly, A.K., Vickers, K., and Turner, S.R. (2003). Interactions among three distinct CesA proteins essential for cellulose synthesis. PNAS 100, 1450-1455.

Taylor, N.G., Scheible, W.-R., Cutler, S., Somerville, C.R., and Turner, S.R. (1999). The irregular *xylem3* locus of Arabidopsis encodes a cellulose synthase required for secondary cell wall synthesis. Plant Cell 11, 769-779.

Thitamadee, S., Tuchihara, K., and Hashimoto, T. (2002). Microtubule basis for left-handed helical growth in Arabidopsis. Nature 417, 193-196.

Vale, R.D. (1991). Severing of stable microtubules by a mitotically activated protein in Xenopus egg extracts. Cell 64, 827-839.

Van Volkenburgh, E. (1999). Leaf expansion-an integrating plant behaviour. Plant, Cell and Environment 22, 1463-1473.

Wasteneys, G.O. (2000). The cytoskeleton and growth polarity. Current Opinion in Plant Biology 3, 503-511.

Webb, M., Jouannic, S., Foreman, J., Linstead, P., and Dolan, L. (2002). Cell specification in the Arabidopsis root epidermis requires the activity of ECTOPIC ROOT HAIR 3-a katanin-p60 protein. Development 129, 123-131.

Whittington, A.T., Vugrek, O., Wei, K.J., hasenbein, N.G., Sugimoto, K., Rashbrooke, M.C., and Wasteneys, G.O. (2001). MOR1 is essential for organizing cortical microtubules in plants. Nature 411, 610-613.

Williamson, R.E., Burn, J.E., and Hocart, C.H. (2002). Toward the mechanism of cellulose synthesis. Trends in Plant Science 7, 461-467.

Williamson, R.E., Burn, J.E., Birch, R., Baskin, T.I., Arioli, T., Betzner, A.S., and Cork, A. (2001). Morphology of *rsw1*, a cellulose-deficient mutant of Arabidopsis thaliana. Protoplasma 215, 116-127.

Zhong, R., Burk, D.H., Morrison, W.H., and Ye, Z.-H. (2002). A kinesin-like protein is essential for oriented deposition of cellulose microfibrils and cell wall strength. Plant Cell 14, 3101-3117.

Zuo, J., Niu, Q.-W., Nishizawa, n., Wu, Y., Kost, B., and Chua, N.-H. (2000). KORRIGAN, an Arabidopsis endo-1,4-β-glucanase, localizes to the cell plate by polarized targeting and is essential for cytokinesis. Plant Cell 12, 1137-115

CHAPTER 2

A KATANIN-LIKE PROTEIN REGULATES NORMAL CELL WALL BIOSYNTHESIS AND CELL ELONGATION[1]

[1]Burk, D.H., Liu, B., Zhong, R., Morrison, W.H., and Ye, Z.-H. 2001. *Plant Cell*. 13:807-827. Reprinted here with permission of the American Society of Plant Biologists.

ABSTRACT

Fibers are one of the mechanical tissues that provide structural support to the plant body. To understand how the normal mechanical strength of fibers is regulated, we isolated an Arabidopsis fragile fiber (*fra2*) mutant defective in the mechanical strength of interfascicular fibers in the inflorescence stems. Anatomical and chemical analyses showed that the *fra2* mutation caused a reduction in fiber cell length and wall thickness, a decrease in cellulose and hemicellulose contents, and an increase in lignin condensation, indicating that the fragile fiber phenotype of *fra2* is a result of alterations in fiber cell elongation and cell wall biosynthesis. In addition to the effects on fibers, the fra2 mutation resulted in a remarkable reduction in cell length and an increase in cell width in all organs, which led to a global alteration in plant morphology. The *FRA2* gene was shown to encode a protein with high similarity to katanin (hence *FRA2* was renamed as *AtKTN1*), a protein shown to be involved in regulating microtubule disassembly by severing microtubules. Consistent with the putative function of AtKTN1 as a microtubule-severing protein, immunolocalization demonstrated that the *fra2* mutation caused delays in the disappearance of perinuclear microtubule array and in the establishment of transverse cortical microtubule array in interphase and elongating cells. Together, these results suggest that AtKTN1, a katanin-like protein, is essential not only for normal cell wall biosynthesis and cell elongation in fiber cells but also for cell expansion in all organs.

INTRODUCTION

The plant cell wall, as an exocytoskeleton, provides structural support to the cells and to the entire plant body. Plant cells can be grouped, according to their wall thickening, into three basic types: parenchyma, collenchyma, and sclerenchyma. Both parenchyma and collenchyma cells, consisting of the primary wall, provide the main structural support in growing regions of the plant body. Sclerenchyma cells, having both primary wall and thick secondary wall, provide the major mechanical support in nonelongating regions of the plant body (Carpita and McCann, 2000). The molecular mechanisms that control the deposition of cell wall materials and that determine cell wall mechanical strength are not yet known.

Because cell walls delimit the boundaries of individual cells, the shapes of individual cell walls determine cell morphology and whole plant morphology. Thus, understanding of how cells make walls will help us to discover the molecular mechanisms that control cell morphology. The essential roles of cell walls in regulating cell morphology and cell elongation have been demonstrated in mutants defective in genes involved in cell wall biosynthesis or modification. It has been shown that disruption of crystalline cellulose biosynthesis in the *rsw1* mutant results in a swollen cell phenotype, indicating the direct role of cellulose in maintaining cell morphology (Arioli et al., 1998). The importance of normal cell wall biosynthesis or modification in regulating cell elongation has been demonstrated by the *kor* mutants defective in a gene encoding endo-1,4-β-glucanase (Nicol et al., 1998; Zuo et al., 2000). The *kor1* mutation causes abnormal cell wall structure and aberrant cell plate formation. Cells in the *kor1* mutants could not elongate normally, resulting in an extremely dwarf phenotype. This finding suggests that proper modification of cell wall materials during cytokinesis and cell expansion is essential for normal cell morphology.

Because cellulose microfibrils must be oriented properly for directional cell expansion, it is obvious that cellulose microfibril deposition must be regulated by cellular machinery. Several lines of evidence have shown that the cytoskeletal microtubules regulate exoskeletal cellulose microfibril orientation (Giddings and Staehelin, 1991; Baskin, 2000). First, cortical microtubule arrays are aligned inside the plasma membrane parallel with newly synthesized cellulose microfibrils, both of which are oriented transversely to the axis of cell elongation. Second, pharmacological studies have proven the direct role of microtubules in determining cellulose microfibril orientation and cell elongation. Disruption of microtubule orientation in parenchyma cells with colchicin, a microtubule-destabilizing drug, effectively disrupts the orientation of cellulose microfibrils and changes the direction of cell expansion. Based on these observations, it has long been accepted that microtubules direct the orientation of cellulose microfibrils, which controls cell elongation. However, it is not known whether microtubules influence cell wall biosynthesis (Seagull and Falconer, 1991).

Fibers have traditionally been used as a model for the study of cell differentiation, cell elongation, and cell wall biosynthesis (Aloni, 1987). Fiber initial cells typically undergo considerable elongation at both ends. For example, in *Boehmeria nivea*, fiber initials approximately 20 μm long can elongate up to 550 mm. At maturity, a massive amount of secondary wall is laid down inside the primary wall, which enables fiber cells to function as an excellent mechanical tissue (Mauseth, 1988). Therefore, fiber cells are a remarkable example of the coordinated regulation of cell elongation and cell wall biosynthesis. It is conceivable that studying the mechanisms that control fiber formation will help us understand the mechanisms that regulate cell elongation and cell wall biosynthesis in general.

In this article, we describe the characterization of the Arabidopsis *fra2* mutant with a defect in fiber strength and the molecular cloning of the *FRA2* gene. We show that

the reduction in the mechanical strength of fibers in *fra2* inflorescence stems is associated with alterations of fiber cell elongation and cell wall biosynthesis. We present evidence that the *fra2* mutation not only alters fiber cell elongation but also changes cell expansion in all organs, thereby leading to a global alteration in plant morphology. We demonstrate that the *FRA2* gene encodes a protein with high similarity to katanin that is involved in severing microtubules. Our results provide direct evidence that a katanin-like protein is essential for cell wall biosynthesis and cell elongation.

RESULTS

ISOLATION OF THE *FRA2* MUTANT WITH A DEFECT IN THE MECHANICAL STRENGTH OF FIBERS

Our previous work has shown that the mechanical strength of the inflorescence stems of Arabidopsis is conferred mainly by interfascicular fibers. Elimination of interfascicular fibers, as in the *ifl1* mutants, dramatically reduces the breaking strength of the inflorescence stems, which results in a pendent shoot phenotype (Zhong et al., 1997; Zhong and Ye, 1999). To further investigate the mechanisms controlling fiber differentiation and fiber mechanical strength, we screened ethyl methanesulfonate–mutagenized Arabidopsis populations for mutants with reduced normal mechanical strength in the inflorescence stems. We found several mutants with a dramatic reduction in the breaking strength of the inflorescence stems. One of them was chosen for this study because of its alteration in cell elongation. Quantitative analysis showed that the force required to break the mutant stems was twofold to threefold less than that for the wild-type stems (Figure 2.1). The mutant stems (Figure 2.2B) developed interfascicular fiber cells like those in the wild type (Figure 2.2A), indicating that the reduction in the breaking strength of mutant stems was due to an alteration in the

mechanical strength of fibers rather than an absence of interfascicular fibers. Thus, we designated the mutant locus as the *fra2* (fragile fiber) locus.

ANATOMICAL EXAMINATION OF FIBER MORPHOLOGY

Reduction in the mechanical strength of fibers could result from alterations in cell wall composition, cell wall structure, fiber cell length, or adhesion of fiber cells. To investigate which specific alterations occurred in the *fra2* fibers, we first examined fiber cell length and fiber cell wall thickness. Longitudinal sections of mature inflorescence stems showed a dramatic alteration in fiber cell length in *fra2* (Figure 2.2). In the wild type, fiber cells were narrow and long with two tapered ends (Figure 2.2C). However, fiber cells in *fra2* (Figure 2.2D) were much shorter than those in the wild type. Furthermore, fiber cell walls in *fra2* (Figure 2.2A, inset) appeared to be much thinner than those in the wild type (Figure 2.2B, inset). These results indicate that the *fra2* mutant is defective in both fiber cell elongation and fiber cell wall thickening, which most likely contributes to the reduction in the mechanical strength of *fra2* fibers.

CHEMICAL ANALYSIS OF CELL WALL COMPOSITION

The finding that the *fra2* mutation caused reduced thickness of the fiber cell wall prompted us to investigate whether it caused any alterations in cell wall biosynthesis. Analysis of crystalline cellulose in stems showed that the amount of cellulose in *fra2* stems was reduced to 80% of that in the wild type (Table 1). The reduction of cellulose level in the *fra2* mutant was further demonstrated by sugar composition analysis of stem cell walls. Glucose levels were reduced by 24% in fra2 compared with the wild type (Table 2.1). Intriguingly, the amounts of other sugars such as xylose, arabinose, and rhamnose were also decreased significantly. However, the *fra2* mutation did not affect the levels of sugars such as mannose and galactose. Because glucose and xylose are the

two sugars that constitute cellulose and hemicellulose, respectively, in the secondary cell wall, the *fra2* mutation caused a reduction in cellulose and hemicellulose in fibers.

Table 2.1 Sugar Composition of Stems of the Wild Type and the *fra2* Mutant (mg/g)

Sample	Rhamnose	Arabinose	Xylose	Mannose	Galactose	Glucose	Fucose	Cellulose
Wild type[a]	5.0 ± 0.7 (100%)	17.2 ± 1.6 (100%)	149.7 ± 15.6 (100%)	14.6 ± 1.2 (100%)	12.8 ± 0.7 (100%)	186.7 ± 9.7 (100%)	1.7 ± 0.5 (100%)	230 ± 7 (100%)
fra2[b]	3.9 ± 0.5 (78%)	11.5 ± 2.1 (68%)	105.5 ± 15.5 (70%)	13.9 ± 1.9 (90%)	13.0 ± 1.2 (102%)	141.7 ± 4.7 (76%)	1.8 ± 0.2 (106%)	184 ± 5 (80%)

[a] Data in parentheses are the sugar contents in the wild type taken as 100.
[b] Data in parentheses are the sugar contents in *fra2* expressed as a percentage of that in the wild type.

Lignin is another main component in the secondary cell wall in addition to cellulose and hemicellulose. Because the *fra2* mutation resulted in reductions in both cellulose and hemicellulose, we investigated whether it caused any changes in lignin content or structure. Analysis of Klason lignin showed a slight decrease in lignin content (Table 2.2). Surprisingly, the levels of base-extractable guaiacyl and syringyl lignin units in *fra2* were decreased 58 and 35%, respectively, compared with the levels in the wild type (Table 2.2). Because guaiacyl and syringyl lignin units in *fra2* are much less extractable by base than those in the wild type, this finding indicates that lignin in *fra2* is much more condensed than that in the wild type.

IN-SOURCE PYROLYSIS MASS SPECTROMETRY OF CELL WALLS

To confirm the results from the chemical analysis, we applied in-source pyrolysis mass spectrometry to examine the relative levels of different cell wall materials. The results showed that the relative intensities of the mass markers for cellulose, hemicellulose, and lignin were altered significantly, with the carbohydrate markers making a greater contribution to the spectrum of *fra2* (Figure 2.3B) than to the spectrum of the wild type (Figure 2.3A). Examination of the mass markers for dimeric lignin (van der Hage et al., 1993) showed that the mass spectrum of *fra2* cell walls exhibited a higher proportion of these markers than that of the wild type (Figures 2.3A and 2.3B, insets), suggesting that the lignin in *fra2* is more thermal stable than that in the wild type. This is consistent with

the results from the chemical analysis indicating that lignin in *fra2* is more condensed than that in the wild type.

Table 2.2. Lignin Content and Composition in the Wild Type and the *fra2* Mutant

	Klason Lignin[a]		Lignin Composition (mg/g Cell Wall)[b]		
Plant	% of Cell Wall[c]	% of Wild-Type Klason Lignin	Guaiacyl Lignin[c]	Syringyl Lignin[c]	S/G[d]
Wild type	15.8 ± 0.4	100	34.0 ± 0.3 (100%)	15.6 ± 1.4 (100%)	0.46
fra2	14.4 ± 0.6	91	14.2 ± 4.2 (42%)	10.2 ± 3.6 (65%)	0.72

[a] Klason lignin was assayed according to Kirk and Obst (1988).
[b] Lignin monolignol composition was analyzed according to Akin et al. (1993).
[c] Each data point is the mean ±SE of two separate assays. Data in parentheses are guaiacyl or syringyl lignin units taken as either 100 in the wild type or a percentage of the wild type in *fra2*.
[d] G (guaiacyl) is the sum of vanillin, acetovanillin, and vanillic acid; S (syringyl) is the sum of syringaldehyde, acetosyringaldehyde, and syringic acid.

PLANT MORPHOLOGY

In addition to the defects in fiber cell elongation and cell wall biosynthesis, the *fra2* mutant exhibited a dramatic alteration in plant morphology (Figure 2.4A). The height of mature inflorescence stems in *fra2* reached only ~50% of the height of the wild type (Table 2.3). Measurement of internode number and length showed no change in internode number but a dramatic reduction in internode length (Figures 2.4B and 2.4C; Table 2.3), indicating that the decrease in plant height in *fra2* was caused by a reduction in internode length.

It was noted that the length of all other organs was reduced in *fra2*. The leaves of *fra2* plants were much shorter than those of the wild type (Figures 2.4G and 2.4I), which resulted in more compact rosette leaves compared with the wild type (Figures 2.4F and 2.4H). The length of leaf blades and petioles of *fra2* plants was reduced to 70 and 40%, respectively, of those in the wild type (Figures 2.5A and 2.5C). However, the width of *fra2* leaf blades did not show significant changes (Figure 2.5B).

Table 2.3. Morphology of Inflorescence Stems and Trichomes of the Wild Type and the *fra2* Mutant

Morphology	Wild Type	*fra2*
Main inflorescence stem[a]		
Height (cm)	27.2 ± 3.3	13.6 ± 1.5
Diameter (mm)[b]	1.7 ± 0.4	2.5 ± 0.4
Cauline branch number	7.3 ± 1.8	6.9 ± 1.8
Internode length (mm)		
First internode	16.5 ± 10.2	5.0 ± 4.8
Second internode	20.2 ± 7.3	4.8 ± 4.1
Third internode	22.1 ± 9.7	6.4 ± 2.5
Trichome branch points (%)[c]		
No points	0.11	7.5
One point	2.41	64.9
Two points	79.7	25.6
Three points	17.8	1.9

[a] Data are mean values ±SE from 10 (wild type) or 20 (*fra2*) plants.
[b] The first internode was used for measurements of the stem diameter.
[c] A total of 1000 trichomes on rosette leaves were counted. The nomenclature of trichome branch points is according to Luo and Oppenheimer (1999).

The length of floral organs was also reduced significantly in the *fra2* mutant. Quantitative examination showed that the length of all four floral organs in *fra2*—including sepal, petal, stamen filament, and carpel—was reduced to 50 to 80% of those of the wild type (Figure 2.6A). However, the width of all four floral organs in *fra2* plants was increased 30 to 40% over wild-type values (Figure 2.6B). The siliques and pedicels were also much shorter than those in the wild type (Figures 2.4D and 2.4E). Quantitative measurements showed that the length of siliques and pedicels of *fra2* mutants was reduced to 30 to 80%, respectively, of those in the wild type (Figures 2.6C and 2.6D). The reduction in organ length was also obvious in young seedlings. One-week-old *fra2* seedlings had much shorter hypocotyls and roots than wild-type seedlings (Figures 2.7A and 2.7D). Together, these results demonstrate that the *fra2* mutation causes a common phenotype: reduction in organ length.

SCANNING ELECTRON MICROSCOPY OF THE MORPHOLOGY OF CELLS AND ORGANS

To investigate whether the reduction in organ length resulted from a reduction in cell length, we examined epidermal cell lengths of different organs. Scanning electron microscopy revealed a significant reduction in the length of epidermal cells of hypocotyls

(Figures 2.7C and 2.7F) and carpels (Figures 2.7I and 2.7L) in *fra2* compared with the wild type. Root hair cells in *fra2* appeared to be more compact than those in the wild type (Figures 2.7B and 2.7E), due to shortening of root epidermal cells. The shapes of epidermal cells in *fra2* leaves were also altered. Ordinary epidermal cells in wild-type leaves exhibited rather convoluted shapes (Figure 2.7H), whereas many of those in *fra2* leaves became tubular in shape with little convolution (Figure 2.7K). Furthermore, most trichomes on *fra2* leaves had one branch point instead of two branch points, as seen in the wild type (Figures 2.7J and 2.7G; Table 2.3). These results indicate that the *fra2* mutation disrupts the normal cell expansion process, which leads to alterations in cell and organ morphology.

Anatomical Examination of Cellular Morphology in Different Organs

To ascertain whether the *fra2* mutation affected the morphology of other cells in addition to fibers and epidermis, we examined the cellular morphology in both transverse and longitudinal sections of *fra2* organs. In inflorescence stems, both epidermal cells and cortical cells beyond the interfascicular regions were much shorter but wider in *fra2* (Figure 2.2D) than those in the wild type (Figure 2.2C). Similar changes were seen in the epidermis and cortex beyond the fascicular regions (Figures 2.8A and 2.8B). It was interesting to note that the tracheary elements in *fra2* also were distorted in shape (Figure 2.8B) compared with the long, straight columns seen in the wild type (Figure 2.8A). The most visible changes occurred in pith. In contrast to the pith cells in the wild type, which were long and tubular and arranged in regular files (Figure 2.8C), pith cells in *fra2* were short and wide and exhibited irregular cell files (Figure 2.8D). It was evident that the appearance of some randomly arranged pith cells resulted from irregular placement of cell division planes (Figure 2.8D), a phenotype similar to that of the *tangled1* mutant, in which leaf cell divisions are oriented nearly randomly (Smith et al., 1996; Cleary and Smith, 1998). The number of pith cells from one vascular bundle to another in a cross-

section remained the same as in the wild type. Therefore, the increase in the width of pith cells apparently accounted for the increase of the stem diameter in *fra2* (Table 2.3).

Examination of sections from leaves, hypocotyls, and roots also showed a reduction in cell length. In cross-sections of leaf blades, columnar palisade cells became shorter and less regular in shape in *fra2* (Figure 2.8F) than in the wild type (Figure 2.8E). It was also obvious that some epidermal cells in *fra2* (Figure 2.8F) were much wider than those in the wild type (Figure 2.8E), which most likely corresponded to the long, tubular cells revealed by electron scanning microscopy (Figure 2.7K). The most noticeable change was seen in the spongy mesophyll region. The spongy mesophyll cells in wild-type leaves were typically loosely distributed, leaving large air spaces between them (Figure 2.8E), whereas those in the *fra2* mutant were closely packed with little space between. It was apparent that the spongy mesophyll cells in *fra2* were much larger than those in the wild type, thus filling the arenchymatous spaces.

In leaf petioles, the parenchyma cells in *fra2* (Figure 2.8J) were enlarged radially but shortened longitudinally compared with the wild type (Figure 2.8I). It was also noted that cells in the wild type were arranged in regular files, whereas some cells in *fra2* were placed irregularly. The alteration in the cell file pattern in *fra2* appeared to be caused by irregular orientation of cell division planes, which was similar to what occurred in pith cells (Figure 2.8D). Significant reduction in cell length was also evident in the cortical cells of *fra2* hypocotyls (Figures 2.8G and 2.8H). Together, the anatomical examination of cell morphology in different organs clearly demonstrated that the *fra2* mutation causes reduced cell length but increased cell width in all organs. It also indicated that the *fra2* mutation might cause an irregular placement of cell division planes in some of the parenchyma cells of pith and petioles.

POSITIONAL CLONING OF THE *FRA2* GENE

The phenotypic characterization of the *fra2* mutant clearly showed its main defects in cell wall biosynthesis and cell elongation. Because the molecular mechanisms that control cell wall biosynthesis and cell elongation are still poorly understood, the isolation of genes such as *FRA2* will be instrumental in dissecting the molecular control of these processes. We used a positional cloning approach to isolate the *FRA2* gene. We first determined whether the *fra2* mutation was monogenic and recessive. All F1 plants that resulted from the cross of *fra2* and wild-type Columbia exhibited wild-type phenotypes, indicating that the *fra2* mutation was recessive. In a population of 210 F2 plants from the cross, 159 plants exhibited wild-type phenotypes and 51 plants showed *fra2* mutant phenotypes. This gave a segregation ratio of 3:1 ($\chi^2 = 0.1$, $P > 50\%$), indicating that the *fra2* mutation was monogenic.

To map the *fra2* locus, *fra2* mutants in a Columbia background were crossed with wild-type Landsberg *erecta*. The F2 plants that resulted from the cross were screened for the *fra2* mutant phenotype and used for mapping. Codominant amplified polymorphic sequence (CAPS) markers were used to map the *fra2* locus to an individual chromosome. When CAPS markers from chromosomes 2 to 5 were used for mapping, no linkages between those markers and *fra2* were found, indicating that the *fra2* mutation did not occur on these chromosomes. When the CAPS marker ADH (Konieczny and Ausubel, 1993) from chromosome 1 was used, a close linkage was found between ADH and *fra2*. Of 538 F2 mutant plants used for mapping, 43 had crossovers between ADH and *fra2*, which placed the *fra2* locus 4.0 centimorgan (cM) away from ADH (Figure 9). To determine on which side of ADH the *fra2* locus was located, we used markers located on both sides of ADH for further mapping. Use of the CAPS marker g11447, which is located to the left of ADH, and marker g17311, which is located to the right of ADH, gave results that suggested that the *fra2* locus was located between ADH and g17311

(Figure 2.9). Of 192 F2 mutant plants used for mapping, 4 plants had crossovers between g17311 and *fra2*, which placed *fra2* 1.0 cM away from g17311. Further mapping with GL2 showed 4 crossovers out of 444 plants used for mapping. Because these four plants showing crossovers with GL2 also had crossovers with ADH but not with g17311, *fra2* appeared to be located 0.5 cM away on the right side of GL2 (Figure 2.9).

Having mapped the *fra2* locus to a small region between GL2 and g17311, we searched the Arabidopsis database and located three overlapping bacterial artificial chromosome (BAC) clones (F19K16, F18B13, and F5I6) covering a 230-kb region between GL2 and g17311 (Figure 9). All three of these BAC clones had been sequenced by the Arabidopsis sequencing project, and putative genes had been annotated. This allowed us to tentatively select and test possible candidates responsible for the *fra2* mutant phenotypes. Because FRA2 was a global regulator of cell wall biosynthesis and cell expansion, we reasoned that FRA2 candidates most likely could be cell wall–modifying enzymes, proteins involved in cytoskeletal regulation, or transcription factors. Of 57 putative genes within these three BAC clones, 4 genes fell into these categories. These putative genes showed high sequence similarities to microtubule-severing proteins, cyclins, auxin responsive proteins, or ring finger proteins. Considering the known roles of microtubules in directing the deposition of cell wall materials, the most likely candidate lay in the F5I6.10 gene encoding a putative microtubule-severing protein located between nucleotide residues 33019 and 35570 in BAC clone F5I6. Sequencing of this gene in the *fra2* mutant identified a deletion mutation that occurred at nucleotide residue 33241 of F5I6 (Figure 2.10A), suggesting that the gene encoding the putative microtubule-severing protein most likely represents the *FRA2* gene. This was confirmed by complementation analysis showing that the wild-type DNA fragment covering this gene (Figure 2.10A) was able to rescue the *fra2* mutant phenotypes when it was transferred into the *fra2* mutant (data not shown).

SEQUENCE ANALYSIS OF THE *FRA2* GENE

To confirm the predicted exons and introns of the *FRA2* gene as shown in the annotation of BAC clone F5I6, we isolated and sequenced the full length *FRA2* cDNA fragment. The longest open reading frame was 1572 nucleotides in length, encoding a polypeptide of 523 amino acids with a predicted molecular mass of 57 kD. Comparison of the *FRA2* gene and its cDNA identified seven exons and six introns in the gene sequence. The *fra2* mutation occurred in the seventh exon, in which the A at nucleotide residue 2329 was deleted (Figure 2.10A). This resulted in a frameshift of the coding sequence, which led to the creation of a premature stop codon in the *fra2* cDNA (Figure 2.10B). The mutant *fra2* protein lacked 78 amino acids at the C-terminal region. The deletion mutation in *fra2* was further confirmed by sequencing of the *fra2* cDNA and by detection of a polymorphism between the wild-type and mutant *fra2* cDNAs (Figure 2.10C).

Sequence comparison of FRA2 with proteins in the GenBank database revealed a high sequence similarity to a group of microtubule-severing proteins called katanins. FRA2 exhibited the highest amino acid sequence identity (43% identity and 56% similarity in the entire open reading frame) to sea urchin katanin (Figure 2.11), which was the first katanin cDNA isolated and confirmed to have microtubule-severing activity (Hartman et al., 1998). The highest sequence similarity (62% identity and 75% similarity) was seen in the putative ATP binding module between amino acid residues 236 and 454 of *fra2*. The amino acid sequence of *fra2* at the N-terminal region before the ATP binding module had 26% sequence identity (38% similarity) with sea urchin katanin. No significant amino acid sequence similarity was found between FRA2 and other proteins except katanins. These analyses strongly suggest that *FRA2*, a gene regulating cell wall biosynthesis and cell expansion, encodes a katanin-like protein. Hence *FRA2* was renamed as *AtKTN1*.

Examination of *AtKTN1* expression patterns showed that the *AtKTN1* gene was expressed in all organs examined, including stems, leaves, flowers, and roots (Figure 2.12). This is consistent with the *fra2* phenotypes of alterations in cell elongation in all organs.

MICROTUBULE ORGANIZATION IN *FRA2* CELLS

The finding that the *AtKTN1* gene encodes a katanin-like protein prompted us to examine microtubule organization in the *fra2* cells because microtubules are essential for cell morphogenesis. In wild-type root tip cells, a cortical array of parallel microtubules was always detected in interphase cells (Figure 2.13A). Microtubules were not detected when we focused away from the cell cortex (Figure 2.13B). In the *fra2* mutant, abnormal microtubule distribution was detected in flat cells which were considered to be cells exited from cell division recently (Figures 2.13C to 2.13F). In these cells, microtubules started to appear at the cell cortex in a converged pattern (Figures 2.13C and 2.13E). However, on the nuclear envelope, microtubule converging points could be clearly detected (Figures 2.13D and 2.13F). Such converging points clearly accounted for aster-like microtubule organization pattern towards cell cortex (Figure 2.13E). Such a microtubule configuration has never been detected in interphase cells among higher plants. In most of the elongating cells, the microtubule converging pattern could no longer be detected on the nuclear envelope, and microtubules gradually organized into parallel pattern in the cell cortex (Figures 2.13G and 2.13H). However, some elongating cells (Figures 2.13G and 2.13H) still remain having the microtubule converging pattern, indicating that disappearance of the microtubule aggregation points during cell elongation was not synchronous. In wild type cells undergoing elongation, cortical microtubules retained a parallel pattern mostly perpendicular to the growth axis (Figure 2.13I). Although the *fra2* cells had very limited elongation activity, cortical microtubules gradually became parallel to the growth axis (Figures 2.13J and 2.13K). In the *fra2* cells

which had become highly vacuolated (Figure 2.13L), typical cortical microtubules could still be visualized.

Because mammalian katanin is largely responsible for microtubule severing during mitosis or meiosis (McNally and Thomas, 1998; Srayko et al., 2000), we investigated whether abnormal microtubule organization could be detected when *fra2* cells undergo cell division. In somatic cells, a cortical microtubule band, the preprophase band is present during late G2 phase to prophase to predict the future division plane. Both wild-type and *fra2* had clear preprophase bands starting in a broad ring in the cell cortex (Figures 2.14A to 2.14D). During later stages, narrower microtubule bands could be detected in both wild-type and mutant cells (data not shown). Before the nuclear envelope breaks down, the preprophase band microtubules are depolymerized while spindle microtubules get organized. We detected normal metaphase spindles in wild-type and *fra2* mutant (Figures 2.14E and 2.14F). Spindle microtubules undergo rapid reorganization (both depolymerization and polymerization) during anaphase. Concomitant with the reorganization of spindle microtubules, sister chromatids are separated. In both wild-type and *fra2*, cells at late anaphase presented a similar microtubule configuration with microtubules starting to accumulate in the central spindle (Figures 2.14G and 2.14H). Following the nuclear division, the phragmoplast, which contains two sets of anti-parallel microtubules oriented perpendicular to the cell plate, is formed to guide vesicles bound for the division site to give rise to the new plasma membrane and the new cell wall. During the centrifugal expansion of cell plate, the phragmoplast microtubules depolymerize centrifugally as well. Identical phragmoplast microtubules arrays were found in a wild-type cell (Figure 2.14I) and a *fra2* cell (Figure 2.14J). Therefore, our data indicate that in the *fra2* cells microtubule reorganization during mitosis and cytokinesis is not affected.

DISCUSSION

It has long been accepted that cortical microtubule arrays regulate cellulose microfibril orientation. Cortical microtubules undergo dynamic rearrangement in direction during different stages of cell expansion and differentiation. Cellulose microfibril orientation accompanies the dynamic alterations of cortical microtubules, thereby regulating the direction of cell expansion. A variety of mechanisms have been proposed as regulators of the dynamic changes of cortical microtubules in plants, such as assembly and disassembly and microtubule translocation (Cyr and Palevitz, 1995). Our finding that a katanin-like protein is essential for cell wall biosynthesis and cell elongation suggests that microtubule-severing proteins also might contribute to the dynamic changes of cortical microtubule arrays.

THE *AtKTN1* GENE ENCODES A KATANIN-LIKE PROTEIN

Katanin, a microtubule-severing protein, couples ATP hydrolysis to disassemble microtubules into tubulin subunits. The microtubule-severing activity was first identified in the mitotic extracts of *Xenopus laevis* eggs (Vale, 1991). Biochemical characterization of katanin from sea urchin oocytes has shown that katanin is a heterodimer of 60- and 80-kD subunits and requires ATP hydrolysis for its microtubule-severing activity (McNally and Vale, 1993). Subsequently, the genes encoding the 60- and 80-kD subunits were cloned from sea urchin (Hartman et al., 1998). The katanin 60-kD subunit was found to be a novel member of the AAA (ATPase associated with diverse cellular activity) family of ATPases. The 60-kD subunit alone possesses both microtubule-stimulating ATPase activity and microtubule-severing activity. The katanin 80-kD subunit contains WD40 repeats and is suggested to target katanin to the centrosome. Katanins have been localized to the centrosome in interphase cells and to the spindle poles in sea urchin, *X. laevis*, and human cells, indicating their roles in the cell cycle regulation of microtubule arrays (McNally et al., 1996; McNally and Thomas, 1998; Ahmad et al., 1999). Katanin-like

microtubule-severing activity is also implicated in flagellar excision in *Chlamydomonas reinhardtii* (Lohret et al., 1998) and meiotic spindle organization in *Caenorhabditis elegans* (Srayko et al., 2000). However, no katanin-like microtubule-severing protein is known to be involved in any cellular activities in higher plants.

Sequence analysis of AtKTN1 revealed that it shares significant amino acid sequence similarity with katanins from sea urchin and *C. elegans* (Hartman et al., 1998; Srayko et al., 2000). The highest sequence identity between AtKTN1 and katanin from sea urchin resides in the ATP binding module located in the C-terminal region. This similarity pattern was also found between sea urchin katanin and *C. elegans* MEI-1, which was shown to possess microtubule-severing activity (Srayko et al., 2000). However, unlike MEI-1, in which the N-terminal region has no similarity to sea urchin katanin, AtKTN1 exhibited significant sequence similarity to sea urchin katanin in the N-terminal region outside the ATP binding module. These lines of evidence strongly indicate that *AtKTN1* encodes a katanin-like protein, a possible ortholog in plants. Definite proof of whether AtKTN1 possesses microtubule-severing activity awaits further investigation.

THE *FRA2* MUTATION DELAYS THE ESTABLISHMENT OF CORTICAL MICROTUBULE ARRAY

Microtubule orientations undergo dynamic changes during cell division, expansion, and differentiation (Hush et al., 1994; Yuan et al., 1994; Marc et al., 1998; Mathur and Chua, 2000). For example, during the transition from isotropic to anisotropic cell expansion, cortical microtubules reorient from a random pattern to a transversely positioned pattern along the elongation axis. After transverse positioning, cortical microtubules must reorient constantly at different angles to direct cellulose microfibril deposition. Although a number of possible mechanisms to control the dynamic changes in microtubules have been proposed, none has been demonstrated to be critical during cell elongation (Cyr and

Palevitz, 1995). The finding that *AtKTN1*, a gene that regulates cell elongation, encodes a katanin-like protein suggests that microtubule-severing activity might play an important role in regulating the dynamic changes in microtubules during the initiation and subsequent maintenance of cell elongation.

Our results indicate that the *fra2* mutation renders a clear phenotype in microtubule organization in early stages during establishment of the cortical microtubule array. However, the mutation appears not to affect the organization of microtubule arrays when cells are undergoing mitosis and cytokinesis. During late stages of cytokinesis in somatic plant cells, a perinuclear microtubule array can be detected transiently (Hasezawa et al., 1991). When cells exit from cytokinesis, perinuclear microtubule array rapidly depolymerizes while cortical microtubule array arises, and two arrays do not overlap (Hasezawa et al., 1991). Therefore, a rapid microtubule depolymerization event takes place during the transition between two arrays. We propose that the plant katanin-like protein AtKTN1 is required for such a rapid microtubule depolymerization activity. Tubulins from the depolymerization of the perinuclear array could supply subunits for the cortical array. Because the perinuclear microtubules can not be rapidly depolymerized on the nuclear envelope, these microtubules may be aggregated together possibly by microtubule motors and/or proteins of microtubule-organizing centers, e.g. γ-tubulin. Because of the phenotypes of microtubule organization and cell elongation defects in the *fra2* mutant cells, we further hypothesize that the defects in cell wall biosynthesis and cell elongation caused by the *fra2* mutation is due to the inefficiency in converting the perinuclear array to the cortical array. Our finding that the plant katanin-like protein AtKTN1 plays a role in severing microtubules after cells exit from cell division is in contrast to animal katanins which play a role in severing microtubules during mitosis. Interestingly, the interphase-specific microtubule-severing activity has also been detected

in the green alga *Chlamydomonas reinhardtii* during deflagellation (Lohret et al., 1999; Quarmby, 2000).

Although the establishment of the cortical microtubule array is delayed in the *fra2* mutant cells, the cortical array eventually emerges. We do not rule out the possibility that AtKTN1 also affects the dynamics of cortical microtubules during cell elongation. It is likely that the *fra2* mutation might also impair the microtubule turnover rate, thereby contributing to a decrease in cell elongation but an increase in radial expansion, although a direct link between microtubule turnover and cell elongation has not been established in the cells of higher plants. Further study is required to directly establish the effects of the *fra2* mutation on microtubule turnover rate.

The defects in the microtubule organization observed in the *fra2* mutant is very different from that of the *fass* mutants, which also are defective in cell elongation (Torres-Ruiz and Jurgens, 1994; Traas et al., 1995; McClinton and Sung, 1997). The *fass* mutation causes disorganization of cortical microtubule arrays and the absence of a preprophase band, suggesting that the mutation affects the organization of microtubules. Therefore, the defect in cell elongation in *fass* mutants is caused by an inability to form cortical microtubule arrays in transverse orientation (McClinton and Sung, 1997). The effect of the *fra2* mutation on plant morphology also is distinguishable from *fass* mutant phenotypes. *fra2* plants have an almost normal shoot architecture except for shortening of all organs (Figure 2.4), whereas *fass* plants exhibit a ball-like shape (McClinton and Sung, 1997).

THE *FRA2* MUTATION ALTERS CELL WALL BIOSYNTHESIS

It is generally accepted that the orientation of cellulose microfibrils synthesized from the cellulose synthase complex is regulated by underlying microtubules beneath the plasma membranes. The trafficking of vesicles containing noncellulosic materials synthesized in the Golgi body also may be guided by microtubules. Thus, it is conceivable that alteration

of the normal dynamic changes in cortical microtubules might result in an inability of microtubules to guide efficiently the deposition of cell wall materials, thereby leading to a delay of cell wall biosynthesis. Our finding that the *fra2* mutation reduces cellulose and hemicellulose contents provides strong evidence to support this possibility. It suggests that microtubules not only guide the orientation of cellulose microfibril deposition, which in turn regulates cell elongation, but also might influence cell wall biosynthesis in general.

It is intriguing that the *fra2* mutation caused the formation of more condensed lignin. In particular, the guaiacyl lignin unit is much more highly condensed than the syringyl lignin unit. This is consistent with the structure of the guaiacyl lignin unit, which has an additional 5-C on the aromatic ring exposed for cross-linking. It is possible that reduction of cellulose in secondary walls and possible alteration of cellulose microfibril orientation may cause a change in the distribution of monolignols across the secondary walls. This might result in an accumulation of monolignols in certain wall areas, thereby leading to the formation of a highly condensed lignin structure. It will be interesting to determine whether there is any alteration in the distribution of lignin within the walls of fiber cells.

THE *FRA2* MUTATION DRAMATICALLY REDUCES THE MECHANICAL STRENGTH OF FIBERS

The *fra2* mutant was isolated based on its marked reduction in the breaking strength of the stems. Because the mechanical strength of the mature stems is conferred largely by the presence of interfascicular fibers, the *fra2* mutant must have a dramatic decrease in the mechanical strength of interfascicular fibers. Anatomical and chemical analyses indicate that the reduction in the mechanical strength of fibers is caused by alterations in fiber cell length and cell wall composition. Because AtKTN1 shows high similarity to microtubule-severing proteins, microtubule-severing activity might be essential for

normal fiber cell elongation and normal synthesis of fiber walls with strong mechanical strength.

In conclusion, we have shown that the *fra2* mutation results in a reduction in cellulose and hemicellulose contents, the formation of highly condensed lignin, a decrease in fiber cell length and fiber mechanical strength, a global alteration in cell elongation and plant morphology, and a delay in the establishment of the normal cortical microtubule array. Based on the finding that the *AtKTN1* gene encodes a protein similar to katanin that severs microtubules, we propose that AtKTN1 regulates the dynamic changes of microtubules during early stages of establishment of the cortical microtubule array as well as during cell elongation, which in turn influences cell morphogenesis, the biosynthesis and deposition of cell wall materials, and cell wall strength.

METHODS

MUTANT SCREENING

Ethyl methanesulfonate–mutagenized M_2 *Arabidopsis thaliana* (ecotype Columbia) plants were grown in a greenhouse. The inflorescence stems of 8-week-old plants were measured for their mechanical strength. Plants showing a dramatic reduction in normal stem strength were selected for further analysis. Mutant lines were backcrossed with the wild type three times to reduce background mutations.

BREAKING STRENGTH MEASUREMENT

The main inflorescence stems of 8-week-old plants were used for breaking force measurement (Reiter et al., 1993) with a digital force/length tester (model DHT 4-50; Larson Systems, Minneapolis, MN). Each stem was divided into four equal segments. The ends of stem segments with a space of 1 cm between were clamped, and a force was

applied manually until the stem segments were broken. Stems from 15 plants were tested for the breaking force.

HISTOLOGY

Tissues were fixed in 2% glutaraldehyde in PBS (33 mM Na_2HPO_4, 1.8 mM NaH_2PO_4, and 140 mM NaCl, pH 7.3) at 4°C overnight. After fixation, segments were dehydrated through a gradient of ethanol, cleared in propylene oxide, and embedded in Araldite resin (Electron Microscopy Sciences, Fort Washington, PA). One-micrometer-thick sections were cut with a microtome and stained with toluidine blue for observation of anatomy.

SCANNING ELECTRON MICROSCOPY

Tissue samples were fixed in 2% glutaraldehyde, dehydrated in ethanol, and then dried in a Samdri critical point dryer (Tousimis, Rockville, MD) before being mounted on stubs with carbon paste. Samples were coated with gold using an Edwards 306 vacuum evaporator (Edwards High Vacuum International, Wilmington, MA) and viewed with a LEO 982 FE scanning electron microscope (LEO, Thornwood, NY).

CELLULOSE CONTENT ASSAY

Stem materials were ground into powder and extracted twice with 70% ethanol at 70°C for 1 hr. After vacuum drying, cell wall materials were used for cellulose content assays according to Updegraff (1969). The cellulose content was determined with the anthrone reagent. Whatman (Clifton, NJ) 3MM paper was used as standard cellulose for quantitation.

CELL WALL SUGAR COMPOSITION ANALYSIS

Sugars (as alditol acetates) were measured as described by Hoebler et al. (1989), with the initial digestion time increased from 30 to 90 min.

LIGNIN CONTENT AND COMPOSITION ANALYSIS

Ethanol-extracted cell wall materials were used for measurement of Klason lignin according to Kirk and Obst (1988). Lignin content was expressed as a percentage of the original weight of cell wall residues.

Lignin composition was analyzed according to Morrison et al. (1996). Cell wall materials were hydrolyzed in 4 N NaOH at 170°C for 2 hr. The hydrolysate was acidified with 2 N HCl to pH 2.0. Lignin monomers released from base hydrolysis were extracted into diethylether and vacuum dried. The residue was dissolved in 10 µL of pyridine and 10 µL of N,O-bis(trimethylsilyl)trifluoroacetamide and analyzed by gas-liquid chromatography. Compounds were identified by comparing their mass spectra with published spectra or with those of the authentic compounds. All samples were run in duplicate.

IN-SOURCE PYROLYSIS MASS SPECTROMETRY

In-source pyrolysis mass spectrometry was performed on a Finngan GCQ mass spectrometer equipped with a direct exposure probe (rhenium loop) (Thermoquest, San Jose, CA), as described by Morrison and Archibald (1998). Analysis conditions were as follows: ionization energy of 20 electron volts; mass range of 50 to 500 m/z; scan time of 1 sec; temperature increase of ~10°C per sec to 700°C; and ion source temperature of 175°C. All samples were run in triplicate.

GENETIC ANALYSIS

The mutant line was crossed with the wild-type Arabidopsis ecotype Landsberg *erecta* for mapping study. F2 plants showing mutant phenotypes were selected for genetic mapping. Genomic DNA was isolated from the F2 mapping plants and used for polymerase chain reaction (PCR) with codominant amplified polymorphic sequence

(CAPS) markers (Konieczny and Ausubel, 1993). The information on CAPS markers used in this study was from the Arabidopsis database.

GENE EXPRESSION ANALYSIS

The level of *AtKTN1* mRNA in different organs was analyzed with reverse transcription–PCR. One-tenth microgram of total RNA was used for the synthesis of the first strand cDNA, which was further PCR amplified for 20 cycles with gene-specific primers. The PCR products were run on an agarose gel and transferred to a nylon membrane. The membrane was then hybridized with a digoxigenin-labeled *AtKTN1* gene probe, and the hybridized signals were detected with a chemiluminescence detection kit (Reche Molecular Biochemicals, Indianapolis, IN) according to the manufacturer's protocol.

LOCALIZATION OF MICROTUBULES

Seed of the wild type and the *fra2* mutant were germinated on wet filter paper at room temperature for 5 days. Two different protocols were used for microtubule localization. A whole-mount staining protocol was adopted from Sugimoto et al. (2000) to observe cells undergoing elongation. To observe cells undergoing cell division, root tip cells were subject to tubulin staining according to Liu and Palevitz (1992). In brief, seedlings were fixed for 60 min with 4% paraformaldehyde in PME buffer (50 mM PIPES, 5 mM EGTA, 2 mM $MgSO_4$, pH6.9). After being rinsed extensively with the PME buffer, the seedlings were treated with 1% cellulase RS (Yakult, Tokyo, Japan) and 0.1% Macerozyme R-10 (Karlan Research Products, Santa Rosa, CA) in PME for 15 min to partially digest the cell wall. Root tips were exercised from the rest of the seedlings and squashed between a coverslip and a microscopic slide pre-coated with gelatin and chrom-alum. Root cells were treated with 0.5% Triton in PME for 10-min followed by a 10-min treatment with -20^{o}C methanol. The cells were then rehydrated in PBS. Immunolocalization was carried out with an anti-α-tubulin antibody (DM1A, Sigma, St.

Louis, MO) diluted at 1:400 followed by an FITC-conjugated goat anti-mouse IgG antibody (Sigma) diluted at 1:400. Cells were then mounted on a slide in a mounting medium containing 100 mM Tris (pH 9.2), 50% glycerol, 1 mg/mL phenylenediamine, and 1 μg/mL 4′,6-diamidino-2-phenylindole. Roots stained with the whole-mount method were observed either under a Wallac UltraVIEW LCI confocal microscope with an Olympus 60X Plapo objective, or under a Nikon E600 epifluorescence microscope with a 60X Plan-Apo objective. Root tip cells were observed under a Nikon E600 epifluorescence microscope with a 100X Plan Fluor objective. Conventional epifluorescence images were acquired by a CCD camera (ORCA100, Hamamatsu Photonics, Hamamatsu city, Japan) with the ImageProPlus software package (Media Cybernetics, Silver Spring, MD). Final assembly of images in Figures 13 and 14 was carried out with the Adobe Photoshop software (Adobe, San Jose, CA).

ACKNOWLEDGMENTS

We thank M.H. Zhou and J.M. Scholey for their help with the confocal microscopy, Jan Nadeau for information on CAPS markers, G. Freshour and E. Richardson for their assistance in sectioning, J. Shields and M. Farmer for their help on scanning electron microscopy, B. Palevitz for stimulating discussions and helpful suggestions, and the editor and reviewers for their comments and suggestions. D.H.B. was supported by a Plant Evolution Training Grant from the National Science Foundation. This work was supported in part by the Cooperative State Research, Education, and Extension Service, U.S. Department of Agriculture.

REFERENCES

Ahmad, F.J., Yu, W., McNally, F.J., and Baas, P.W. (1999). An essential role for katanin in severing microtubules in the neuron. J. Cell Biol. 145, 305-315.

Akin, D.E., Morrison, W.H., and Himmelsbach, D.S. (1993). Characterization of digestion residues of alfalfa and orchardgrass leaves by microscopic, spectroscopic and chemical analysis. J. Sci. Food Agric. 63, 339-347.

Aloni, R. (1987). Differentiation of vascular tissues. Annu. Rev. Plant Physiol. 38, 179-204.

Arioli, T., Peng, L., Betzner, A.S., Burn, J., Wittke, W., Herth, W., Camilleri, C., Höfte, H., Plazinski, J., Birch, R., Cork, A., Glover, J., Redmond, J., and Williamson, R.E. (1998). Molecular analysis of cellulose biosynthesis in Arabidopsis. Science 279, 717-720.

Baskin, T.I. (2000). The cytoskeleton. In Biochemistry and Molecular Biology of Plants, B.B. Buchanan, W. Gruissem, and R.L. Jones, eds (Rockville, MD: American Society of Plant Physiologists), pp. 202-258.

Carpita, N., and McCann, M. (2000). The cell wall. In Biochemistry and Molecular Biology of Plants, B.B. Buchanan, W. Gruissem, and R.L. Jones, eds (Rockville, MD: American Society of Plant Physiologists), pp. 52-108.

Cleary, A.L., and Smith, L.G. (1998). The *tangled1* gene is required for spatial control of cytoskeletal arrays associated with cell division during maize leaf development. Plant Cell 10, 1875-1888.

Cyr, R.J., and Palevitz, B.A. (1995). Organization of cortical microtubules in plant cells. Curr. Opin. Cell Biol. 7, 65-71.

Giddings, T.H., and Staehelin, L.A. (1991). Microtubule-mediated control of microfibril deposition: A re-examination of the hypothesis. In The Cytoskeletal Basis of Plant Growth and Form, C.W. Lloyd, ed (San Diego, CA: Academic Press), pp. 85-99.

Hartman, J.J., Mahr, J., McNally, K., Okawa, K., Iwamatsu, A., Thomas, S., Cheesman, S., Heuser, J., Vale, R.D., and McNally, F.J. (1998). Katanin, a microtubule-severing protein, is a novel AAA ATPase that targets to the centrosome using a WD40-containing subunit. Cell 93, 277-287.

Hasezawa, S., Marc, J., and Palevitz, B. A. (1991). Microtubule reorganization during the cell cycle in synchronized BY-2 tobacco suspensions. Cell Motil. Cytoskeleton 18, 94-106.

Hoebler, C., Barry, L.D., and Delort-Laval, J. (1989). Rapid hydrolysis of plant cell wall polysaccharides by gas-liquid chromatography. J. Agric. Food Chem. 37, 360-367.

Hush, J.M., Wadsworth, P., Callaham, D.A., and Hepler, P.K. (1994). Quantification of microtubule dynamics in living plant cells using fluorescence redistribution after photobleaching. J. Cell Sci. 107, 775-784.

Kirk, T.K., and Obst, J.R. (1988). Lignin determination. Methods Enzymol. 161, 87-101.

Konieczny, A., and Ausubel, F.M. (1993). A procedure for mapping Arabidopsis mutations using co-dominant ecotype-specific PCR-based markers. Plant J. 4, 403-410.

Liu, B., and Palevitz, B.A. (1992). Organization of cortical microfilaments in dividing root cells. Cell Motil. Cytoskeleton 23, 252-264.

Lohret, T.A., McNally, F.J., and Quarmby, L.M. (1998). A role for katanin-mediated axonemal severing during *Chlamydomonas* deflagellation. Mol. Biol. Cell 9, 1195-1207.

Lohret, T. A., Zhao, L. F., and Quarmby, L. M. (1999). Cloning of Chlamydomonas p60 katanin and localization to the site of outer doublet severing during deflagellation. Cell Motil. Cytoskeleton 43: 221-231.

Luo, D., and Oppenheimer, D.G. (1999). Genetic control of trichome branch number in Arabidopsis: the roles of the *FURCA* loci. Development 126, 5547-5557.

Marc, J., Granger, C.L., Brincat, J., Fisher, D.D., Kao, T.-H., McCubbin, A.G., and Cyr, R.J. (1998). A *GFP-MAP4* reporter gene for visualizing cortical microtubule rearrangements in living epidermal cells. Plant Cell 10, 1927-1939.

Mathur, J., and Chua, N.-H. (2000). Microtubule stabilization leads to growth reorientation in Arabidopsis trichomes. Plant Cell 12, 465-477.

Mauseth, J.D. (1988). Plant Anatomy. (Menlo Park, CA: Benjamin/Cummings Publishing).

McClinton, R.S., and Sung, Z.R. (1997). Organization of cortical microtubules at the plasma membrane in Arabidopsis. Planta 201, 252-260.

McNally, F.J., and Vale, R.D. (1993). Identification of katanin, an ATPase that severs and disassembles stable microtubules. Cell 75, 419-429.

McNally, F.J., and Thomas, S. (1998). Katanin is responsible for the M-phase microtubule-severing activity in *Xenopus* eggs. Mol. Biol. Cell 9, 1847-1861.

McNally, F.J., Okawa, K., Iwamatsu, A., and Vale, R.D. (1996). Katanin, the microtubule-severing ATPase, is concentrated at centrosomes. J. Cell Sci. 109, 561-567.

Morrison, W.H., and Archibald, D.D. (1998). Analysis of graded flax fiber and yarn by pyrolysis mass spectrometry and pyrolysis gas chromatography mass spectrometry. J. Agric. Food Chem. 46, 1870-1876.

Morrison, W.H., Akin, D.E., Ramaswamy, G., and Baldwin, B. (1996). Evaluating chemically retted kenaf using chemical, histochemical, and microspectrophotometric analyses. Text. Res. J. 66, 651-656.

Nicol, F., His, I., Jauneau, A., Vernhettes, S., Canut, H., and Höfte, H. (1998). A plasma membrane-bound putative endo-1,4-β-D-glucanase is required for normal wall assembly and cell elongation in Arabidopsis. EMBO J. 17, 5563-5576.

Quarmby, L. (2000). Cellular Samurai: katanin and the severing of microtubules. J. Cell Sci. 113: 2821-2827.

Reiter, W.-D., Chapple, C.C.S., and Somerville, C.R. (1993). Altered growth and cell walls in a fucose-deficient mutant of Arabidopsis. Science 261, 1032-1035.

Seagull, R.W., and Falconer, M.M. (1991). In vitro xylogenesis. In The Cytoskeletal Basis of Plant Growth and Form, C.W. Lloyd, ed (San Diego, CA: Academic Press), pp. 183-194.

Smith, L.G., Hake, S., and Sylvester, A.W. (1996). The *tangled1* mutation alters cell division orientations throughout maize leaf development without altering leaf shape. Development 122, 481-489.

Srayko, M., Buster, D.W., Bazirgan, O.A., McNally, F.J., and Mains, P.E. (2000). MEI-1/MEI-2 katanin-like microtubule severing activity is required for Caenorhabditis elegans meiosis. Genes Dev. 14, 1072-1084.

Sugimoto, K., Williamson, R. E., and Wasteneys, G. O. (2000). New techniques enable comparative analysis of microtubule orientation, wall texture, and growth rate in intact roots of Arabidopsis. Plant Physiol. 124, 1493-1506.

Torres-Ruiz, R.A., and Jurgens, G. (1994). Mutations in the *FASS* gene uncouple pattern formation and morphogenesis in Arabidopsis development. Development 120, 2967-2978.

Traas, J., Bellini, C., Nacry, P., Kronenberger, J., Bouchez, D., and Caboche, M. (1995). Normal differentiation patterns in plants lacking microtubular preprophase bands. Nature 375, 676-677.

Updegraff, D.M. (1969). Semimicro determination of cellulose in biological materials. Anal. Biochem. 32, 420-424.

Vale, R.D. (1991). Severing of stable microtubules by a mitotically activated protein in *Xenopus* egg extracts. Cell 64, 827-839.

van der Hage, E.R.E., Mulder, M.M., and Boon, J.J. (1993). Structural characterization of lignin polymers by temperature-resolved in-source pyrolysis-mass spectrometry and

Curie-point pyrolysis-gas chromatography/mass spectrometry. J. Anal. Appl. Pyrolysis 25, 149-183.

Yuan, M., Shaw, P.J. Warn, R.M., and Lloyd, C.W. (1994). Dynamic reorientation of cortical microtubules, from transverse to longitudinal, in living plant cells. Proc. Natl. Acad. Sci. USA 91, 6050-6053.

Zhong, R., and Ye, Z.-H. (1999). *IFL1*, a gene regulating interfascicular fiber differentiation in Arabidopsis, encodes a homeodomain-leucine zipper protein. Plant Cell 11, 2139-2152.

Zhong, R., Taylor, J.J., and Ye, Z.-H. (1997). Disruption of interfascicular fiber differentiation in an Arabidopsis mutant. Plant Cell 9, 2159-2170.

Zuo, J., Niu, Q.-W., Nishizawa, N., Wu, Y., Kost, B., and Chua, N.-H. (2000). KORRIGAN, an Arabidopsis endo-1,4-β-glucanase, localizes to the cell plate by polarized targeting and is essential for cytokinesis. Plant Cell 12, 1137-1152.

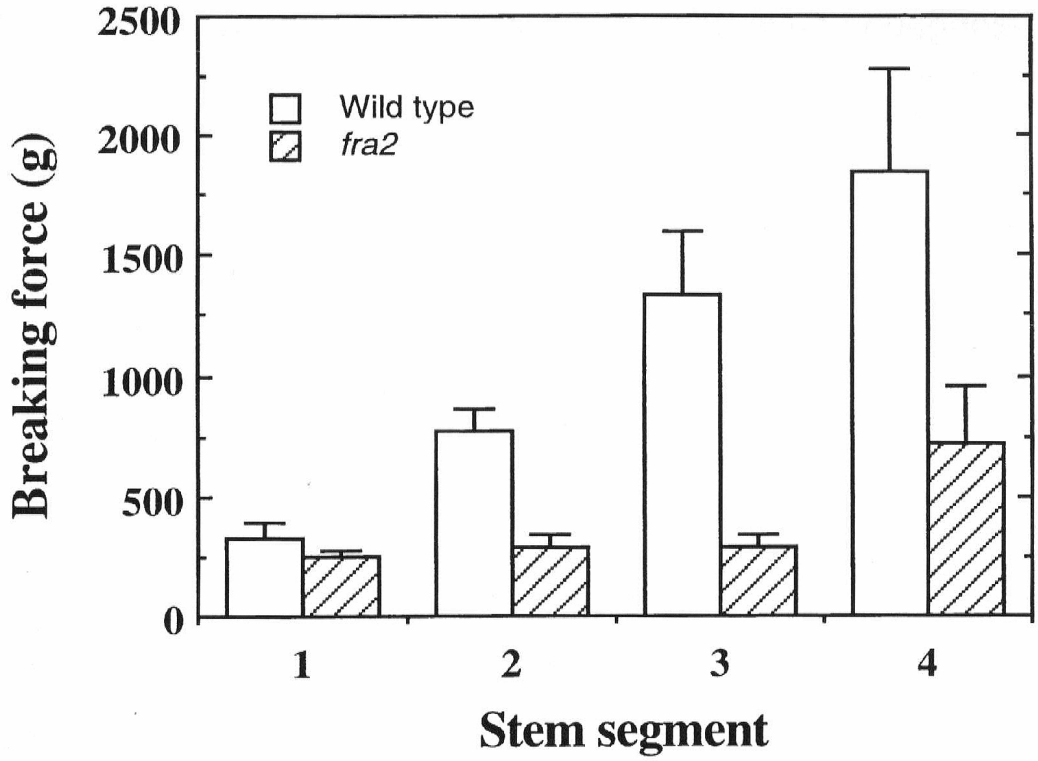

Figure 2.1. Breaking Force Measurement in Stems of the Wild Type and the *fra2* Mutant.

The main inflorescence stems of 8-week-old plants were divided into four equal segments and measured for the force required to break the stems. Segments were numbered in order from the top to the bottom of the stems. Data are mean values ± SE for 15 plants.

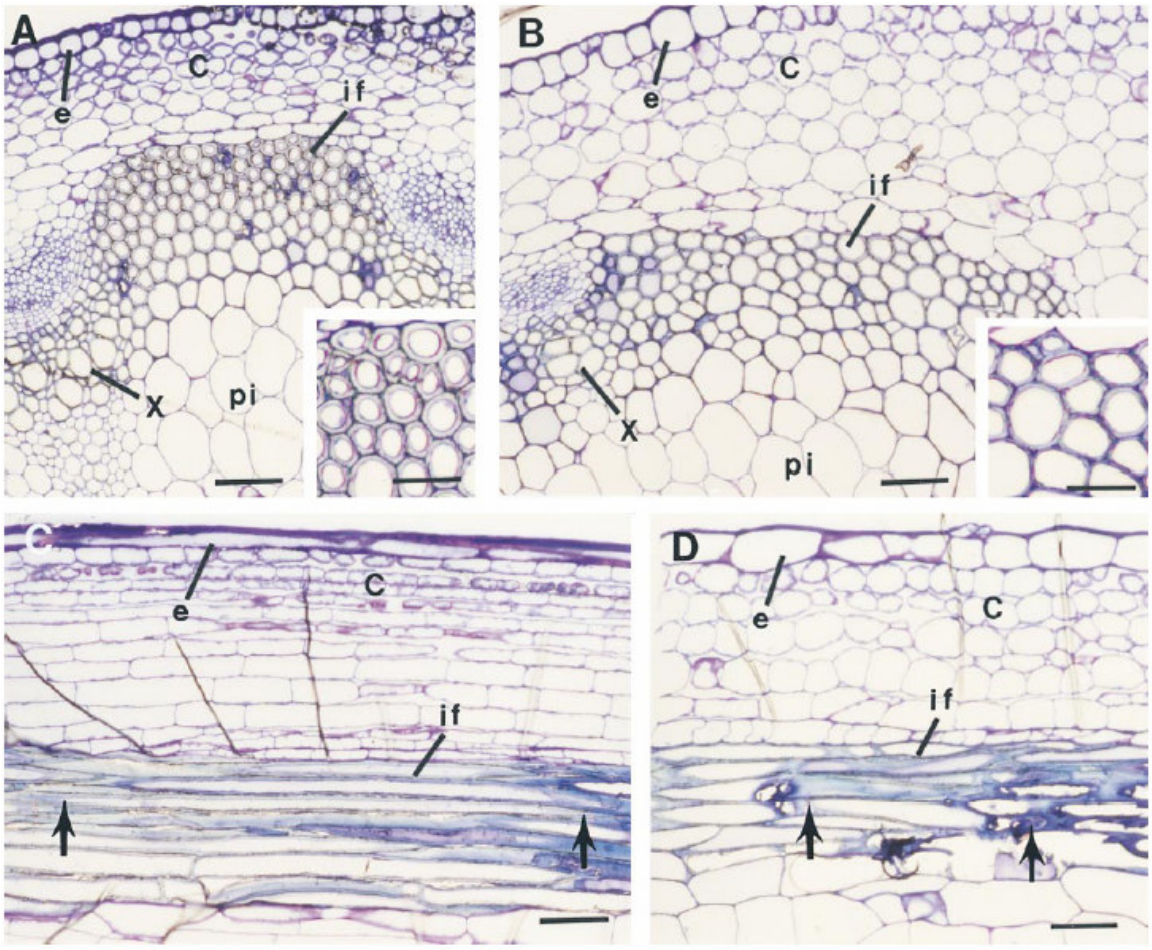

Figure 2.2. Anatomy of Interfascicular Fibers in Stems of the Wild Type and the *fra2* Mutant.

(A) and (B) Cross-sections of the stems of wild type (A) and *fra2* (B) showing the presence of interfascicular fibers. Insets show enlarged fiber cells. It is evident that the fiber cell wall in the wild type (A) is much thicker than that in *fra2* (B).

(C) and (D) Longitudinal sections of the stems of wild type (C) and *fra2* (D). Fiber cells in *fra2* (D) are much shorter and wider than those in the wild type (C). Arrows mark the ends of a fiber cell.

Abbreviations: c, cortex; e, epidermis; if, interfascicular fiber; pi, pith; x, xylem. Bars = 55 μm for (A) to (D) and 28 μm for insets in (A) and (B).

Figure 2.3. In-Source Pyrolysis Mass Spectrometry of Cell Walls of the Wild Type (WT) and the *fra2* Mutant.

Mass peaks of guaiacyl lignin had mass−charge ratio (m/z) values of 124, 137, 138, 150, 152, 164, 166, 178, and 180. Mass peaks of syringyl lignin had m/z values of 154, 167, 168, 180, 182, 194, 196, 208, and 210. Mass peaks of cellulose and amylose had m/z values of 57, 60, 73, 85, 86, 96, 98, 100, 102, 110, 112, 126, and 144. Mass peaks of hemicellulose had m/z values of 58, 85, 86, and 114. Insets show the expanded portions of the spectra of mass markers for dimeric lignin, with m/z values of 272, 302, 312, 320, 326, 328, 332, 358, 388, and 418. The relative intensities of mass peaks for cell wall polysaccharides and lignin were altered significantly between the wild type and the *fra2* mutant.

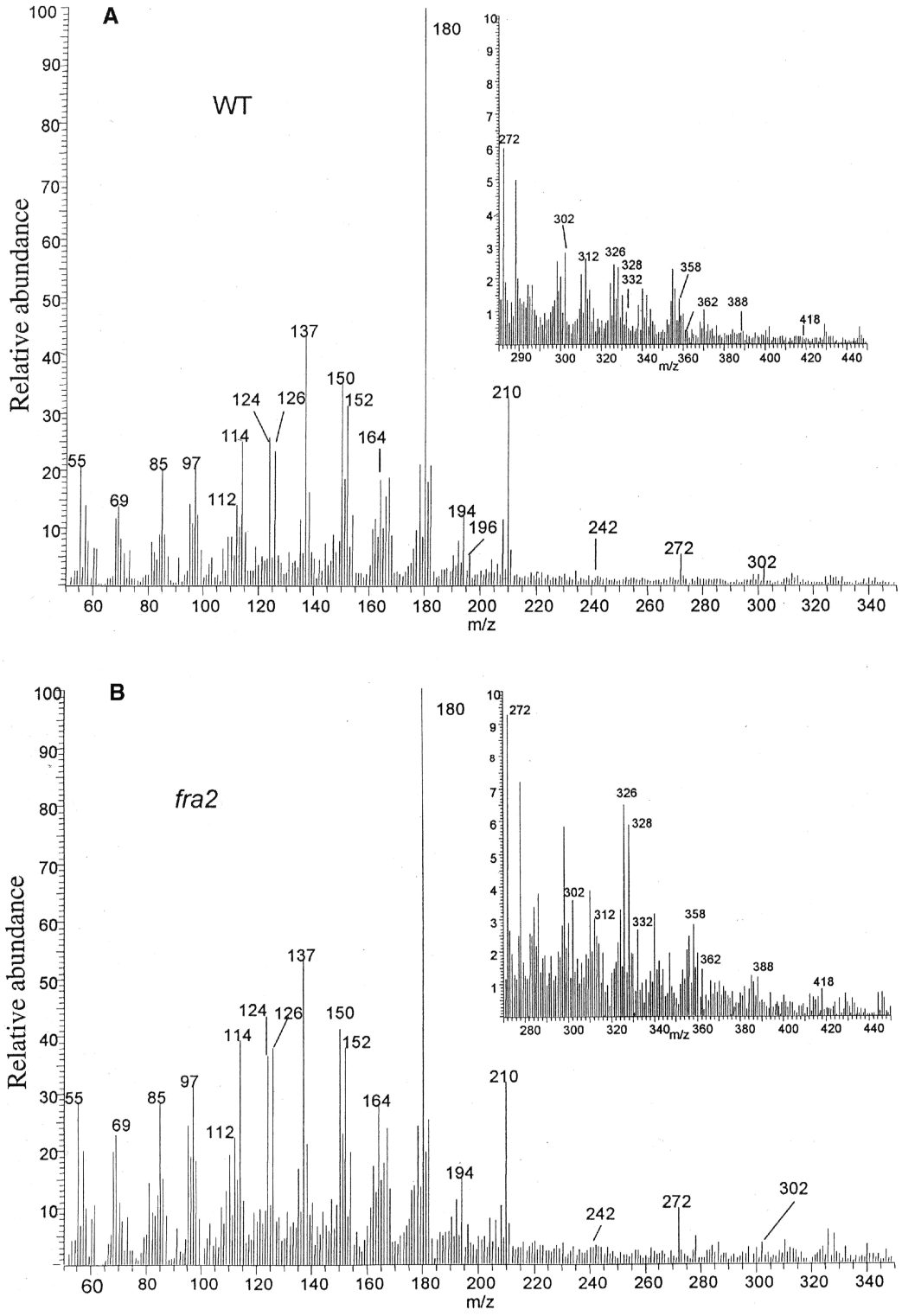
A
WT
Relative abundance
m/z
180
137
150
124
126
152
210
114
164
55
85
97
69
112
194
196
242
272
302
B
fra2
Relative abundance
m/z
180
272
326
328
302
312
332
358
362
388
418
137
124
126
150
114
152
210
97
55
85
164
69
112
194
242
272
302

Figure 2.4. Morphology of the Wild Type and the *fra2* Mutant.

(A) Morphology of 8-week-old plants. The main inflorescence stem of a *fra2* plant (right) is much shorter than that of a wild-type plant (left).

(B) and (C) The main inflorescence stems. The *fra2* stem (C) has reduced internode length compared with the wild-type stem (B).

(D) and (E) Siliques of wild type (D) and *fra2* (E).

(F) and (H) The rosette leaves of a 5-week-old *fra2* plant (H) are more compact than those of a wild-type plant (F).

(G) and (I) Individual leaves of 5-week-old plants. The length of both blades and petioles in *fra2* (I) is reduced compared with wild type (G). From left to right, the leaves are arranged according to the order from cotyledons to the youngest leaves.

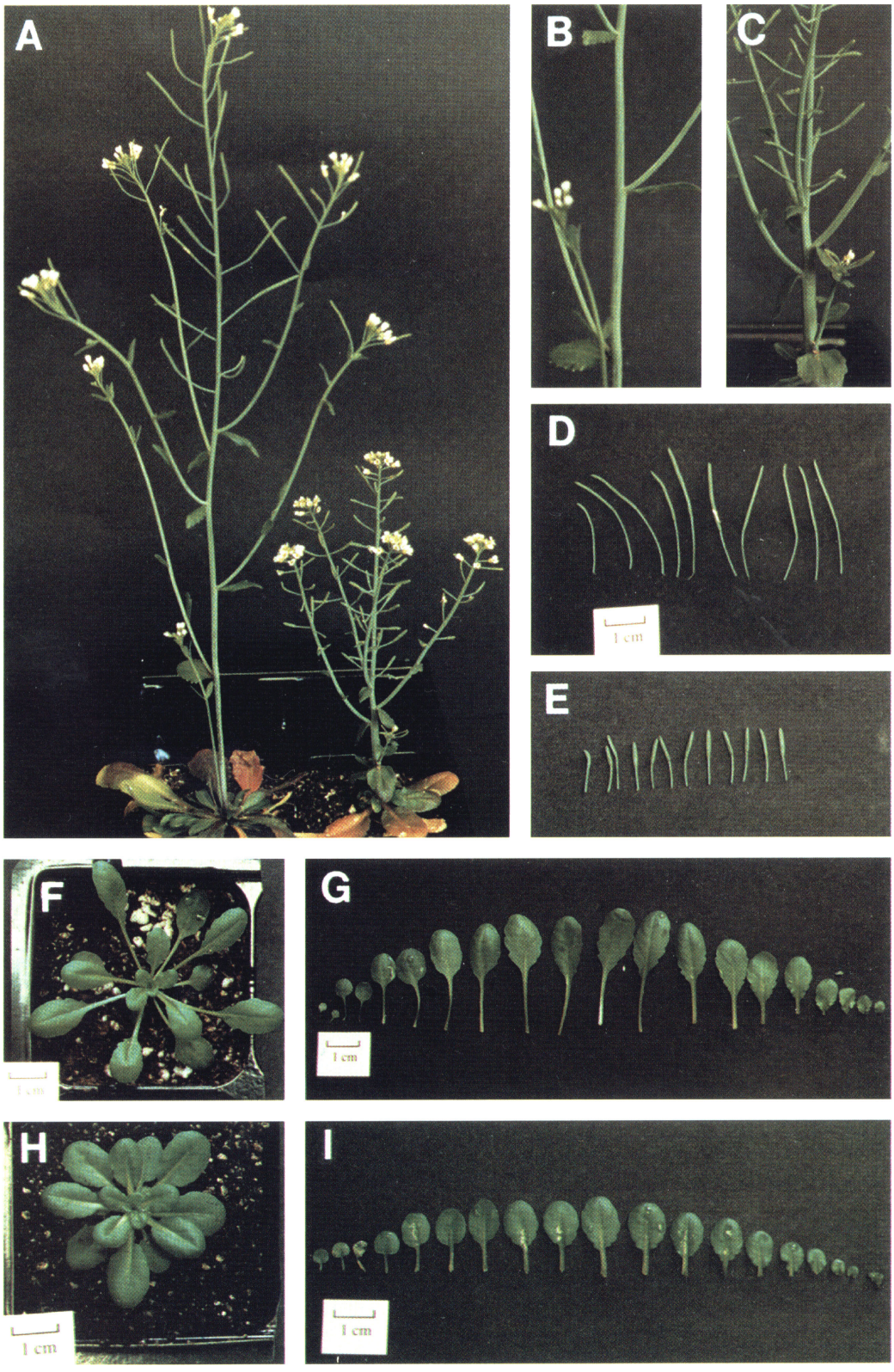
A
B
C
D
1 cm
E
F
1 cm
G
1 cm
H
1 cm
I
1 cm

Figure 2.5. Measurement of the Length and Width of Leaves.

The fifth to ninth leaves of 5-week-old plants were measured for their length and width. Data are means ± SE of 10 leaves.

(A) Length of leaf blades, showing a reduction in *fra2* compared with wild type.

(B) Width of leaf blades, showing little change in *fra2* compared with wild type.

(C) Length of petioles, showing a dramatic reduction in *fra2* compared with wild type.

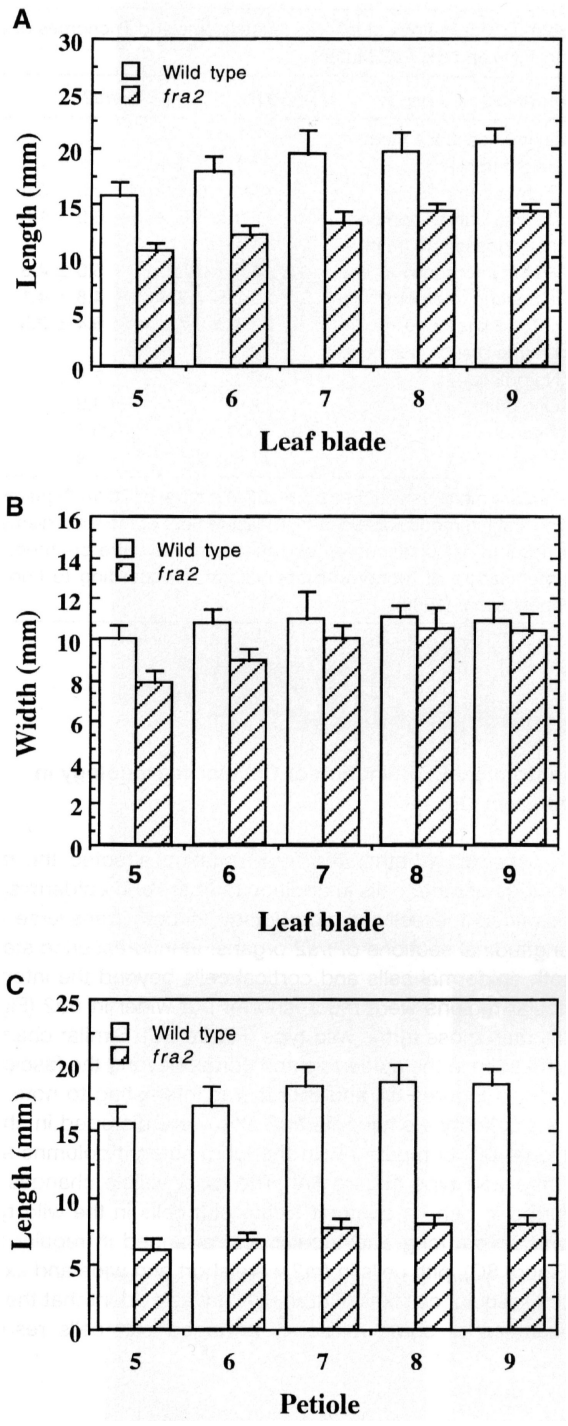
A
Wild type
fra2
Length (mm)
30
25
20
15
10
5
0
5
6
7
8
9
Leaf blade
B
Wild type
fra2
Width (mm)
16
14
12
10
8
6
4
2
0
5
6
7
8
9
Leaf blade
C
Wild type
fra2
Length (mm)
25
20
15
10
5
0
5
6
7
8
9
Petiole

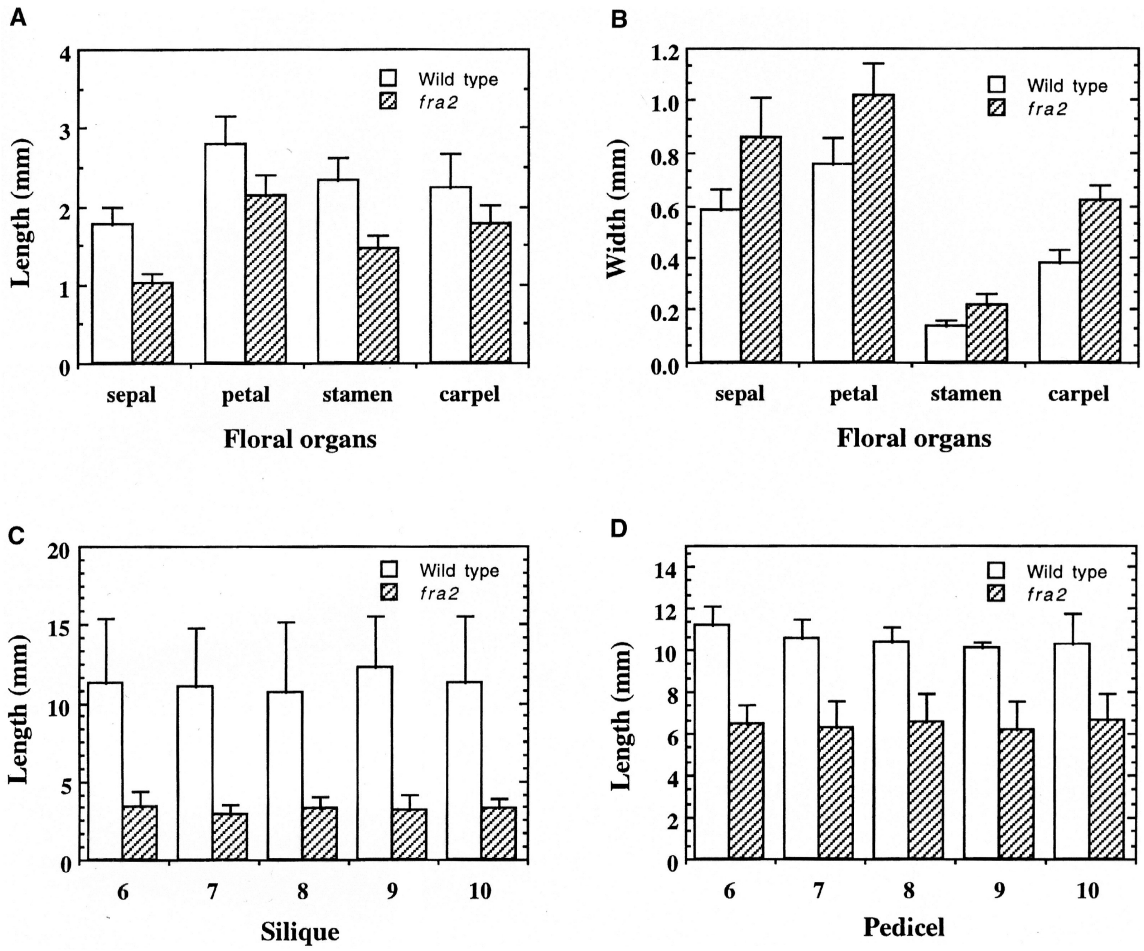

Figure 2.6. Measurement of the Length and Width of Floral Organs.

The sixth to tenth siliques of 8-week-old plants were measured for their length and width. Data are means ± SE of 30 samples.

(A) and (B) Length and width of floral organs, showing reduced length (A) but increased width (B) in *fra2* compared with wild type.

(C) and (D) Length of silique and pedicel, showing a reduction in *fra2* compared with wild type.

Figure 2.7. Scanning Electron Micrographs of Epidermal Cell Morphology.

(A) and (D) Five-day-old seedlings showing that *fra2* (D) has shorter hypocotyl and root than wild type (A).

(B) and (E) Roots of 5-day-old seedlings showing that root hair cells in *fra2* (E) are more compact than those in wild type (B).

(C) and (F) Hypocotyls of 5-day-old seedlings showing that epidermal cells in *fra2* (F) have reduced length compared with those in wild type (C).

(G) and (J) Trichomes showing that wild type (G) has two branch points and *fra2* (J) has one branch point.

(H) and (K) Upper epidermal cells of leaves showing that *fra2* (K) has less convolution than wild type (H).

(I) and (L) Epidermal cells of carpels showing that *fra2* (L) has reduced length compared with wild type (I).

Bars = 1 mm for (A) and (D); 100 μm for (B), (C), (E) to (H), and (J) and (K); and 50 μm for (I) and (L).

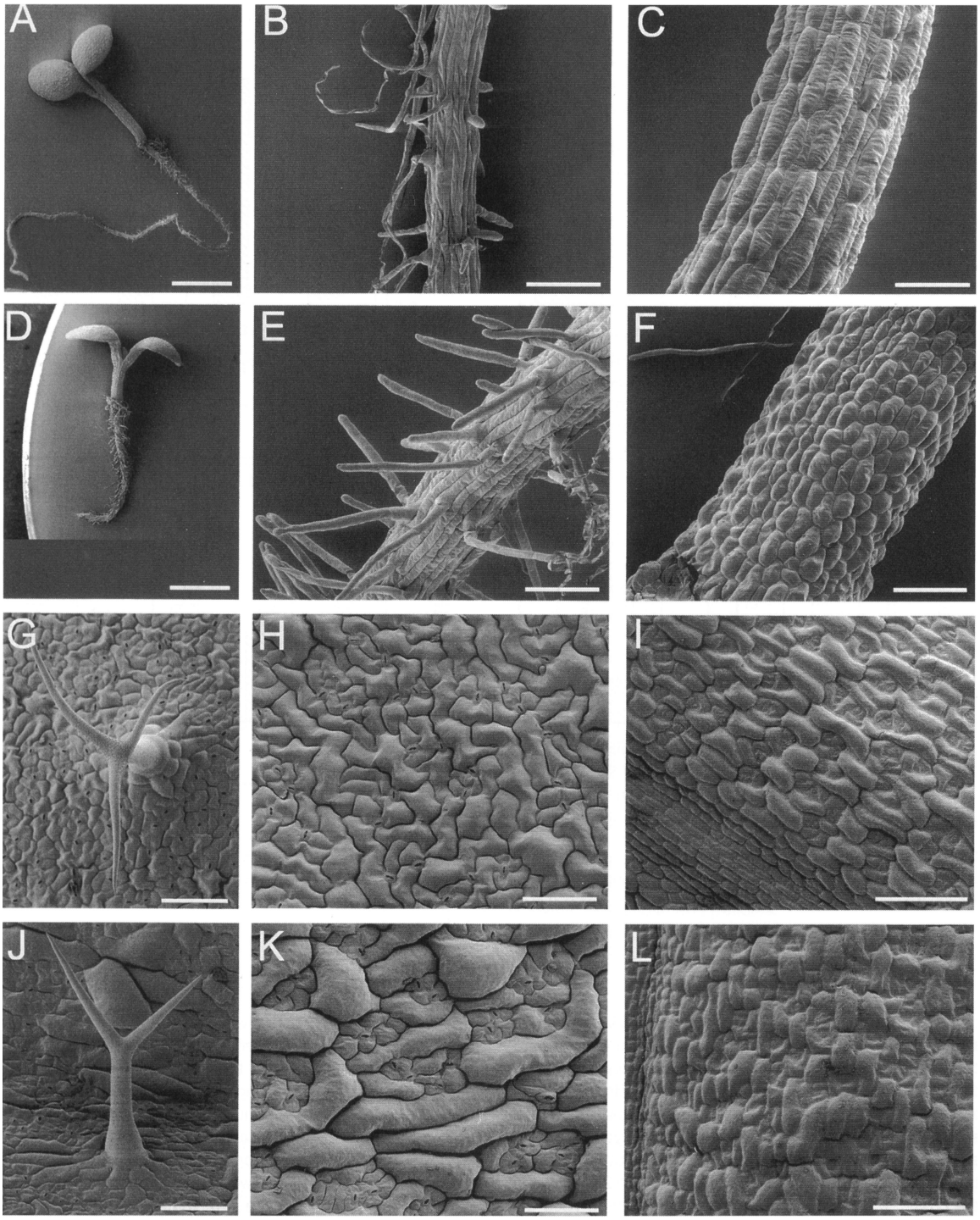
A
B
C
D
E
F
G
H
I
J
K
L

Figure 2.8. Cellular Morphology in Different Organs of the Wild Type and the *fra2* Mutant.

(A) and (B) Longitudinal sections of stems. *fra2* (B) has shorter epidermal and cortical cells and altered shape of tracheary elements compared with wild type (A).

Abbreviations: c, cortex; e, epidermis; ph, phloem; te, tracheary element.

(C) and (D) Longitudinal sections of pith showing reduced cell length and less organized cell files in *fra2* (D) compared with wild type (C).

(E) and (F) Cross-sections of leaves showing enlarged spongy mesophyll cells (sm) in *fra2* (F) compared with wild type (E). The arrow points to a giant epidermal cell in *fra2* (F). pp, palisade parenchyma.

(G) and (H) Longitudinal sections of hypocotyls. Cortical cells in *fra2* (H) have reduced length compared with wild type (G).

(I) and (J) Longitudinal sections of petioles showing reduced cell length and less organized cell files in *fra2* (J) compared with wild type (I).

Bars = 55 μm for (A), (B), (G), and (H); 90 μm for (C) to (F); and 110 μm for (I) and (J).

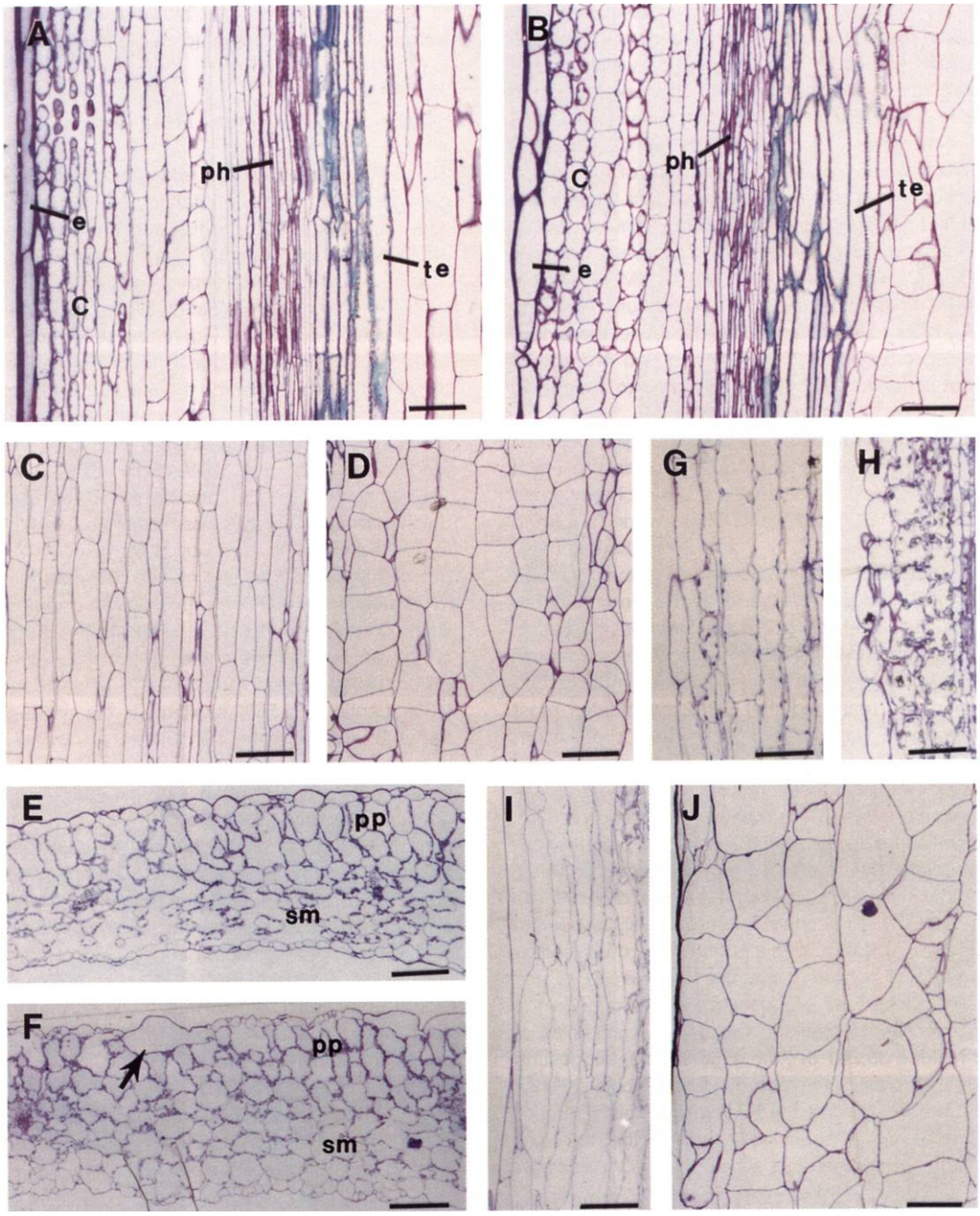
A
ph
e
te
C
B
C
ph
te
e
C
D
G
H
E
pp
sm
F
pp
sm
I
J

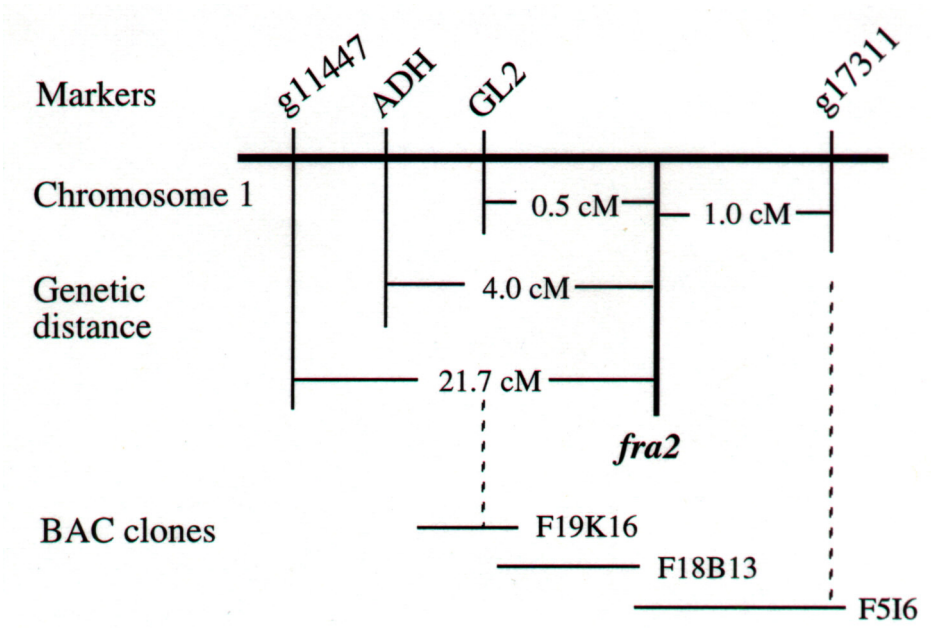

Figure 2.9. Fine Mapping of the *fra2* Locus.

F2 mutant plants segregating from the cross of *fra2* and Landsberg *erecta* were used for mapping with CAPS markers. The *fra2* locus was mapped to a 230-kb region located between GL2 and g17311, which was covered by three overlapping BAC clones. Markers are not positioned on scale.

Figure 2.10. Structure of the *FRA2* Gene and Nature of the *fra2* Mutation.

(A) Exon and intron organization of the *FRA2* gene. The *FRA2* gene has 2554 nucleotides from the start codon (designated nucleotide 1) to the stop codon (designated nucleotide 2554). A single nucleotide deletion was found at nucleotide 2329 in *fra2*. Black boxes indicate exons, and lines between boxes indicate introns.

(B) Effect of the deletion mutation in *fra2* on the translation of the predicted protein. Shown are nucleotide sequences and their amino acid sequences around the deletion site. Deletion of the nucleotide A (marked with an asterisk in the wild type and with an inverted triangle in *fra2*) leads to a frameshift of codons, thereby generating a premature stop codon at the second codon after the mutation site.

(C) Elimination of a BsmAI site in the mutant *fra2* cDNA. The deletion mutation in *fra2* happens to occur at a BsmAI site. This is readily revealed by digesting PCR-amplified cDNA fragments with BsmAI, which shows that one BsmAI site is missing in *fra2* cDNA compared with the wild-type (WT) *FRA2* cDNA.

A

B

Wild type	DNA	TAC	AGT	GGA	GAC*	GAT	CTG	ACT
	Protein	Y	S	G	D	D	L	T
fra2	DNA	TAC	AGT	GGA	GCG▽	ATC	TGA	CT
	Protein	Y	S	G	A	I	STOP	

C

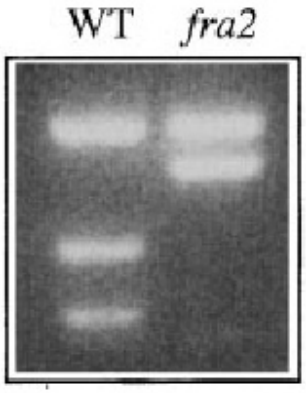

Figure 2.11. Alignment of the Deduced Amino Acid Sequences of AtKTN1 and Katanin (SuKTN) from Sea Urchin.

AtKTN1 exhibits 56% sequence similarity in the entire open reading frame with katanin from sea urchin. The ATP binding module, which shares 75% sequence similarity between AtKTN1 and katanin, is underlined. The GenBank accession number for the AtKTN1 cDNA sequence data is AFK23578.

```
AtKTN1  MVGSSNSLAGLQDHLKLAREYALEGSYDTSVIFFDGAIAQ 40
SuKTN        M:VDEICENT:MG:::::L:N:E::LVYYQ:VLQ: 35

AtKTN1  INKHLNTLDDPLARTKWMNVKKAIMEETEVVKQLDAERRA 80
SuKTN   :Q:L:TSVHE:QRKHQ:QTIRQELSQ:Y:H::NITKTLNG 75

AtKTN1  FKEAPTGRRAASPPINTKSSFVFQPLDEYPTSSGGGPMDD 120
SuKTN   ::SE:----::PE:APNHRAAP:SHHQHAAKPAAAE:AR: 111

AtKTN1  PDVWRPPTRDVTSRRPARAGQTGTRKSPQDGAWARGPTTR 160
SuKTN   ::::P:::--PVDH::SPPY:RAA::D:PRRSEPSK:AN: 149

AtKTN1  TGPASRGGRGGATSKSTAGARSSTAGKKGAASKSNKAESM 200
SuKTN   APGND:::::PSDRRGDARSGGGGRGGARGSDKDKNRGGK 189

AtKTN1  NGDA------EDGKSKRGLYEGPDEDLAAMLERDVLDSTP 234
SuKTN   SDKDKKAPSG:E:DE:KFDPA:Y:K::VEN::::IVQRN: 229

AtKTN1  GVRWDDVAGLSEAKRLLEEAVVLPLWMPEYFQGIRRPWKG 274
SuKTN   N:H:A:I:::T:::::::::::::::::D::K:::::::: 269

AtKTN1  VLMFGPPGTGKTLLAKAVATECGTTFFNVSSATLASKWRG 314
SuKTN   :::V::::::::M:::::::::::::::::::S:T::YH: 309

AtKTN1  ESERMVRCLFDLARAYAPSTIFIDEIDSLCNSRGGSGEHE 354
SuKTN   :::KL::L::EM::F:::::::::::::I:SK::TGS::: 349

AtKTN1  SSRRVKSELLVQVDGVSNTATNEDGSRKIVMVLAATNFPW 394
SuKTN   A:::::::::I:M::::GPSAG:ES:-:M:::::::::: 388

AtKTN1  DIDEALRRRLEKRIYIPLPDFESRKALININLRTVBVASD 434
SuKTN   ::::::::::::::::::EIDG:EQ:LR:::KE:PL:D: 428

AtKTN1  VNIEDVARRTEGYSGDDLTNVCRDASMNGMRRKIAGKTRD 474
SuKTN   IDLKSI:EKMD::::A:I:::::::::MA:::R:Q:LRPE 468

AtKTN1  EIKNMSKDDISNDPVAMCDFEEAIRKVQPSVSSSDIEKHE 514
SuKTN   ::RHIP:EEL-:Q:STPA::LL:LQ::SK::GKE:LV:YM 507

AtKTN1  KWLSEFGSA                                523
SuKTN   A:ME::::V                                 516
```

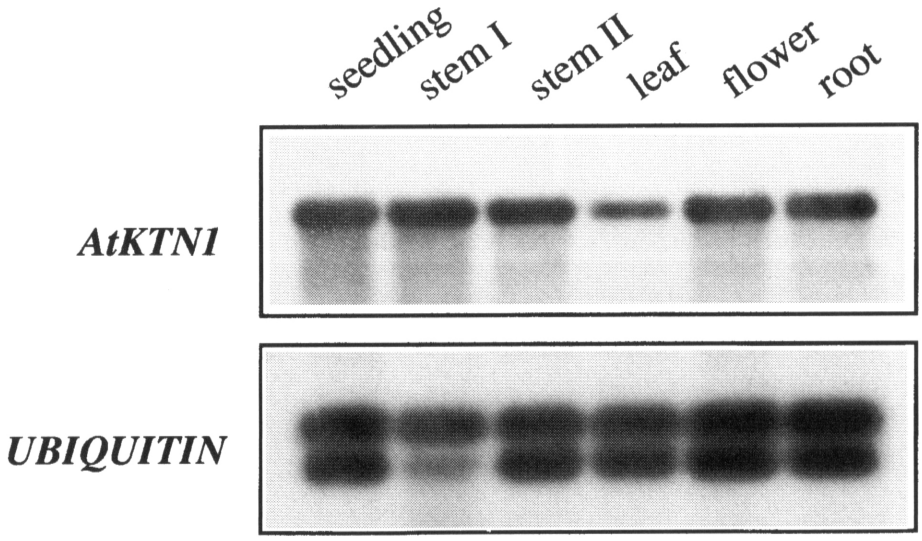

Figure 2.12. Analysis of *AtKTN1* Gene Expression in Arabidopsis Organs.
Total RNA was isolated from different organs of Arabidopsis plants and used for reverse transcription–PCR. The ubiquitin gene was used as an internal control for PCR. The seedlings were 3 weeks old. Leaves, roots, and flowers were from 8-week old plants. Stem I and stem II were from 4- and 8-week-old plants, respectively.

Figure 2.13. Immunostaining of Microtubules in Root Cells of Wild Type and *fra2*. Young roots from 5-day-old seedlings were treated with cell wall–digesting enzymes, probed with the antibodies against α-tubulin and fluorescein isothiocyanate–conjugated secondary antibodies, and visualized with an epifluorescence microscope or a confocal microscope.

(A) and (B) A Surface view (A) of a wild-type interphase cell which has yet to undergo elongation, showing the parallel cortical microtubule network. A midplane view (B) of the same cell showing no obvious microtubules.

(C) and (D) A surface view (C) of the *fra2* interphase cells, displaying microtubules in a converged pattern near the cell cortex. A midplane view (D) of the same cells, showing microtubule aggregation points.

(E) Close-up of a surface view of the uppermost cell in (C), showing the converging microtubule organization pattern.

(F) Close-up of a mid plane view of the uppermost cell in (D), showing the microtubule aggregation points (arrows), which are the centers of three microtubule asters facing towards the cell cortex (E).

(G) and (H) Surface (G) and midplane (H) views of the *fra2* elongating cells showing the disappearance of microtubule aggregation patterns, except the tope left cell, which retains the microtubule converging pattern.

(I) A whole-mount view of the wild-type root, showing cortical microtubules in a transverse pattern in the cell cortex of elongating epidermal cells.

(J) and (K) A whole-mount view of the *fra2* root showing cortical microtubules aligned in the cell cortex of elongating epidermal cells. Note that the *fra2* epidermal cells are much shorter in length compared with the wild type (I).

(L) A surface view of a highly vacuolated *fra2* cell with well-organized cortical microtubules.

Bar in (L) = 5 μm. for (A) to (D), (G), (H), and (L); bar in (F) = 5 μm for (E) and (F); bar in (K) = 5 μm for (I) to (K).

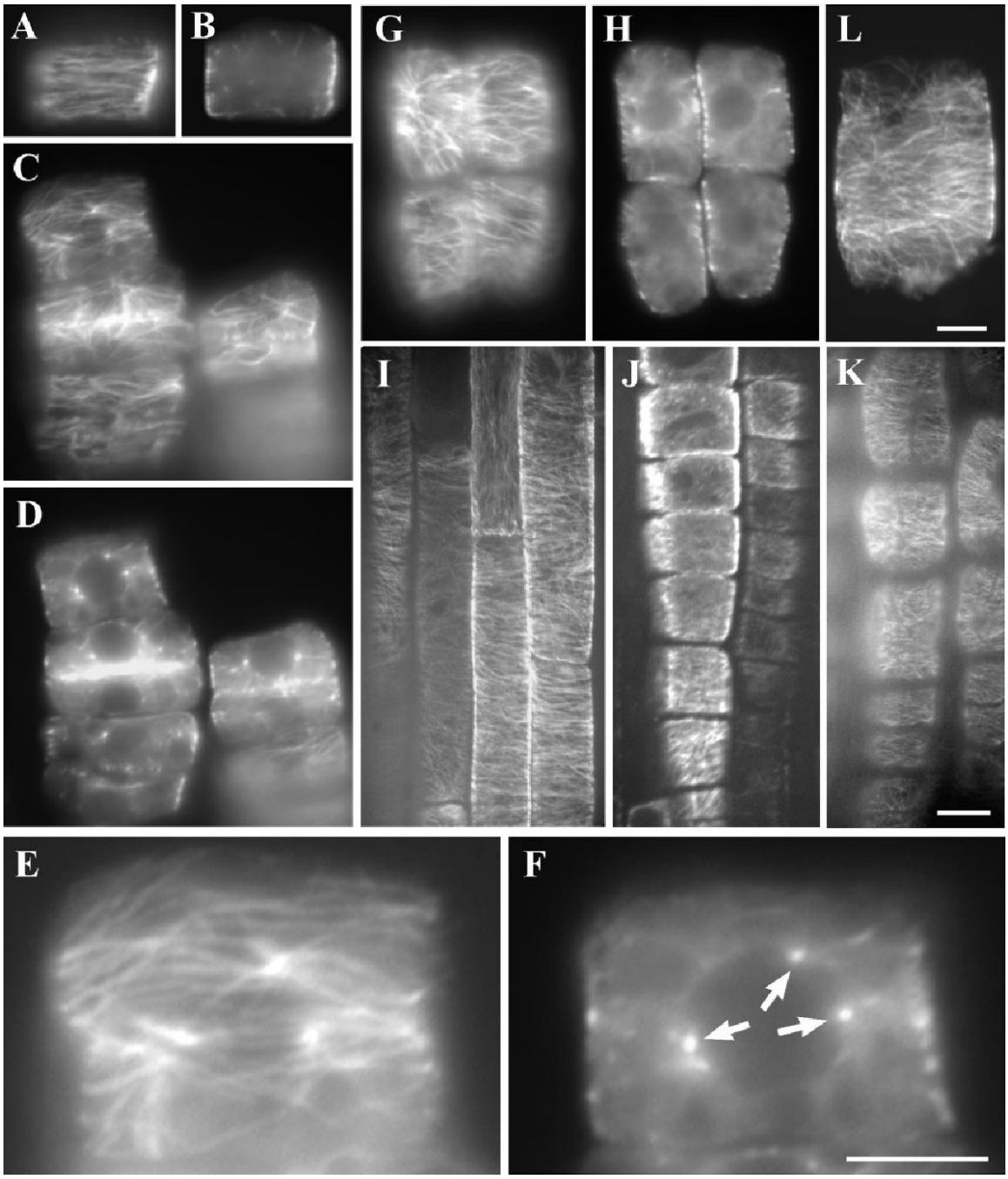

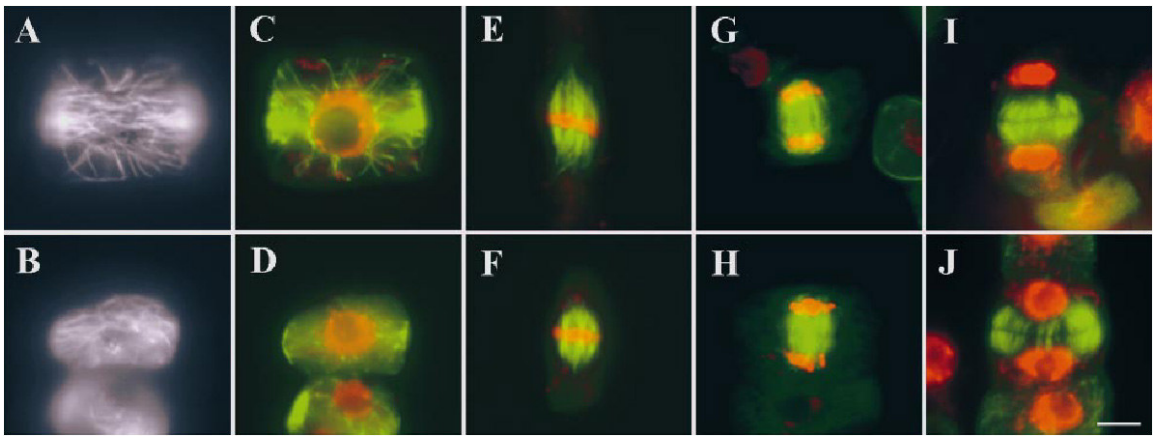

Figure 2.14. Immunostaining of Microtubules in Dividing Root Cells of Wild Type and *fra2*.

Microtubules were pseudocolored in green, and DNA was pseudocolored in red in (C) to (J).

(A) to (D) The microtubules in early broad preprophase bands in a wild-type cell ([A] and [C]), and a *fra2* mutant cell ([B] and [D]). (A) and (B) were in the focus at the cell cortex, and (C) and (D) were in the middle.

(E) and (F) Metaphase spindles in wild-type (E) and *fra2* mutant (F) cells.

(G) and (H) Microtubule spindles between two sets of segregated chromatids of a wild-type cell (G) and a *fra2* mutant cell (H) during late anaphase.

(I) and (J) Typical phragmoplast microtubule arrays in a wild-type cell (I) and a *fra2* mutant cell (J). Microtubules have already started to depolymerize in the central region in the phragmoplast shown in (J). Bar in (J) = 5 μm for (A) to (J).

CHAPTER 3

ALTERATION OF ORIENTED DEPOSITION OF CELLULOSE MICROFIBRILS BY MUTATION OF A KATANIN-LIKE MICROTUBULE-SEVERING PROTEIN[1]

[1]Burk, D.H., and Ye, Z.-H. 2002. Plant Cell. 14:2145-2160.

ABSTRACT

It has long been hypothesized that cortical microtubules (MTs) control the orientation of cellulose microfibril deposition, but no mutants with alterations of MT orientation have been shown to affect this process. We have previously shown that in *Arabidopsis thaliana* the *fra2* mutation causes aberrant cortical MT orientation and reduced cell elongation, and the gene responsible for the *fra2* mutation encodes a katanin-like protein. In this study, using field emission scanning electron microscopy, we found that the *fra2* mutation altered the normal orientation of cellulose microfibrils in walls of expanding cells. While cellulose microfibrils in walls of wild-type cells were transversely oriented along the elongation axis, cellulose microfibrils in walls of *fra2* cells often formed bands and ran in different directions. The *fra2* mutation also caused aberrant deposition of cellulose microfibrils in secondary walls of fiber cells. The aberrant orientation of cellulose microfibrils was shown to be correlated with disorganized cortical MTs in several cell types examined. In addition, the thickness of both primary and secondary cell walls was significantly reduced in the *fra2* mutant. These results indicate that the katanin-like protein is essential for oriented cellulose microfibril deposition and normal cell wall biosynthesis. We further demonstrated that the Arabidopsis katanin-like protein possessed MT-severing activity in vitro, thus it is an ortholog of animal katanin. We propose that the aberrant MT orientation caused by mutation of katanin results in the distorted deposition of cellulose microfibrils, which in turn leads to a defect in cell elongation. These findings strongly support the hypothesis that cortical MTs regulate the oriented deposition of cellulose microfibrils that determines the direction of cell elongation.

INTRODUCTION

Newly divided cells in plants undergo significant elongation before they mature into different cell types, such as fiber cells, tracheary elements, and sieve elements. The direction and degree of elongation determine the morphology of cells, thus, dissecting the molecular mechanisms regulating cell elongation will help us understand cellular morphogenesis. Because plant cells are encased in rigid cell walls made of networks of cellulose, hemicellulose, and other matrix components, the patterned deposition of cell walls and subsequent loosening of the cell wall networks are critical for the directional elongation of cells. Cellulose microfibrils, which are deposited in a transverse direction along the axis of elongating cells, have been proposed to control cellular morphogenesis (Green, 1962). Disruption of the normal deposition of cellulose microfibrils by mutation of a cellulose synthase gene in the temperature sensitive *rsw1* mutant is correlated with alteration of cell elongation (Sugimoto et al., 2001). The transverse deposition of cellulose microfibrils along the axis of elongating cells presumably allows directional expansion through loosening of the cellulose and hemicellulose network. Enzymes such as expansins are proposed to be involved in the cell wall loosening process during cell elongation (Cosgrove, 1988).

The transverse deposition of cellulose microfibrils along the long axis of elongating cells has long been proposed to be controlled by the transversely oriented cortical microtubules (MTs) lying underneath the plasma membrane, a hypothesis called MT/microfibril parallelism. Two lines of evidence support this hypothesis. First, cortical MTs often align in parallel with cellulose microfibrils in elongating cells. Since the first observation by Ledbetter and Porter (1963), the coalignment of MTs and microfibrils has been confirmed in both algae and land plants (Giddings and Staehelin, 1991; Baskin, 2001). Second, alteration of the orientation of cortical MTs by drugs has been shown to cause changes in the oriented deposition of cellulose microfibrils (Giddings and Staehelin, 1991; Baskin, 2001). Treatment with MT depolymerizing drugs, such as

colchicine and amiprophos-methyl, causes randomization of both MTs and newly-deposited cellulose microfibrils. Treatment with taxol, a MT-stabilizing drug, results in stabilization of MT patterns and concomitant coalignment of cellulose microfibrils. The coalignment of MTs and microfibrils has been demonstrated in both elongating cells and cells undergoing secondary wall thickening (Baskin, 2001).

Although it seems certain that cortical MTs control the orientation of cellulose microfibril deposition, which determines the direction of cell elongation, there are some exceptions that appear not to favor MT/microfibril parallelism (Preston, 1988). It has been observed that cellulose microfibrils appear to be transversely oriented earlier than do cortical MTs before the onset of cell elongation, which questions the obligate nature of MT/microfibril parallelism (Sugimoto et al., 2000; Wasteneys, 2000). In addition, cells with tip growth such as pollen tubes and root hairs obviously do not exhibit the coalignment of MTs and cellulose microfibrils, indicating that cellulose microfibril deposition in tip growing cells is independent of MT orientation (Emons et al., 1992). An alternative hypothesis has been proposed which states that the coalignment of MTs and cellulose microfibrils might be determined by cellular geometry rather than by MT control of microfibril order (Emons and Mulder, 1998). It has also been suggested that simultaneous alteration of the orientations of MT and cellulose microfibrils by pharmacological drugs could be caused by a disruption of cell growth which evokes a second parameter that could be responsible for the observed effect (Emons et al., 1992). Due to these exceptions, it is necessary to use genetic tools to further investigate the phenomenon of MT/microfibril parallelism. Use of mutants with direct alteration of cortical MTs or cellulose microfibril patterns could eliminate possible nonspecific effects that may occur with the use of pharmacological drugs. Cellulose microfibrils have been proposed to be able to impose the orientation of MTs (Williamson, 1990; Emons et al, 1992), and this is substantiated by pharmacological studies showing that drug inhibition of cellulose synthesis could alter the pattern of MTs (Fisher and Cyr, 1998). However,

study of the *rsw1* mutant which has a defect in cellulose biosynthesis demonstrates that while the orientation of cellulose microfibrils in the mutant is dramatically distorted, the cortical MT pattern retains an appearance of that in the wild type (Sugimoto et al., 2001). It was therefore proposed that there is no direct control of MT orientation by cellulose microfibrils.

Several Arabidopsis mutants, such as *fass* (Torres-Ruiz and Jürgens, 1994; McClinton and Sung, 1997), *ton1* and *ton 2* (Traas et al., 1995; Thion et al., 1998), *cho* (Mayer et al., 1999), *hal* (Mayer et al., 1999), *pfi* (Mayer et al., 1999), *por* (Mayer et al., 1999), *fra2/bot1* (Bichet et al., 2001; Burk et al., 2001), and *mor1* (Whittington et al., 2001), have been shown to alter cortical microtubule patterns and affect cellular morphology. Genes of two of these mutants have been cloned and characterized. The *MOR1* gene encodes a large MT-associated protein that is required for MT stability, and mutation of the *MOR1* gene causes fragmentation of cortical MTs and swollen cells (Whittington et al., 2001). The gene responsible for the *fra2* mutation encodes a katanin-like protein (abbreviated as AtKTN1) that is essential for the normal cortical MT patterns during the initiation and continuation of cell elongation (Burk et al., 2001). The katanin-like protein, also abbreviated as AtKSS, appears to be localized in the cytoplasm and around the nuclear envelope (McClinton et al., 2001). Because MOR1 and katanin-like protein are directly involved in regulation of cortical MT patterns, these mutants offer ideal opportunities for testing roles of MTs in the control of oriented cellulose microfibril deposition.

Mutation of the katanin-like protein in the *fra2* mutant caused a dramatic reduction in the length and an increase in the width of all cell types examined except tip growing cells. Examination of MT organization in roots showed that the *fra2* mutation caused delays in the disassembly of perinuclear MT arrays and in the assembly of cortical MT arrays in expanding cells. As a result, cortical MTs in expanding cells of *fra2* did not show a uniform transverse orientation as seen in the wild type (Burk et al., 2001). The

defects in cell elongation and MT pattern have also been demonstrated in the *bot1* mutant (Bichet et al., 2001) which is believed to be allelic to the *fra2* mutant. The correlation between the disruption of normal cortical MT pattern and reduction in cell elongation in the *fra2/bot1* mutants suggests a direct role of MTs in the control of cell elongation. In this study, we investigate whether the altered MT pattern caused by the *fra2* mutation affects the oriented deposition of cellulose microfibrils. Using field emission scanning electron microscopy, we show that the *fra2* mutation dramatically alters the orientation of cellulose microfibrils in expanding cells. While cellulose microfibrils in elongating cells of the wild type run in a transverse direction along the long axis, microfibrils in expanding cells of *fra2* often form bands and run in different directions. We also show that cortical MTs in cells of *fra2* stems and petioles are severely disorganized. In addition, the primary and secondary walls of *fra2* cells are significantly thinner than those of the wild type. We demonstrate that the Arabidopsis katanin-like protein possesses in vitro MT-severing activity. These results suggest that the katanin-like protein, through influencing MT patterns, affects the oriented deposition of cellulose microfibrils, cell wall biosynthesis, and directional cell elongation.

RESULTS

ORIENTATION OF CELLULOSE MICROFIBRILS IN ELONGATING ROOT CELLS

Arabidopsis primary roots are an ideal source for examination of cells at different phases of cell elongation. It has been shown that cells at the early elongating, rapidly elongating or late elongating phases all have cortical MTs transversely aligned along the axis of elongation (Sugimoto et al., 2000). In parallel with the MT orientation, cellulose microfibrils at the innermost layer of the cell wall are also positioned in a transverse pattern (Sugimoto et al., 2000; Figure 1). This indicates that Arabidopsis roots are an excellent system to investigate roles of MTs in the oriented deposition of microfibrils and cell elongation. We have previously shown that mutation of a katanin-like protein in the

fra2 mutant causes alterations in cortical MT orientation and cell elongation (Burk et al., 2001). To investigate whether the *fra2* mutation reduces cell elongation by altering cellulose microfibril deposition, we examined the orientation of cellulose microfibrils in elongating root cells of the wild type and the *fra2* mutant (Figures 3.1 and 3.2). Using field emission scanning electron microscopy, we visualized cellulose microfibrils in the innermost layer of cell walls that represent the most recently deposited microfibrils. After exiting the apical meristem zone, cortical cells of *fra2* roots (Figure 3.2A) underwent much less elongation compared with the wild type (Figure 3.1A). Cellulose microfibrils in walls of cortical cells from expanding regions of *fra2* roots (Figures 3.2B and 3.2C) were dramatically distorted in orientation compared with the uniform transverse orientation seen in the wild type (Figures 3.1B to 3.1E). Some microfibrils appeared to form bands in groups of 8 to 12 individuals and ran in different directions with twists and turns. It was noticed that some microfibril bands made a 180^{o}C turn within a small area (Figures 3.2B and 3.2C). These results clearly indicated that the *fra2* mutation altered the oriented deposition of cellulose microfibrils in elongating root cells.

ORIENTATION OF CORTICAL MTS IN ELONGATING ROOT CELLS

Previous work has shown that the cortical MT orientation in root cells of *fra2*/*bot1* is altered (Bichet et al., 2001; Burk et al., 2001), but no clear, detailed images of cortical MT pattern in cells from early expanding and rapidly expanding regions of *fra2*/*bot1* roots have been shown. To investigate in detail the cortical MT pattern in elongating cells of the wild type and *fra2* mutant, we performed immunoflorescence labeling of MTs in root cells.

In wild-type roots (Figure 3.3A), cortical MTs were transversely oriented along the long axis of both early elongating and rapidly elongating cells (Figures 3.3B and 3.3C). In contrast, in *fra2* roots (Figure 3.4A), cortical MTs in early expanding cells were severely disoriented (Figures 3.4B to 3.4E) and ran in different directions (Figures 3.4F to 3.4H). It was noted that cortical MTs in some regions of cells aligned in a nearly

transverse orientation (Figures 3.4B and 3.4C). It was evident that many cortical MTs converged at some common sites in both early expanding (Figures 3.4D and 3.4E) and rapidly expanding (Figure 3.4H) cells, a pattern similar to the aster-like MTs seen around the perinuclear envelope of the *fra2* cells during the initiation of cell expansion (Burk et al., 2001).

Optical sectioning through the nuclear envelope did not show any apparent convergent MT sites around the nuclear envelope in the expanding *fra2* cells (data not shown). It appeared that the elongation of epidermal cells (Figure 3.4A) in *fra2* roots was less affected than that of cortical cells (Figure 3.2A). These results indicated that the *fra2* mutation caused a dramatic alteration in the orientations of both cortical MTs and cellulose microfibrils during different stages of cell elongation in roots.

ORIENTATION OF CELLULOSE MICROFIBRILS IN ELONGATING CELLS OF HYPOCOTYLS, STEMS AND PETIOLES

Because the *fra2*/*bot1* mutations cause a dramatic reduction in cell length in all organs, such as roots, hypocotyls, stems, leaf blades, petioles and floral organs (Bichet et al., 2001; Burk et al., 2001), we investigated whether an alteration in the oriented cellulose microfibril deposition occurred in other organs in addition to roots. In walls of elongating cortical cells of wild-type hypocotyls (Figure 5A), cellulose microfibrils were transversely oriented along the axis of elongation (Figure 5B). In contrast, the microfibril orientation was apparently disorganized in walls of expanding cortical cells of *fra2* hypocotyls (Figures 3.5C and 3.5D). Like the microfibrils in walls of expanding root cells, it appeared that groups of 6 to 12 microfibrils often formed bands that ran in different directions.

The most severely affected cell types by the *fra2* mutation were pith cells in inflorescence stems and parenchyma cells in petioles (Burk et al., 2001). These cells were often isodiametric in the mutant instead of cylindrical as seen in the wild type. Some of the *fra2* pith cells were so severely reduced in length that the cell width was longer than

the length (Burk et al., 2001). Field emission scanning electron microscopy showed that the microfibrils in the walls of *fra2* pith and petiole cells were also affected.

In wild-type elongating pith cells (Figure 3.6A), cellulose microfibrils ran in parallel and were oriented in a transverse direction (data not shown), or with a small angle relative to the transverse direction (Figure 3.6B). In expanding pith cells of *fra2* (Figure 3.6C), the cellulose microfibrils often formed bands and were oriented in different directions (Figure 3.6D). Similarly, cellulose microfibrils in walls of parenchyma cells of petioles were transversely oriented along the elongating axis in the wild type (Figures 3.7A and 3.7B), whereas bands of microfibrils ran in various directions in the *fra2* mutant (Figures 3.7C and 3.7D). Together, these results indicated that the *fra2* mutation dramatically altered the cellulose microfibril deposition pattern in primary walls of elongating cells from various organs.

ORIENTATION OF CELLULOSE MICROFIBRILS IN THE SECONDARY WALL OF FIBER CELLS

Arabidopsis inflorescence stems develop interfascicular fiber cells next to the endodermis (Zhong et al., 1997 and 2001). Interfascicular fiber cells in the *fra2* mutant have shortened length and reduced thickness of secondary cell walls (Burk et al., 2001). To investigate whether the *fra2* mutation affects the oriented cellulose microfibril deposition during secondary wall formation, we examined the orientation of cellulose microfibrils in the innermost layer of walls of mature fiber cells.

Cellulose microfibrils in the middle part of wild-type fiber cells uniformly ran in the same direction with an angle of 15 to 25 degrees relative to the transverse orientation (Figures 3.8A and 3.8B). At the tip of fiber cells, cellulose microfibrils ran in parallel with the elongation axis (data not shown). By contrast, the orientation of cellulose microfibrils in secondary walls of *fra2* fiber cells was severely distorted (Figures 3.8C and 3.8D). Cellulose microfibrils often formed bands and ran in different directions in a

swirl-like pattern. This indicated that the *fra2* mutation also altered the pattern of cellulose microfibril deposition in secondary walls of fiber cells.

QUANTITATIVE ANALYSIS OF CELLULOSE MICROFIBRIL ORIENTATIONS

The above results have clearly shown that the orientation of cellulose microfibrils in *fra2* cell walls was altered compared with that in wild-type cell walls (Figures 3.1, 3.2, 3.5-3.8). To quantify the degree of distortion of cellulose microfibril orientation in *fra2* cell walls, we measured the angles of individual cellulose microfibrils. Most microfibrils in the walls of wild-type root (Figure 3.9A) and pith (Figure 3.9B) cells were transversely oriented with <30° deviation from the transverse direction. Cellulose microfibrils in walls of *fra2* root (Figure 3.9A) and pith (Figure 3.9B) cells had a much wider angle of deviation from the transverse orientation, especially those in walls of pith cells that lacked predominant angle peaks. This finding indicated that cellulose microfibrils in *fra2* cells were oriented more randomly than those in wild-type cells.

ORIENTATION OF CORTICAL MTS IN ELONGATING CELLS OF STEMS AND PETIOLES

Because we have demonstrated that the aberrant cellulose microfibril deposition in root cells was correlated with disorganized cortical MTs in the *fra2* mutant, we next investigated whether the altered cellulose microfibril deposition pattern in cells of other organs was also accompanied with disrupted pattern of cortical MTs. We performed immunolocalization of cortical MTs in stems and petioles. In elongating pith cells of the wild type, cortical MTs were oriented transversely along the elongation axis (Figure 3.10A). A close-up of wild-type cells showed that cortical MTs were aligned in parallel with a small degree of deviation (Figure 3.10B). Visualization of cortical MTs in *fra2* pith cells showed a sharp contrast to those in wild-type cells. Cortical MTs in *fra2* cells were oriented aberrantly and lost their typical parallel alignment pattern (Figure 3.10C). It was noted that a few cells had cortical MTs oriented in a nearly transverse pattern. A close-up of MTs in *fra2* cells clearly showed the aberrant organization of cortical MTs (Figures 3.10D and 3.10E) compared with the wild type (Figure 3.10B). Furthermore,

many cortical MTs in *fra2* cells appeared to converge into some common sites. Quantitative analysis of cortical MT angles showed that most cortical MTs in wild-type pith cells were oriented transversely, with <20° deviation from the transverse direction, whereas those in *fra2* pith cells were oriented in various angles with a wide deviation from the transverse direction (Figure 3.11).

Immunolocalization of cortical MTs in petioles of the wild type and *fra2* showed patterns similar to those in stems (Figure 3.12). Although cortical MTs in wild-type cells were transversely aligned along the elongation axis (Figure 3.12A), those in *fra2* cells apparently were disorganized and often converged to some common sites (Figure 3.12B). These results demonstrate that the katanin-like protein is required for the normal transverse parallel alignment of cortical MTs, and the abnormal MT pattern is directly correlated with the aberrant deposition of cellulose microfibrils in the *fra2* mutant.

ANATOMICAL STRUCTURE OF PRIMARY AND SECONDARY WALLS

To investigate whether the distorted orientation of cellulose microfibrils affected cell wall morphology, we examined the ultrastructure of cell walls in the *fra2* mutant. Transmission electron microscopy revealed that interfascicular fiber cells in the *fra2* mutant were much larger in the radial dimension (Figure 3.13C) and that their walls were dramatically reduced in thickness (Figure 3.13D) compared with the same features in wild-type cells (Figures 3.13A and 3.13B).

In addition, although secondary walls of wild-type fiber cells were well stained and had distinct layers of wall thickening (Figure 3.13B), secondary walls of *fra2* fiber cells stained less and lacked clear layers of wall thickening (Figure 3.13D). The middle lamella of fiber cell walls in both wild type and *fra2* were well stained (Figures 3.13B and 3.13D). Additionally, the inner wall surface of wild-type fiber cells was smooth (Figure 3.13B), whereas the inner wall surface of *fra2* fiber cells appeared undulated (Figure 3.13D).

Similarly, examination of pith cells in the inflorescence stems showed that the wall thickness was significantly reduced and the inner wall surface was uneven in the *fra2* mutant (Figures 3.14B and 3.14C) compared with the wild type (Figure 3.14A). Quantitative analysis showed that the wall thickness of *fra2* pith cells and fiber cells was reduced to 63% and 58% of that in the wild type, respectively (Table 3.1). Longitudinal sections of fiber and pith cells did not show dramatic alterations in surface area of these cells between the wild type and the *fra2* mutant (Burk et al., 2001). This indicated that the *fra2* mutation dramatically affected the wall thickening of both pith cells and fiber cells.

Table 1. Wall Thickness of Pith Cells and Fiber Cells in the Wild Type and the *fra2* Mutant

	Wall Thickness (μm)[a]	
Cell Type	Pith Cell[b]	Fiber Cell[c]
Wild type	0.35 ± 0.09	2.09 ± 0.50
fra2	0.22 ± 0.07	1.21 ± 0.41

[a] Wall thickness was measured from transmission electron micrographs of cells. Data shown are means ±SE from 15 to 20 cells.
[b] Pith cells from nonelongating internodes of inflorescence stems were used for the measurement of wall thickness.
[c] Interfascicular fiber cells from nonelongating internodes of inflorescence stems were used for the measurement of wall thickness.

THE ARABIDOPSIS KATANIN-LIKE PROTEIN POSSESSES IN VITRO MT-SEVERING ACTIVITY

The Arabidopsis katanin-like protein shows high sequence similarity to katanin from sea urchin, a protein known to sever MTs in vitro in an ATP-dependent manner (Hartman et al., 1998). Our finding that mutation of the katanin-like protein in the *fra2* mutant disrupts the normal pattern of cortical MTs in elongating cells supports roles of katanin in regulating MT organization. To confirm that the Arabidopsis katanin-like protein is a MT-severing protein, we tested its ability to sever MTs in vitro.

Recombinant Arabidopsis katanin-like protein expressed in insect cells was able to sever MTs (Figure 3.15). Taxol-stabilized, rhodamine-labeled MTs were fragmented into

much shorter lengths after 5 min of incubation with the recombinant protein (Figure 3.15B). The length of MTs was reduced from the original average of 28 μm to an average of 4 μm in length (Figures 3.15B and 3.15E). After 10 min of incubation, most MTs disappeared although a few very short MTs (<2 μm) were still visible (Figure 3.15C). When MTs were incubated with a control protein, they remained intact with an average length of 28 μm (Figures 3.15D and 3.15E). These results demonstrate that the Arabidopsis katanin-like protein does possess MT-severing activity in vitro. They suggest that it is an ortholog of animal katanin and it might affect MT patterns by controlling MT disassembly processes.

DISCUSSION

It has been proposed that cortical MTs undergo constant disassembly and assembly during cell elongation and their overall transverse orientation along the elongation axis regulates the transverse pattern of cellulose microfibril deposition (Cyr and Palevitz, 1995; Baskin, 2001). Our findings demonstrate that the Arabidopsis katanin is essential for normal cortical MT patterns and the oriented deposition of cellulose microfibrils during cell elongation. These results provide genetic evidence in support of the hypothesis that cortical MTs control the pattern of cellulose microfibril deposition (Baskin, 2001).

ARABIDOPSIS KATANIN IS ESSENTIAL FOR THE TRANSVERSE ORIENTATION OF CORTICAL MTS

After cells exit from cytokinesis, MTs first appear around the nuclear envelope as a perinuclear MT array. MTs extend from the perinuclear area into the cortical region during the initial stage of cell expansion. It has been proposed that the MT nucleation sites are located around the nuclear envelope, and that cortical MTs originate from these nucleation sites (Hasezawa and Hagata, 1991; Hagata et al., 1994; Hasezawa et al.,

2000). During cell elongation, cortical MTs must adjust their orientation constantly to keep up with the increasing cell length. This constant change in MT organization, or MT dynamics, was proposed to be performed by the rapid disassembly, assembly, and translocation of MTs (Cyr and Palevitz, 1995).

The findings that the *fra2* mutation delays the disappearance of the perinuclear MT array during the initiation of cell elongation (Burk et al., 2001) and alters the normal cortical MT pattern throughout cell elongation (Figure 3.4) indicate that the katanin-like protein is essential for the normal MT patterns found during both the initiation and the continuation of cell elongation. The Arabidopsis katanin-like protein has been shown to possess MT-severing activity (Figure 3.15); thus, it is an ortholog of animal katanin and it most likely functions in the disassembly of the perinuclear MT array during the initiation of cell elongation (Figure 3.16A).

Disassembly of the perinuclear MT array by Arabidopsis katanin could be mediated by releasing perinuclear MTs that are then translocated to the cortical region or by severing perinuclear MTs into dimers that are then reassembled into MTs in the cortical region. During cell elongation, katanin is likely involved in the disassembly of cortical MTs that is essential to establish a transverse orientation (Figure 3.16A). In our model, lack of katanin MT-severing activity causes a delay in the disassembly of perinuclear MTs and, consequently, a delay in the appearance of cortical MTs during the initiation of cell elongation (Figure 3.16B). During cell elongation, lack of katanin MT-severing activity causes an alteration in normal cortical MT dynamics that in turn results in aberrant orientations of cortical MTs (Figure 3.16B).

It is important to note that, in addition to the aster-like MT pattern seen around the nuclear envelope during the initiation of cell expansion in the *fra2* mutant (Burk et al., 2001), many cortical MTs also appeared to converge at some common sites in the cortical region of expanding *fra2* cells (Figures 3.4, 3.10, and 3.12). It has been proposed that cortical MTs are likely nucleated at the cortical region (Vaughn and Harper, 1998); thus,

these converged MT sites at the cortical region might be nucleation sites of cortical MTs during cell elongation. In the wild type, the katanin MT-severing activity might constantly release MTs from these sites, so that the converged MTs are not detectable. Lack of katanin MT-severing activity in the *fra2* mutant might cause a delay in the release of MTs from these sites, enabling the converged MTs to be visualized at the cortical region.

It is tempting to propose that a timely release of MTs from these converged sites by katanin is essential for formation of transversely oriented cortical MTs. A role of katanin MT-severing activity in the release of MTs from putative nucleation sites at the nuclear envelope and the cortical region is similar to the proposed roles of katanin MT- severing proteins in animal cells. Katanins in sea urchin embryonic cells (McNally et al., 1996; Hartman et al., 1998) and rat sympathetic neurons (Ahmad et al., 1999) are localized in centrosomes that are MT organization centers. Inactivation of katanin in neurons by microinjection of the katanin antibody resulted in a dramatic accumulation of MTs at the centrosome, indicating roles for katanin in the release of MTs from the centrosome (Ahmad et al., 1999). It will be very interesting to further investigate the nature of these converged MT sites in the *fra2* mutant.

Despite the observation that lack of katanin MT-severing activity in the Arabidopsis *fra2* mutant causes a delay in MT dynamics, cortical MTs ultimately appear in the cortical region, although in aberrant orientations. This fact indicates that katanin MT-severing activity is not the only mechanism involved in the regulation of MT dynamics. Other mechanisms, such as dynamic instability and treadmilling (Walczak, 2000), are also likely involved in the regulation of MT dynamics in plants. However, these other mechanisms apparently could not compensate fully for the loss of katanin MT-severing activity in Arabidopsis.

ARABIDOPSIS KATANIN IS REQUIRED FOR ORIENTED CELLULOSE MICROFIBRIL DEPOSITION AND CELL ELONGATION

The *fra2/bot1* mutations cause a dramatic reduction in cell length and an increase in cell width (Bichet et al., 2001; Burk et al., 2001). Because cellular morphology is determined by the ordered deposition of cellulose microfibrils, which is thought to be regulated by the pattern of cortical MTs (Baskin, 200; Wasteneys, 2000), it is conceivable that the altered cellular morphology caused by the *fra2/bot1* mutations could be a result of altered cellulose microfibril deposition. This notion was confirmed by field emission scanning electron microscopy showing the distorted orientation of cellulose microfibrils in walls of expanding cells of *fra2*.

Because Arabidopsis katanin is essential for normal MT patterns, we propose that katanin facilitates the transverse orientation of cortical MTs, which in turn dictates the ordered deposition of cellulose microfibrils during cell elongation (Figure 3.16A). Lack of katanin MT-severing activity in the *fra2* mutant causes the formation of abnormal cortical MT patterns, which in turn results in a distorted orientation of cellulose microfibrils, leading to a dramatic reduction in cell elongation (Figure 3.16B).

Our finding that mutation of the katanin gene in the *fra2* mutant alters the orientations of both cortical MTs and cellulose microfibrils provides genetic evidence of the roles that MTs play in the control of oriented cellulose microfibril deposition. Although previous studies have shown the coalignment of MTs and cellulose microfibrils and have documented the simultaneous alteration of their orientations by drugs, the hypothesis of MT and cellulose microfibril parallelism remains controversial (Wasteneys, 2000). Because animal katanin has been shown to target specifically to MTs (Hartman et al., 1998; Quarmby, 2000), it is unlikely that a lack of katanin MT-severing activity in plants would directly affect the movement of cellulose synthase complex in the plasma membrane. Instead, the altered orientation of cellulose microfibrils in the *fra2* mutant is

most likely a result of the aberrant orientation of cortical MTs caused by a lack of katanin MT-severing activity.

Therefore, our results support the hypothesis that cortical MTs regulate the ordered deposition of cellulose microfibrils during cell elongation (Baskin, 2001). However, we could not completely exclude the possibility that the aberrant deposition of cellulose microfibrils in the *fra2* mutant could be caused by the same mechanisms that account for the disorientation of cellulose microfibrils in the *rsw1* mutant (Sugimoto et al., 2001), although it is not known how the *rsw1* mutation causes aberrant orientations of cellulose microfibrils.

It is interesting that, unlike the uniformly aligned microfibrils in walls of wild-type cells, microfibrils in walls of *fra2* mutant cells often form bands and run in different directions. It was proposed that cortical MTs might regulate the oriented deposition of cellulose microfibrils by delimiting the path of cellulose synthase movement (Herth, 1980; Giddings and Staehelin, 1991). If this is the case, the aberrantly oriented MTs in *fra2* cells could cause abnormal delimitation of the path of cellulose synthase movement, which would lead to the formation of bands of microfibrils running in different directions.

In another model, it was hypothesized that cellulose synthase complexes might move directly along cortical MTs located underneath the plasma membrane. This model was first proposed by Heath (1974) and was supported experimentally by Hasezawa and Nozaki (1999). If this is the case, the aberrantly oriented and more stabilized cortical MTs in *fra2* cells could provide prolonged tracks for the movement of cellulose synthase complexes and thus cause the formation of bands of microfibrils. In addition, it has been proposed that the movement of cellulose synthase complexes in the plasma membrane also might be constrained by cellular geometry (Emons and Mulder, 1998). This could explain why the orientations of cellulose microfibrils in *fra2* cells are abnormal but not completely random, although the aberrantly oriented MTs in *fra2* cells might lose their

control of the oriented deposition of cellulose microfibrils. The formation of aberrant cellulose microfibril bands is likely the cause of the uneven inner wall surfaces seen in both primary and secondary walls of *fra2* cells (Figures 3.13 and 3.14). This indicates that an ordered pattern of cortical MTs is not only essential for the oriented deposition of cellulose microfibrils but also important for the uniform thickening of cell walls around the cells.

In addition to its involvement in cell elongation, Arabidopsis katanin apparently is required for the normal branching of trichomes. In the *fra2* mutant, most trichomes have one branch point instead of two branch points seen in the wild type (Burk et al., 2001). Because katanin is essential for the normal organization of MTs, this indicates that the normal patterns of cortical MTs are important in branch initiation during trichome morphogenesis. The roles of cortical MTs in trichome branching have been demonstrated in drug inhibitor experiments (Mathur and Chua, 2000) and in the *fass* mutants, which are known to have altered MT patterns (Torres-Ruiz and Jürgens, 1994; McClinton and and Sung, 1997). Because trichome branching is an anisotropic growth process that needs localized loosening of cellulose microfibrils, the reduced branch formation in the *fra2* mutant might be caused by the altered deposition of cellulose microfibrils. It will be interesting to determine whether the patterns of MTs and cellulose microfibrils are altered in trichomes of the *fra2* mutant.

ARABIDOPSIS KATANIN IS REQUIRED FOR ORIENTED CELLULOSE MICROFIBRIL DEPOSITION DURING SECONDARY WALL THICKENING

In addition to a role in regulating cellulose microfibril deposition in primary walls of elongating cells, cortical MTs are proposed to regulate cellulose microfibril deposition during secondary wall thickening (Baskin, 2001). This is supported by our observation that mutation of the katanin gene in the *fra2* mutant causes aberrant orientations of cellulose microfibrils in fiber cell walls (Figure 3.8). Secondary walls of tracheids and fibers typically are composed of three distinct layers of cellulose microfibrils: S1, S2 and

S3. The S1 and S3 layers have cellulose microfibrils in a flat helix, and the S2 layer has cellulose microfibrils in a steep helix (Harada and Cote, 1985). Cellulose microfibrils in secondary walls have been shown to be aligned in parallel with underlying cortical MTs (Robards and Kidwai, 1972; Seagull, 1992; Abe et al., 1994 and 1995; Prodhan et al., 1995), suggesting that the cortical MTs undergo dynamic changes to form three distinctly oriented patterns during different stages of secondary wall thickening. Our finding that secondary walls of *fra2* fiber cells lack distinct layers indicates that katanin is essential for formation of distinct layers of cellulose microfibrils during secondary wall thickening.

MICROTUBULE DYNAMICS IS REQUIRED FOR NORMAL CELL WALL BIOSYNTHESIS

Although cortical MTs are believed to regulate the orientation of cellulose microfibrils, it was proposed that they do not affect the biosynthesis of cellulose and other cell wall components (Seagull and Falconer, 1991). This idea was based on early pharmacological studies showing that a disturbance of cortical MT organization alters the pattern of cellulose microfibril deposition but does not affect cellulose biosynthesis. However, the effects of cortical MT alterations on cell wall biosynthesis could not be determined easily in drug-treated cells. The *fra2* mutation was shown to reduce the amount of cellulose and hemicellulose and increase the condensation of lignin in total cell wall extracts of stems (Burk et al., 2001). The overall reduction of cell wall components apparently occurs in both primary and secondary walls, as revealed by transmission electron microscopy (Figures 3.13 and 3.14). This finding indicates that the normal MT pattern is essential not only for the oriented deposition of cellulose microfibrils but also for normal cell wall biosynthesis during primary and secondary wall formation. It is likely that the aberrant MT pattern in *fra2* cells causes a decrease in the rate of cellulose synthase movement, which leads to a reduced amount of cellulose synthesis.

METHODS

MATERIALS

Wild type and *fra2 Arabidopsis thaliana* seeds were germinated on Murashige-Skoog (1962) medium on vertically placed plates and grown in a growth chamber at 24°C under a 16-h-light/8-h-dark photoperiod. Hypocotyls and roots from 3-day-old seedlings were used for the visualization of microtubules (MTs) or cellulose microfibrils. Stems and petioles used for the visualization of cellulose microfibrils were from plants grown in soil in a growth room at 22 °C under a 12-h-light/12-h-dark photoperiod. The first emerging elongating internodes of inflorescence stems were used for the examination of MT and cellulose microfibrils in pith cells. The basal nonelongating internodes of inflorescence stems of 8-week-old plants were used for the examination of cellulose microfibrils in fiber cells.

FIELD EMISSION SCANNING ELECTRON MICROSCOPY OF CELLULOSE MICROFIBRILS

Cellulose microfibrils at the innermost layer of cell walls were visualized using field emission scanning electron microscopy according to Sugimoto et al. (2000). Whole roots and hypocotyls were fixed directly, and elongating stems and petioles were cut longitudinally using a double-edge razor blade before fixation. Mature stems were cut longitudinally through the interfascicular fiber region using a dissection microscope before fixation. Roots and hypocotyls were sectioned longitudinally using a cryo-ultramicrotome (model MT6000-XL with CR2000 attachment, RMC Inc., Tucson, AZ).

After treatment, tissues were dried in a Samdri critical point dryer (Tousimis, Rockville, MD) before being mounted on stubs with carbon paste. Samples were coated with platinum using an Edwards 306 vacuum evaporator (Edwards High Vacuum International, Wilmington, MA), and viewed for cellulose microfibrils under a LEO 982 FE scanning electron microscope (LEO, Thornwood, NY).

IMMUNOLOCALIZATION OF MTS

MTs were visualized by immunolabeling α-tubulins according to Sugimoto et al. (2000). Roots from 3-day old seedlings and young elongating petioles and stems were used for MT localization. Samples were probed first with mouse monoclonal antibody against chicken α-tubulin (1:800 dilution; Sigma) and then incubated with fluorescein isothiocyanate-conjugated goat antibody against mouse IgG (1:800 dilution; Sigma). MTs were visualized using a Leica TCS SP2 spectral confocal microscope (Leica Microsystems, Heidelberg, Germany). Images were saved and processed with Adobe Photoshop version 5.0 software (Adobe, San Jose, CA).

TRANSMISSION ELECTRON MICROSCOPY

Tissues were fixed in 2% (v/v) glutaraldehyde in phosphate buffer (50 mM, pH 7.2) at 4 ^{o}C overnight. After fixation, tissues were postfixed in 2% (v/v) OsO_4 for 2 hr. After being washed in phosphate buffer, tissues were dehydrated in ethanol, infiltrated with Araldite/Embed 812 resin (Electron Microscopy Sciences, Fort Washington, PA), and finally polymerized in Araldite/Embed resin. For electron microscopy, 90-nm-thick sections were cut with a Reichert-Jung ultrathin microtome (C. Reichert Optische Werke AG, Vienna, Austria), mounted on formvar-coated gold slot grids, and post-stained with uranyl acetate and lead citrate. Cell wall structure was visualized with a Zeiss EM 902A electron microscope (Jena, Germany).

QUANTITATIVE ANALYSIS

Images of cellulose microfibrils at the innermost layer of the cell wall were obtained using a field emission scanning electron microscope and used for the measurements of cellulose microfibril angles. Briefly, three to four representative images of wild-type and *fra2* cell walls from different cells were reduced to a fixed size, and a grid was overlaid on the image so that 130 evenly spaced grid points were available for analysis. At each grid point, the angle of the single microfibril that passed through or was closest to the point was measured using the ruler tool of Adobe Photoshop 5.0.

The microfibril was traced along its length to a fixed distance ~0.24 μm from the grid point, and the angle was noted. If at any grid point the microfibrils were not resolved sufficiently for tracing, that point was discarded. All angles were measured relative to the axis perpendicular to the long axis of the cell. This perpendicular axis was arbitrarily given an angle of 0°. Using this method, microfibrils can approach angles of ±90° and correspond to fibrils approaching a longitudinal orientation in a left or right handed helix.

Images of cortical MTs were obtained using a confocal microscope and used for the measurement of cortical MTs. Representative images of wild type and *fra2* cells were overlaid with a grid so that at least 50 evenly spaced grid points were available for analysis within each cell. At selected grid points, the angle of the single MT that passed through or was closest to the point was measured using the ruler tool of Adobe Photoshop 5.0. The MT was traced along its length to a fixed distance ~1 μm from the grid point, and the angle was noted. All angles were measured relative to the axis perpendicular to the long axis of the cell, which is consistent with the measurement technique used for cellulose microfibril angle determination.

INSECT CELL EXPRESSION AND PURIFICATION OF RECOMBINANT ARABIDOPSIS KATANIN

Expression of His-tagged Arabidopsis katanin was performed with an InsectSelect System kit (Invitrogen, Carlsbad, CA). Sf9 cells were grown and maintained as a monolayer at 27^{o}C in TNM-FH medium plus 10% fetal bovine serum. Full-length Arabidopsis katanin cDNA containing a Kozak translation initiation sequence was cloned into BamHI and XbaI sites of the insect expression vector pIZ/V5-His to generate pIZ/AtKTN1-His. pIZ/V5-His vector contains the baculovirus immediate-early promoter OpIE2 that uses the host cell transcription machinery and does not require viral factor for the activation and expression of recombinant protein. pIZ/AtKTN1-His plasmid DNA was transfected into Sf9 cells with Insectin-Plus Liposomes (Invitrogen), and stable cell

lines were selected and maintained in zeocin-containing TNM-FH medium (Invitrogen) plus 10% fetal bovine serum.

Cells expressing recombinant Arabidopsis katanin were suspended in lysis buffer (50 mM Na-phosphate, pH 8.0, 300 mM NaCl, 2 mM $MgCl_2$, 20 mM imidazole, 0.05% [v/v] Nonidet P-40, 1 µg/mL aprotinin, 1 µg/mL leupeptin, and 0.1 mM phenylmethylsulfonyl fluoride) and freeze-thawed five times in a dry ice/ethanol bath and cold water. The cell lysate was centrifuged at 100,000*g* for 30 min to remove cell debris. His-tagged recombinant protein was purified on nickel-nitrilotriacetic acid agarose resin (Qiagen, Chatsworth, CA), and aliquots were frozen at -80°C until use.

MT-SEVERING ACTIVITY ASSAY

Rhodamine-labeled MTs were prepared by incubation of 5 mg/mL unlabeled tubulin and 5 mg/mL rhodamine-labeled tubulin (Cytoskeleton, Denver, CO) in PEM buffer (80 mM Na-PIPES, pH 6.9, 1 mM $MgCl_2$, 1 mM EGTA) containing 1 mM GTP and 5% glycerol at 37°C for 50 min. The MTs were stabilized by adding an equal volume of PEM buffer contaning 40 µM taxol and incubated for 10 min at 37°C. Taxol-stabilized, rhodamine-labeled MTs were kept at room temperature in the dark for 24 hr before being used for the severing assay. In our preparations, the MTs were 20 to 40 µm in length.

MT-severing assays were performed as described by Vale (1991). Briefly, purified recombinant Arabidopsis katanin was diluted 10-fold in assay buffer (20 mM Na-Hepes, pH 7.5, 1 mM $MgCl_2$, 0.1 M EGTA, 1 mM ATP, 20 µM taxol) and combined with fluorescent MTs in a tube by gentle pipetting with a cut tip. Two microliters of the mixture was gently pipetted with a cut tip onto the surface of glass slides and incubated at room temperature. Reactions were stopped at various times by adding 2 µL of 2% glutaraldehyde in PEM buffer containing 20 µM taxol onto the assay mixture and gently covering with a cover slip.

The length of MTs was viewed under a confocal microscope. The MT-severing assays were repeated three times, and similar results were obtained. Typical fields of view for each time point were recorded and measured for MT length distribution. Consistent with previous observations (Vale, 1991), this assay procedure did not cause shearing of long MTs. Although bundling of some long MTs occurred as described (Vale, 1991), the MT severing by recombinant Arabidopsis katanin was obvious. A control protein, His-tagged AtCTL1, a chitinase-like protein (Zhong et al., 2002) expressed in the Sf9 insect cells, was used as a control in the MT-severing activity assay.

Upon request, all novel material described in this publication will be made available in a timely manner for non-commercial research purposes. No restrictions or conditions will be placed on the use of any materials described in this paper that would limit their use on non-commercial research purposes.

ACKNOWLEDGMENTS

We thank R. Zhong for her assistance in recombinant katanin expression and MT-severing activity assay, J. Shields and M. Farmer for their help on scanning electron microscopy, E. Richardson and G. Freshour for their assistance with transmission electron microscopy, B. Palevitz for his helpful suggestions, and the coeditor and reviewer for their suggestions. D.H.B. was supported by a Plant Evolution Training Grant from the National Science Foundation. This work was supported by the Cooperative State Research, Education, and Extension Service, U.S. Department of Agriculture.

REFERENCES

Abe, H., Ohtani, J., and Fukazawa, K. (1994). A scanning electron microscopic study of changes in microtubule distributions during secondary wall formation in tracheids. IAWA J. 15, 185-189.

Abe, H., Funada, R., Imaizumi, H., Ohtani, J., Fukazawa, K. (1995). Dynamic changes in the arrangement of cortical microtubules in conifer tracheids during differentiation. Planta 197, 418-421.

Ahmad, F.J., Yu, W., McNally, F.J., and Baas, P.W. (1999). An essential role for katanin in severing microtubules in the neuron. J. Cell Biol. 145**,** 305-315.

Baskin, T.I. (2001). On the alignment of cellulose microfibrils by cortical microtubules: a review and a model. Protoplasma 215, 150-171.

Bichet, A., Desnos, T., Turner, S., Grandjean, O., and Höfte, H. (2001). *BOTERO1* is required for normal orientation of cortical microtubules and anisotropic cell expansion in Arabidopsis. Plant J. 25, 137-148.

Burk, D.H., Liu, B., Zhong, R., Morrison, W.H., and Ye, Z.-H. (2001). A katanin-like protein regulates normal cell wall biosynthesis and cell elongation. Plant Cell 13, 807-827.

Cosgrove, D.J. (1998). Cell wall loosening by expansins. Plant Physiol. 118, 333-339.

Cyr, R.J., and Palevitz, B.A. (1995). Organization of cortical microtubules in plant cells. Curr. Opin. Cell Biol. 7**,** 65-71.

Emons, A.M.C., Derksen, J., and Sassen, M.M.A. (1992). Do microtubules orient plant cell wall microtubules? Physiol. Plant. 84, 486-493.

Emons, A.M.C., and Mulder, B.M. (1998). The making of the architecture of the plant cell wall: how cells exploit geometry. Proc. Natl. Acad. Sci. USA 95, 7215-7219.

Fisher, D.D., and Cyr, R.J. (1998). Extending the microtubule/microfibril paradigm. Cellulose synthesis is required for normal cortical microtubule alignment in elongating cells. Plant Physiol. 116, 1043-1051.

Giddings, T.H., and Staehelin, L.A. (1991). Microtubule-mediated control of microfibril deposition: A re-examination of the hypothesis. In The Cytoskeletal Basis of Plant Growth and Form, C.W. Lloyd, ed (San Diego, CA: Academic Press), pp. 85-99.

Green, P.B. (1962). Mechanism for plant cellular morphogenesis. Science 138, 1404-1405.

Harada, T., and Coté, W.A. (1985). Structure of wood. In Biosynthesis and Biodegradation of Wood Components, T. Higuchi, ed (San Diego, CA: Acadimic Press), pp. 1-42.

Hartman, J.J., Mahr, J., McNally, K., Okawa, K., Iwamatsu, A., Thomas, S., Cheesman, S., Heuser, J., Vale, R.D., and McNally, F.J. (1998). Katanin, a microtubule-severing protein, is a novel AAA ATPase that targets to the centrosome using a WD40-containing subunit. Cell 93**,** 277-287.

Hasezawa, S., and Nagata, T. (1991). Dynamic organization of plant microtubules at the three distinct transition points during the cell cycle progression of synchronized tobacco BY-2 cells. Bot. Acta 104, 206-211.

Hasezawa, S., and Nozaki, H. (1999). Role of cortical microtubules in the orientation of cellulose microfibril deposition in higher-plant cell. Protoplasma 209, 98-104.

Hasezawa, S., Ueda, K., and Kumagai, F. (2000). Time-sequence observation of microtubule dynamics throughout mitosis in living cell suspensions of stable transgenic Arabidopsis. Direct evidence for the origin of cortical microtubules at M/G_1 interface. Plant Cell Physiol. 41, 244-250.

Heath, I.B. (1974). A unified hypothesis for the role of membrane bound enzyme complexes and microtubules in plant cell wall synthesis. J. Theor. Biol. 48, 445-449.

Herth, W. (1980). Calcofluor white and Congo red inhibit chitin microfibril assembly of *Poterioochromonas*: evidence for a gap between polymerization and microfibril formation. J. Cell Biol. 87, 442-450.

Ledbetter, M.C., and Porter, K.R. (1963). A "microtubule" in plant cell fine structure. J. Cell Biol. 19, 239-250.

Mathur, J., and Chua, N.-H. (2000). Microtubule stabilization leads to growth reorientation in Arabidopsis trichomes. Plant Cell 12, 465-477.

Mayer, U., Herzog, U., Berger, F., Inzé, D., and Jürgens, G. (1999). Mutations in the *PILZ* group genes disrupt the microtubule cytoskeleton and uncouple cell cycle progression from cell division in Arabidopsis embryo and endosperm. Eur. J. Cell Biol. 78, 100-108.

McClinton, R.S., Chandler, J.S., and Callis, J. (2001). CDNA isolation, characterization, and protein intracellular localization of a katanin-like p60 subunit from *Arabidopsis thaliana*. Protoplasma 216, 181-190.

McClinton, R.S., and Sung, Z.R. (1997). Organization of cortical microtubules at the plasma membrane in Arabidopsis. Planta 201**,** 252-260.

McNally, F.J., Okawa, K., Iwamatsu, A., and Vale, R.D. (1996). Katanin, the microtubule-severing ATPase, is concentrated at centrosomes. J. Cell Sci. 109**,** 561-567.

Murashige, T., and Skoog, F**.** (1962). A revised medium for rapid growth and bioassay with tobacco tissue cultures. Physiol. Plant. 15, 473-497.

Nagata, T., Kumagai, F., and Hasezawa, S. (1994). The origin and organization of cortical microtubules during the transition between M and G_1 phases of the cell cycle as observed in highly synchronized cells of tobacco BY-2. Planta 193, 567-572.

Preston, R.D. (1988). Cellulose-microfibril-oriening mechanisms in plant cells walls. Planta 174, 67-74.

Prodhan, A.K.M.A., Funada, R., Ohtani, J., Abe, H., and Fukazawa, K. (1995). Orientation of microfibrils and microtubules in developing tension-wood fibers of Japanese ash (*Fraxinus mandshurica* var. japonica). Planta 196, 577-585.

Quarmby, L. (2000). Cellular Samurai: katanin and the severing of microtubules. J. Cell Sci. 113: 2821-2827.

Robards, A.W., and Kidwai, P. (1972). Microtubules and microfibrils in xylem fibers during secondary wall formation. Cytobiologie 6, 1-21.

Seagull, R.W., and Falconer, M.M. (1991). In vitro xylogenesis. In The Cytoskeletal Basis of Plant Growth and Form, C.W. Lloyd, ed (San Diego, CA: Academic Press), pp. 183-194.

Sugimoto, K., Williamson, R. E., and Wasteneys, G. O. (2000). New techniques enable comparative analysis of microtubule orientation, wall texture, and growth rate in intact roots of Arabidopsis. Plant Physiol. 124, 1493-1506.

Sugimoto, K., Williamson, R. E., and Wasteneys, G. O. (2001). Wall architecture in the cellulose-deficient *rsw1* mutant of Arabidopsis thaliana: microfibrils but not microtubules lose their transverse alignment before microfibrils become unrecognizable in the mitotic and elongation zones of roots. Protoplasma 215, 172-183.

Thion, L., Mazars, C., Nacry, P., Bouchez, D., Moreau, M., Ranjeva, R., and Thuleau, P. (1998). Plasma membrane depolarization-activated calcium channels, stimulated by microtubule-depolymerizing drugs in wild-type *Arabidopsis thaliana* protoplasts, display constitutively large activities and a longer half-life in *ton2* mutant cells affected in the organization of cortical microtubules. Plant J. 13, 603-610.

Torres-Ruiz, R.A., and Jurgens, G. (1994). Mutations in the *FASS* gene uncouple pattern formation and morphogenesis in Arabidopsis development. Development 120**,** 2967-2978.

Traas, J., Bellini, C., Nacry, P., Kronenberger, J., Bouchez, D., and Caboche, M**.** (1995). Normal differentiation patterns in plants lacking microtubular preprophase bands. Nature 375**,** 676-677.

Vale, R.D. (1991). Severing of stable microtubules by a mitotically activated protein in Xenopus egg extracts. Cell 64, 827-839.

Vaughn, K.C., and Harper, J.D.I. (1998). Microtubule-organization centers and nucleating sites in landing plants. Int. Rev. Cytol. 181, 75-149.

Walczak, C.E. (2000). Microtubule dynamics and tubulin interacting proteins. Curr. Opin. Cell Biol. 12, 52-56.

Wasteneys, G.O. (2000). The cytoskeleton and growth polarity. Curr. Opin. Plant Biol. 3, 503-511.

Whittington, A.T., Vugrek, O., Wei, K.J., Hasenbein, N.G., Sugimoto, K., Rashbrooke, M.C., and Wasteneys, G.O. (2001). MOR1 is essential for organizing cortical microtubules in plants. Nature 411, 610-613.

Zhong, R., Burk, D.H., and Ye, Z.-H. (2001). Fibers. A model for studying cell differentiation, cell elongation, and cell wall biosynthesis. Plant Physiol. 126, 477-479.

Zhong, R., Stanley, J.K., Schroeder, B.P., and Ye, Z.-H. (2002). Mutation of a chitinase-like protein causes ectopic deposition of lignin, aberrant cell shapes, and overproduction of ethylene. Plant Cell 14, 165-179.

Zhong, R., Taylor, J.J., and Ye, Z.-H. (1997). Disruption of interfascicular fiber differentiation in an Arabidopsis mutant. Plant Cell 9**,** 2159-2170.

Figure 3.1. Visualization of Cellulose Microfibrils in the Innermost Layer of Walls of Wild-Type Root Cell Walls.

Roots of 3-day-old wild-type seedlings were sectioned longitudinally, and the cellulose microfibrils in the innermost layer of cell walls were observed using field emission scanning electron microscopy. Individual microfibrils are seen as distinct lines. The vertical direction of the cellulose microfibril images in all figures corresponds to the elongation axis. Square marks, if present, at the centers of the images in all figures are the result of beam focusing.

(A) Longitudinal section of a root showing early-elongating (arrow) and rapidly elongating (arrowhead) cells.

(B) and (C) Cellulose microfibrils of rapidly elongating cells showing a transverse orientation along the elongation axis.

(D) and (E) Cellulose microfibrils of early-elongating cells showing a transverse orientation along the elongation axis.

Bar in (A) = 50 μm; bar in (B) = 0.5 μm for (B) to (E).

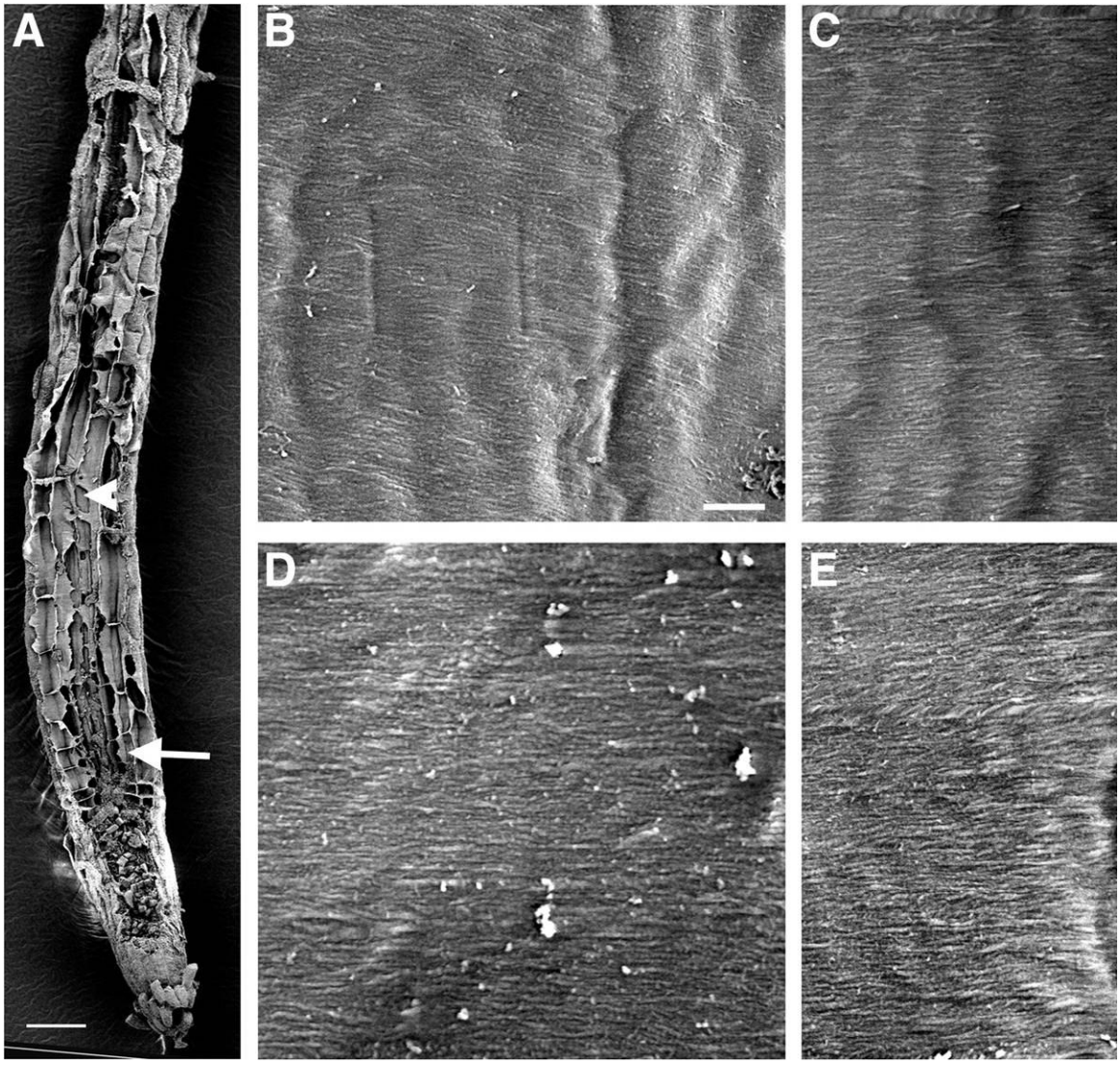
A
B
C
D
E

Figure 3.2. Visualization of Cellulose Microfibrils in the Innermost Layer of *fra2* Root Cell Walls.

(A) Longitudinal section of a root showing early-expanding (arrow) and rapidly expanding (arrowhead) cells.

(B) and (C) Cellulose microfibrils of rapidly expanding (B) and early-expanding (C) cells showing distorted orientations. Note that bands of microfibrils run in different directions. Bar in (A) = 50 µm; bar in (B) = 0.5 µm for (B) and (C).

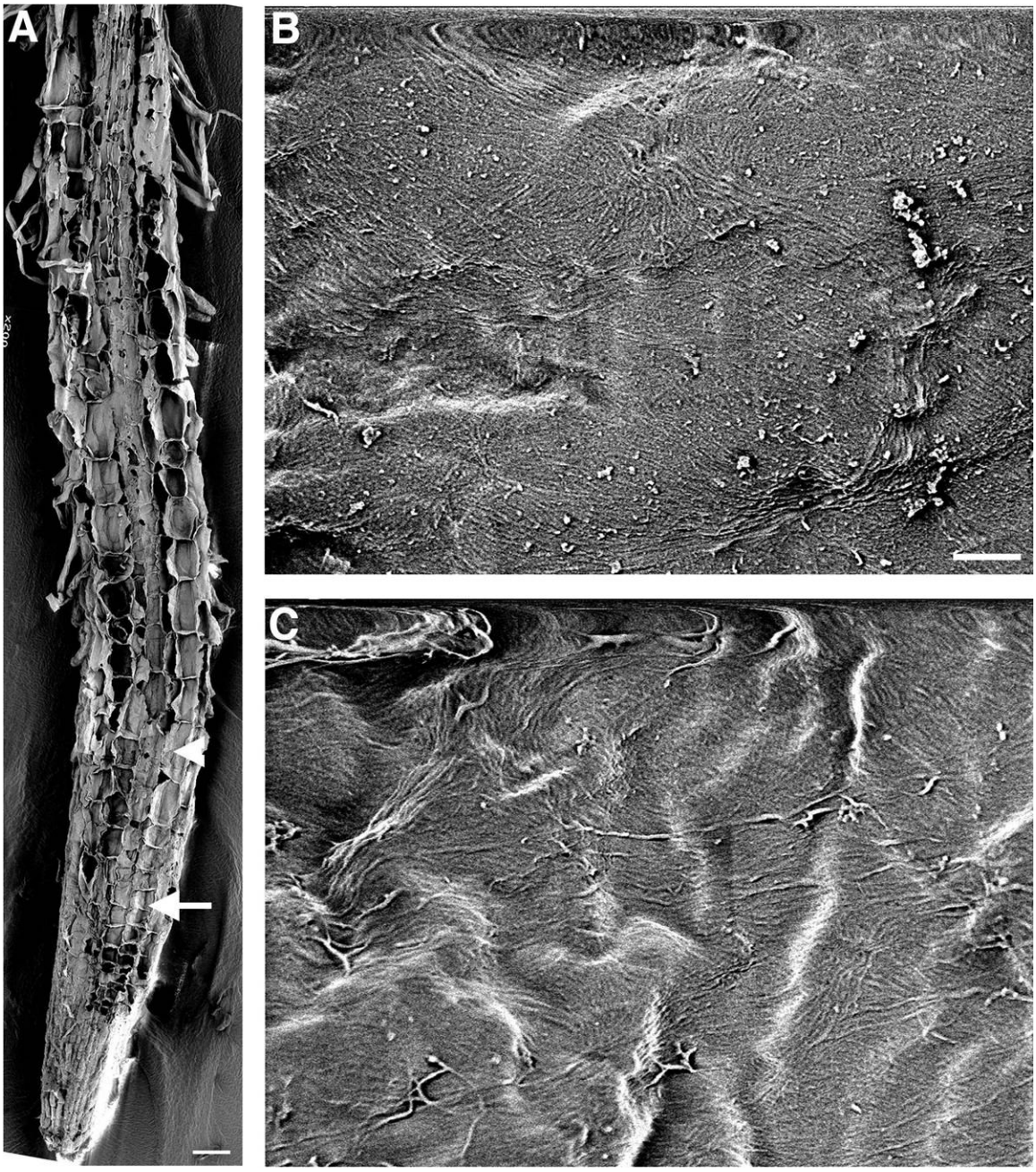
A
B
C

Figure 3.3. Visualization of Cortical MTs in Wild-Type Root Epidermal Cells.
Roots of 3-day-old seedlings were used for MT labeling with a monoclonal antibody against α-tubulin. Antibody-labeled MTs were detected with fluorescein isothiocyanate-conjugated secondary antibodies, and the signals of fluorescent MTs (green) were visualized under a confocal microscope. Double-headed arrows indicate the elongation axis.

(A) View of a whole root tip showing root cap cells (asterisk), early elongating cells (arrow) and rapidly elongating cells (arrowhead).

(B) Rapidly elongating cells showing the transverse orientation of cortical MTs.

(C) Early elongating cells showing the transverse orientation of dense cortical MTs.

Bar in (A) = 40 μm; bars in (B) and (C) = 8 μm.

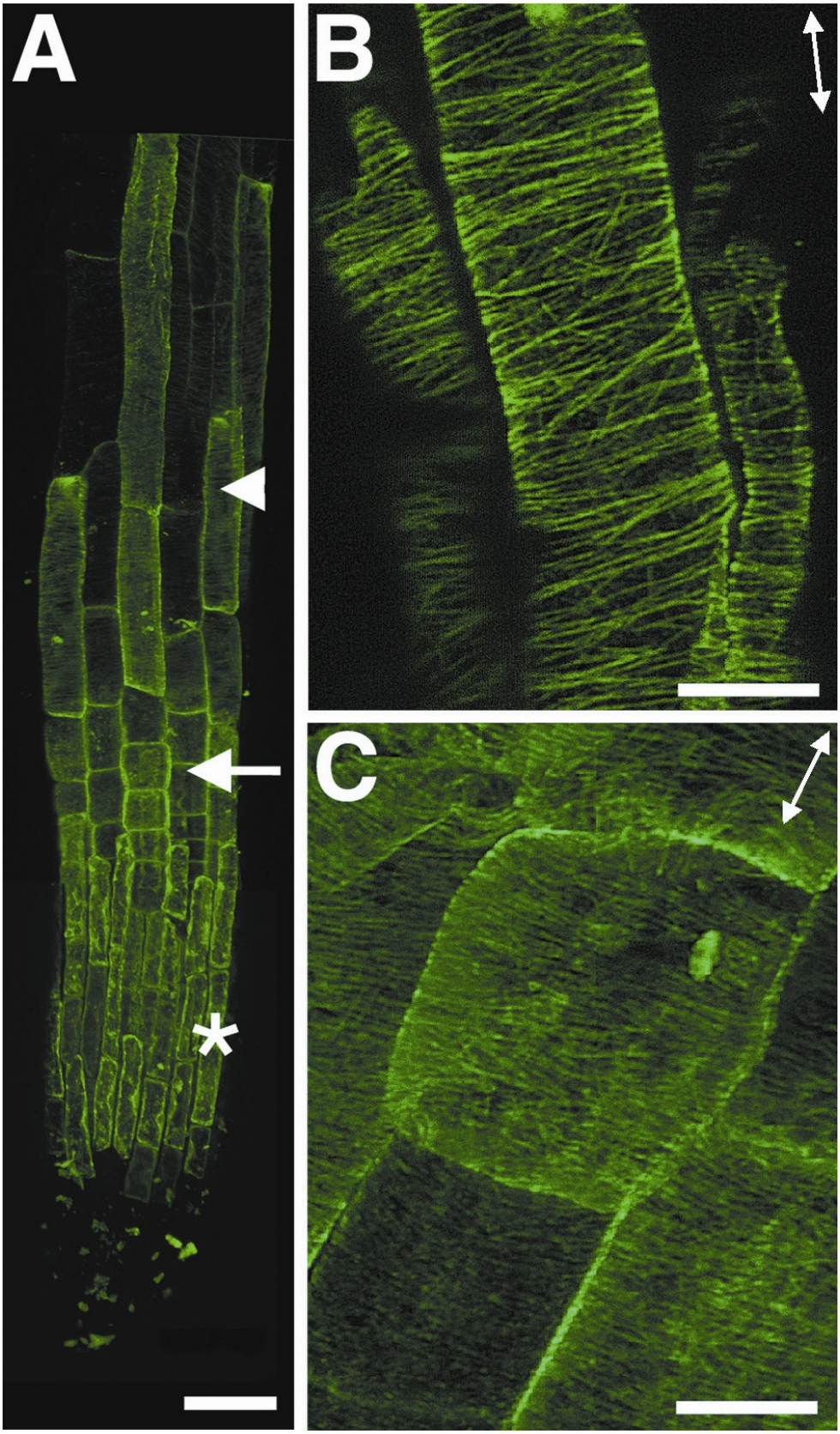
A
B
C

Figure 3.4. Visualization of Cortical MTs in *fra2* Root Epidermal Cells.

Roots of 3-day-old seedlings were used for immunofluorescent labeling of MTs, and the signals of fluorescent MTs (green) were visualized using a confocal microscope. Double-headed arrows indicate the elongation axis.

(A) View of a whole root tip showing root cap cells (asterisk), early expanding cells (arrow) and rapidly expanding cells (arrowhead).

(B) to (E) Early-expanding cells showing aberrant orientations of cortical MTs. Note that many MTs appeared to converge at some common sites. Also note that some regions of cells had cortical MTs aligned in a nearly transverse orientation (arrowheads).

(F) to (H) Rapidly expanding cells showing aberrant orientation of cortical MTs. Note that many MTs in (H) appeared to converge at some common sites.

Bar in (A) = 40 μm; bars in (B), (E) and (G) = 8 μm; bars in (C), (F) and (H) = 4 μm; bar in D = 2 μm.

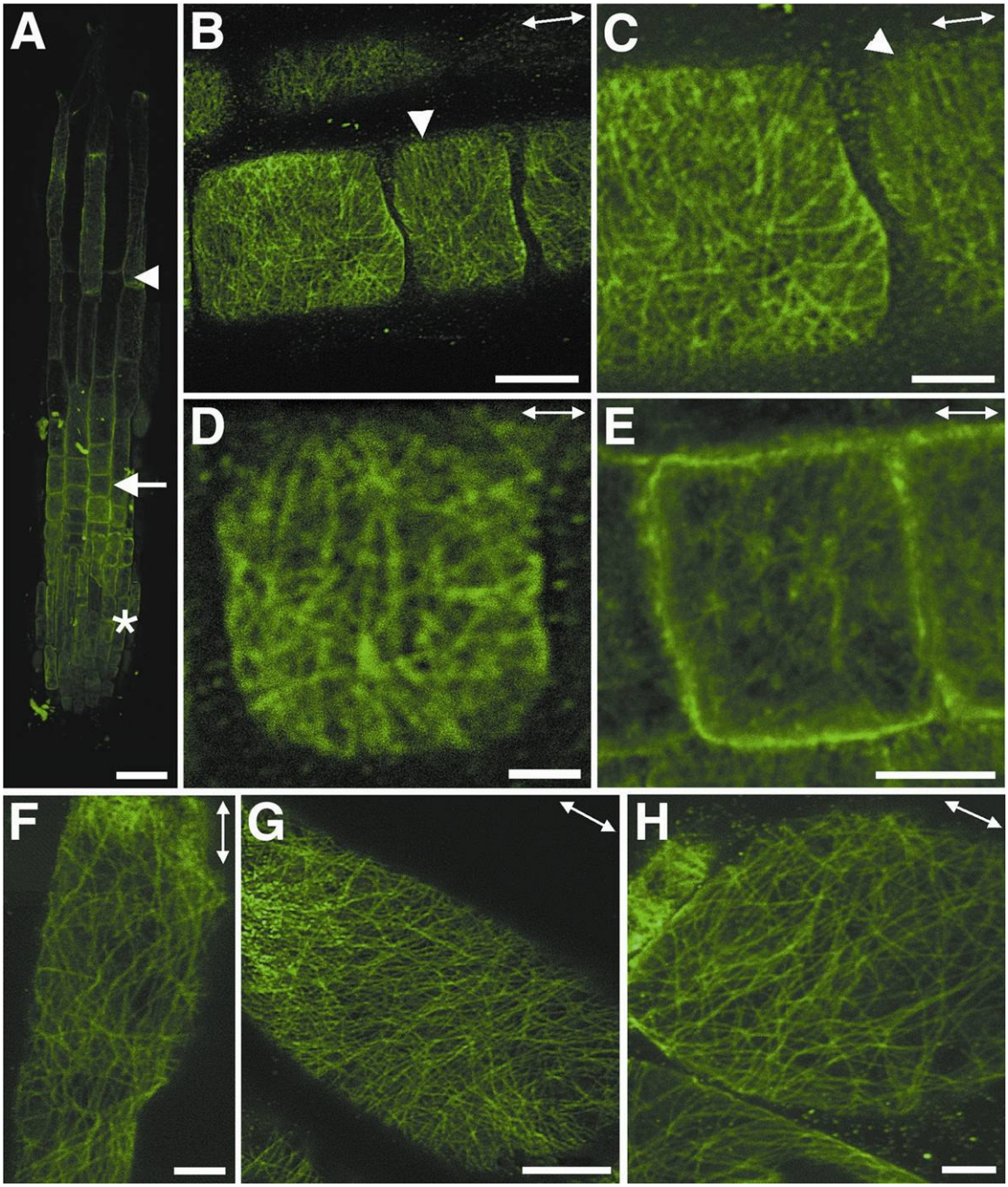
A
B
C
D
E
F
G
H

Figure 3.5. Visualization of Cellulose Microfibrils in the Innermost Layer of Elongating Hypocotyl Cell Walls.

(A) Longitudinal section of a wild-type hypocotyl showing elongating cortical cells (arrow).

(B) Cellulose microfibrils of a wild-type elongation cortical cell showing a transverse orientation.

(C) Longitudinal section of an elongating *fra2* hycopotyl showing cortical cells (arrow).

(D) Cellulose microfibrils of a *fra2* cortical cell showing bands of microfibrils running in different directions.

Bars in (A) and (C) = 50 µm; bars in (B) and (D) = 0.5 µm.

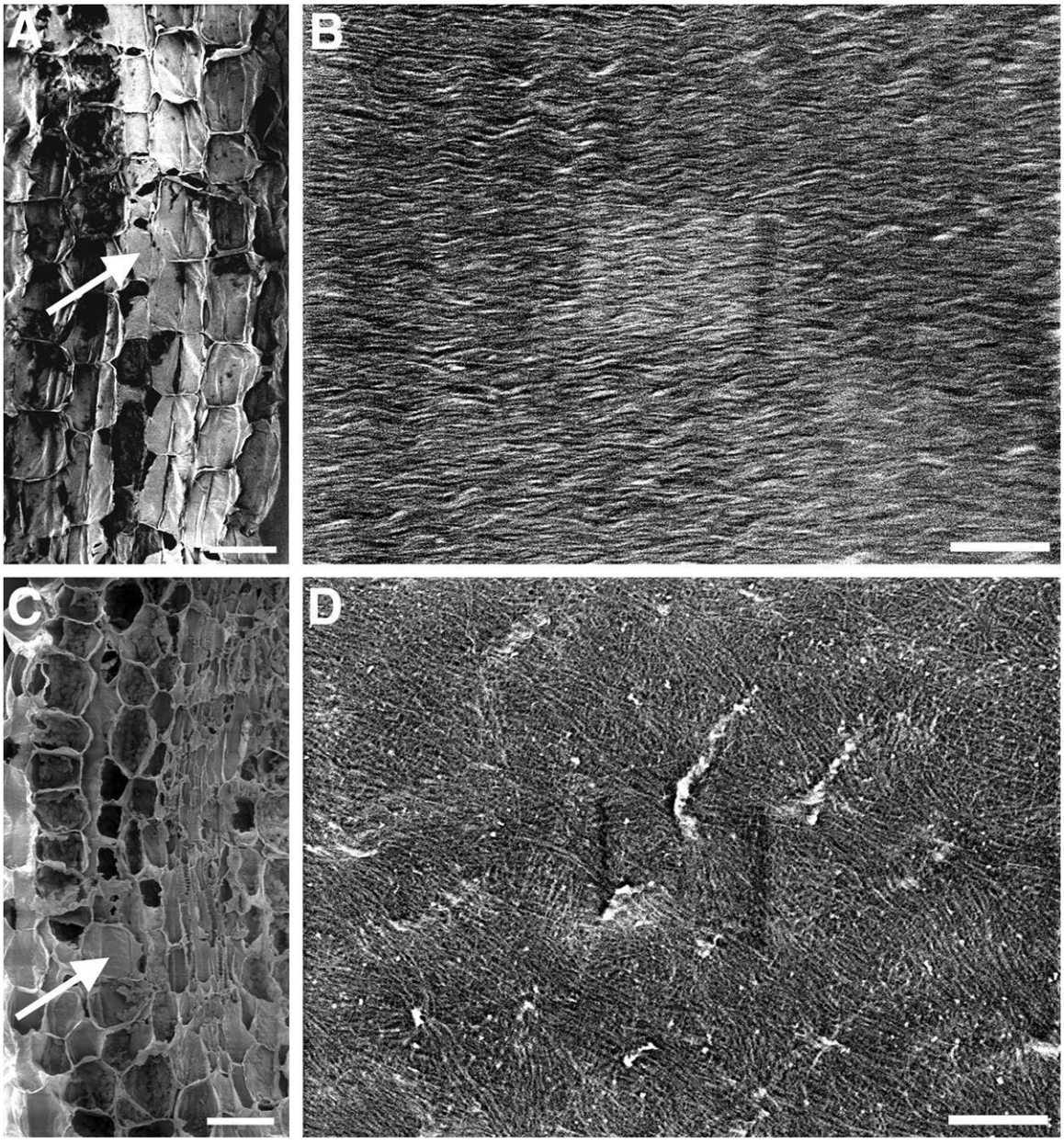
A
B
C
D

Figure 3.6. Visualization of Cellulose Microfibrils in the Innermost Layer of Elongating Pith Cell Walls.

(A) Longitudinal section of the elongating region of a wild-type stem showing pith cells (arrow).

(B) Cellulose microfibrils in wild-type pith cell walls showing a transverse orientation.

(C) Longitudinal section of the elongating region of a *fra2* stem showing pith cells (arrow).

(D) Cellulose microfibrils in *fra2* pith cell walls showing various orientations.

Bars in (A) and (C) = 50 µm; bars in (B) and (D) = 0.25 µm.

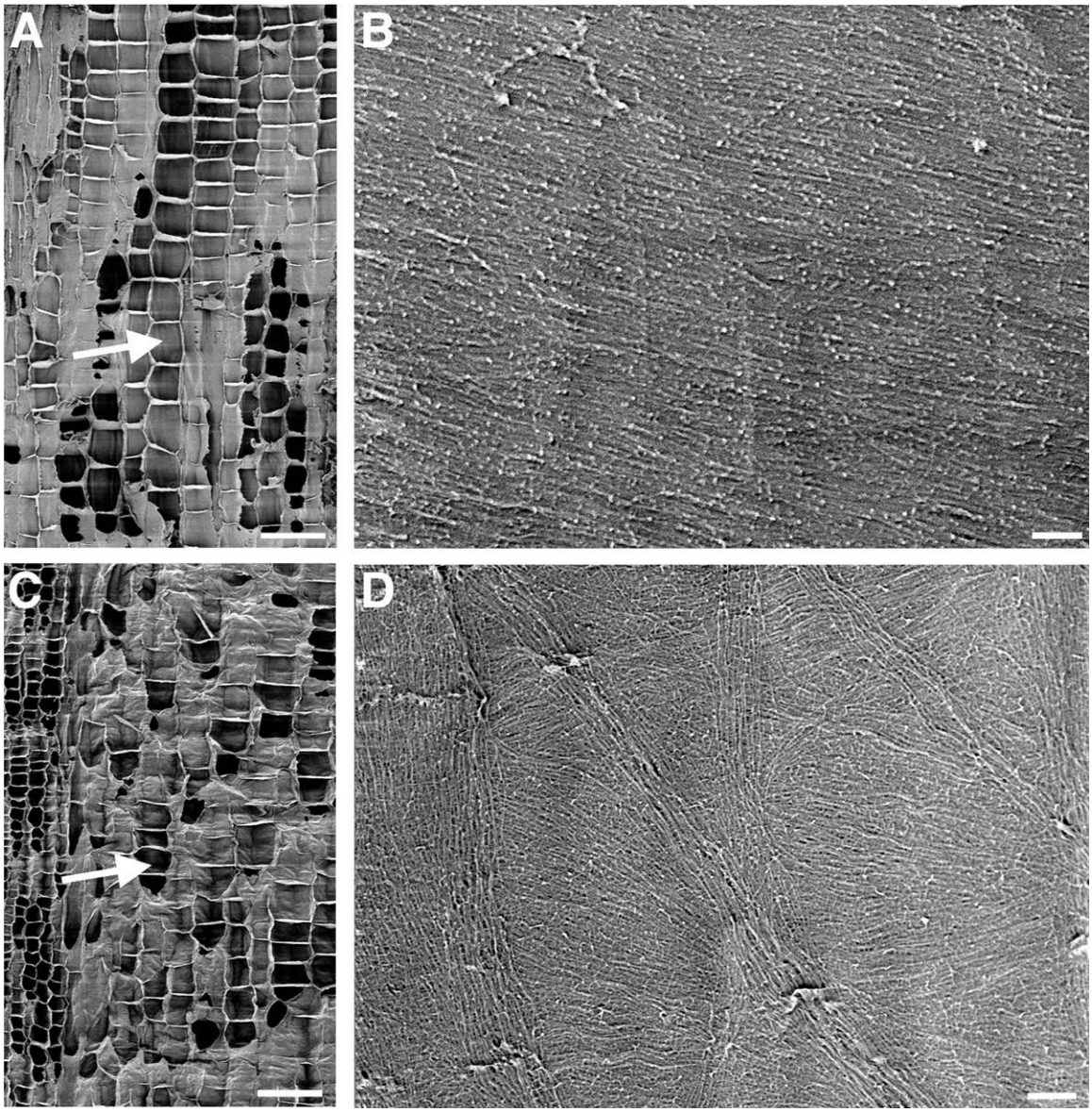
A
B
C
D

Figure 3.7. Visualization of Cellulose Microfibrils in the Innermost Layer of Elongating Petiole Cell Walls.

(A) Longitudinal section of an elongating wild-type petiole showing parenchyma cells (arrow).

(B) Cellulose microfibrils in wild-type parenchyma cell walls showing a transverse orientation.

(C) Longitudinal section of an elongating *fra2* petiole showing parenchyma cells (arrow).

(D) Cellulose microfibrils in *fra2* parenchyma cell walls showing a disoriented pattern.

Bars in (A) and (C) = 50 µm; bars in (B) and (D) = 0.25 µm.

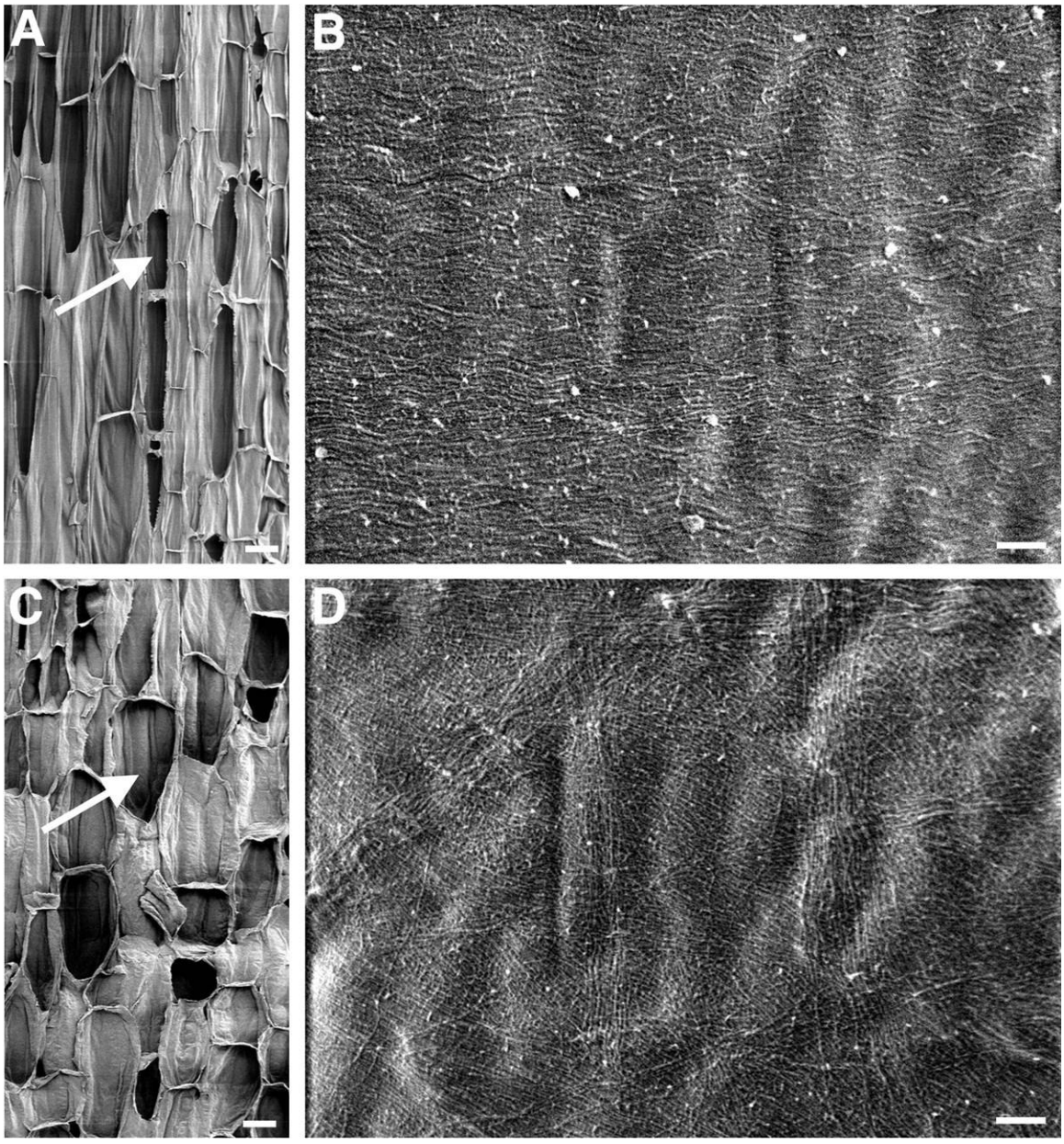
A
B
C
D

Figure 3.8. Visualization of Cellulose Microfibrils in the Innermost Layer of Fiber Cell Walls.

(A) Longitudinal section of the nonelongating region of a wild-type stem showing interfascicular fiber cells (arrow).

(B) Cellulose microfibrils in the middle part of a wild-type fiber cell. Note that microfibrils run in parallel at an angle of 15 to 25° relative to the transverse orientation.

(C) Longitudinal section of the nonelongating region of a *fra2* stem showing interfascicular fiber cells (arrow).

(D) Cellulose microfibrils in the middle part of a *fra2* fiber cell showing a disoriented pattern.

Bars in (A) and (C) = 25 µm; bars in (B) and (D) = 0.5 µm.

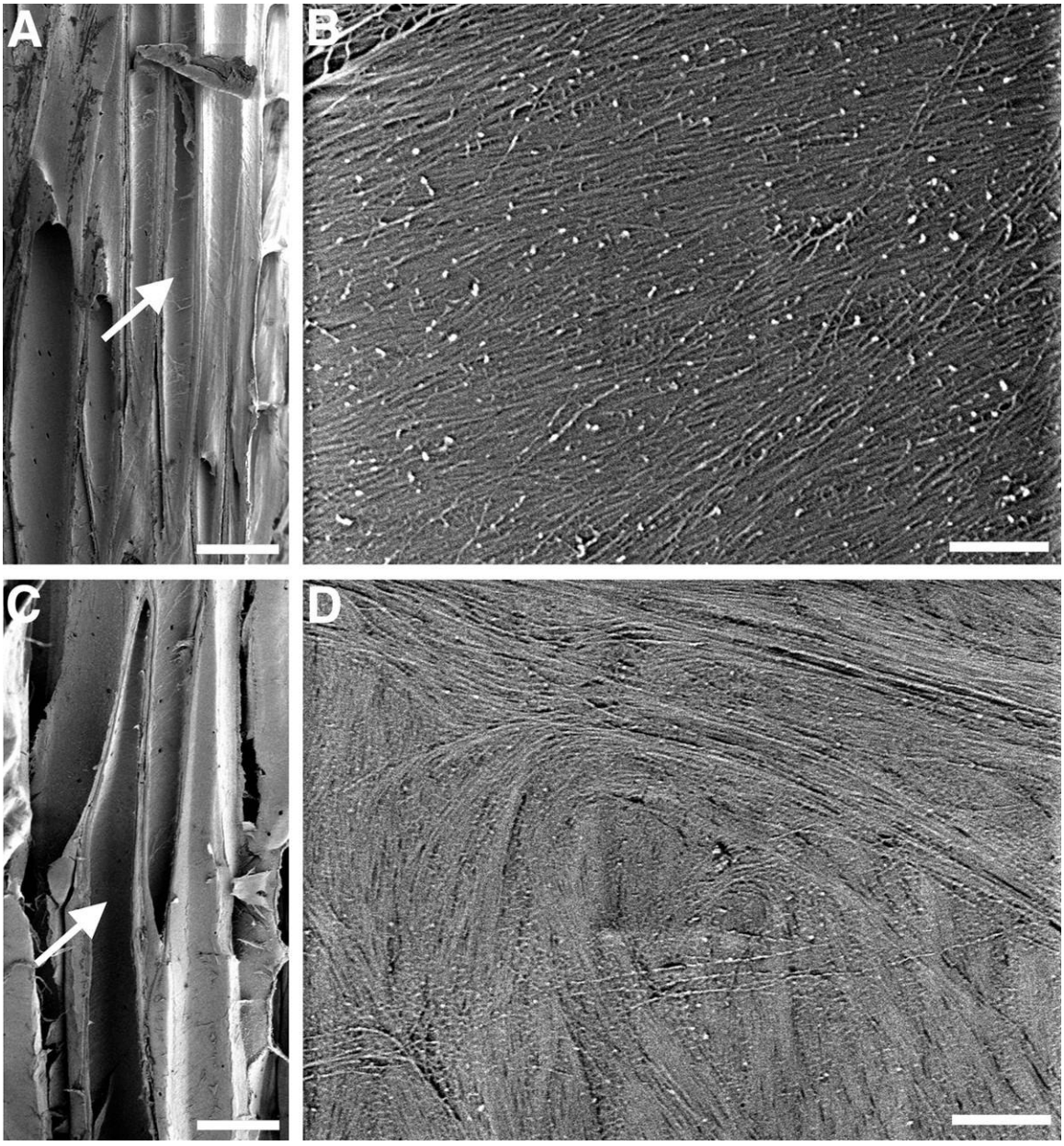
A
B
C
D

Figure 3.9. Quantitative Analysis of the Orientation of Cellulose Microfibrils.
Angles of 450 individual cellulose microfibrils from field emission scanning electron micrographs of the innermost layer of cell walls were measured and represented in angles at 10° increments. Cellulose microfibrils at different angles were calculated as percentage of total microfibrils measured. The transverse direction relative to the elongation axis is arbitrarily defined as 0°, and angles deviating from the transverse orientation are represented by positive or negative numbers of degrees. Insets (a),(b), and (c) show directions of microfibrils corresponding to the defined angles.
(A) Cellulose microfibrils in walls of root cortical cells. Cellulose microfibrils in the wild-type cell walls were oriented mostly in a transverse direction with a slight deviation, whereas the angles of microfibrils in *fra2* cell walls had a much wider distribution.
(B) Cellulose microfibrils in walls of pith cells. Cellulose microfibrils in wild-type cell walls showed a prominent transverse orientation with <30° deviation, whereas the angles of microfibrils in the *fra2* cell walls had a much wider distribution.

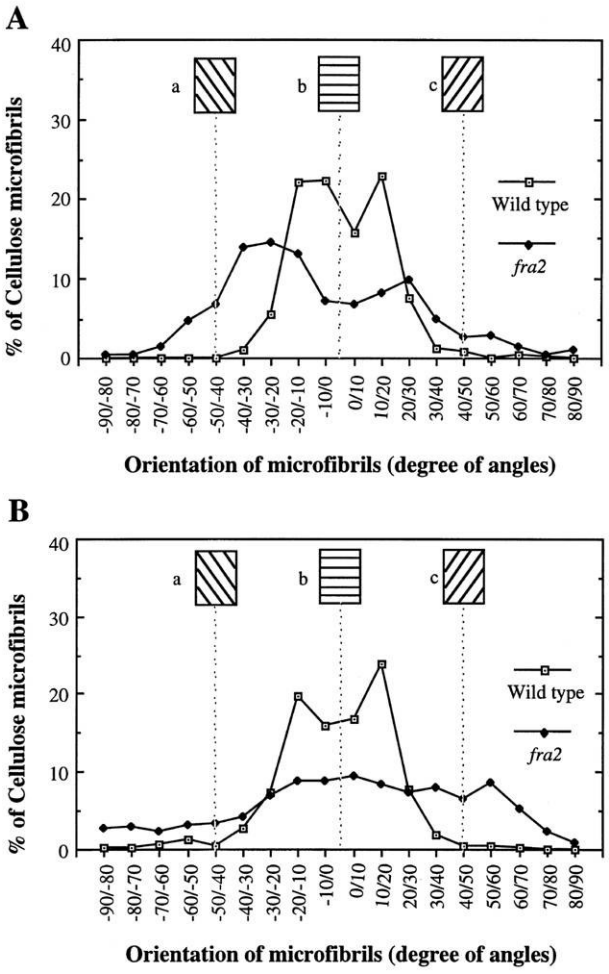
A
% of Cellulose microfibrils
40
30
20
10
0
a
b
c
Wild type
fra2
-90/-80
-80/-70
-70/-60
-60/-50
-50/-40
-40/-30
-30/-20
-20/-10
-10/0
0/10
10/20
20/30
30/40
40/50
50/60
60/70
70/80
80/90
Orientation of microfibrils (degree of angles)
B
% of Cellulose microfibrils
40
30
20
10
0
a
b
c
Wild type
fra2
-90/-80
-80/-70
-70/-60
-60/-50
-50/-40
-40/-30
-30/-20
-20/-10
-10/0
0/10
10/20
20/30
30/40
40/50
50/60
60/70
70/80
80/90
Orientation of microfibrils (degree of angles)

Figure 3.10. Visualization of Cortical MTs in Pith Cells of Stems.

Pith cells from elongating internodes were used for MT labeling with a monoclonal antibody against α-tubulin. Antibody-labeled MTs were detected with fluorescein isothiocyanate-conjugated secondary antibodies, and the signals of fluorescent MTs were visualized under a confocal microscope. Double-headed arrows indicate the elongation axis.

(A) Wild-type pith cells showing the transversely oriented cortical MTs.

(B) High-magnification image of cortical MTs in the wild type showing their transverse alignment.

(C) *fra2* pith cells showing aberrantly oriented cortical MTs. Note that in a few cells, cortical MTs aligned in a nearly transverse orientation (arrowheads).

(D) and (E) High-magnification image of cortical MTs in the *fra2* mutant showing their aberrant patterns and converging sites.

Bars in (A) and (C) = 20 μm; bars in (B), (D) and (E) = 4 μm.

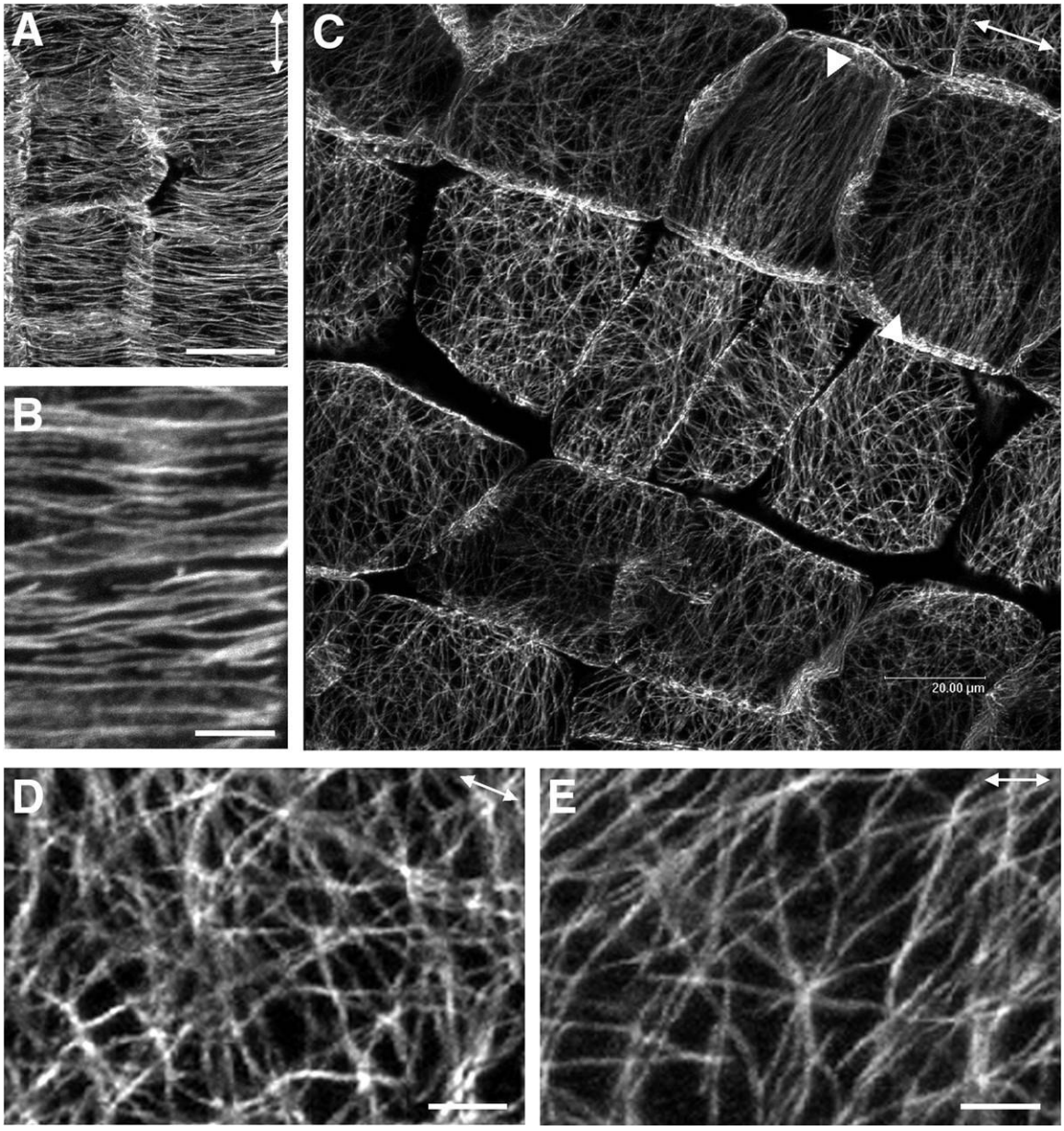
A
B
C
20.00 µm
D
E

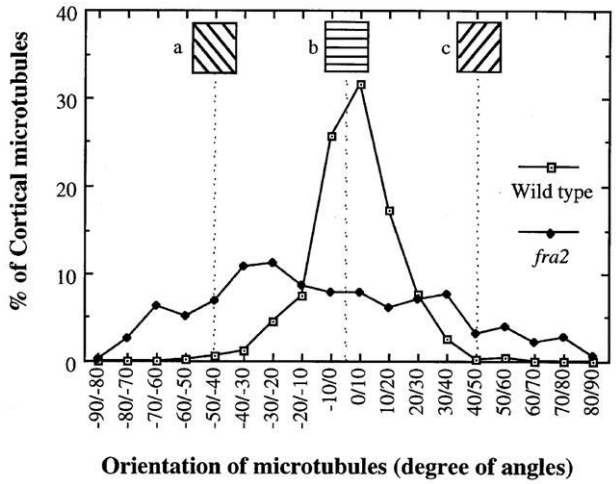

Figure 3.11. Quantitative Analysis of the Orientation of Cortical MTs.

Angles of 535 individual cortical MTs from pith cells of wild type and *fra2* were measured and represented in angles at 10° increments. The number of cortical MTs in a certain angle range was calculated as percentage of total MTs measured. The transverse direction relative to the elongation axis was arbitrarily defined as 0°, and angles deviating from the transverse direction are represented by positive or negative numbers of degrees. Insets (a), (b), and (c) show the directions of cortical MTs corresponding to the defined angles. Cortical MTs in wild-type cells showed a prominent transverse orientation with <20° deviation, whereas the angles of cortical MTs in *fra2* cells had a much wider distribution.

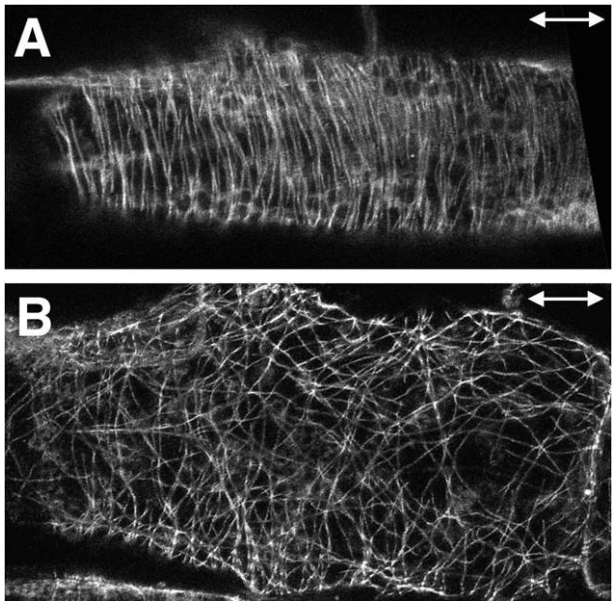

Figure 3.12. Visualization of Cortical MTs in Elongating Petiole Cells.

Parenchyma cells from elongating petioles were used for immunofluorescent labeling of MTs. Double-headed arrows indicate the elongation axis.

(A) A wild-type petiole parenchyma cell showing the transversely oriented cortical MTs.

(B) A *fra2* petiole parenchyma cell showing aberrantly oriented cortical MTs.

Bars in (A) and (B) = 20 µm.

Figure 3.13. Structure of Fiber Cell Walls in the Wild Type and the *fra2* Mutant.
Nonelongating regions of stems of 8-week-old plants were cross-sectioned, and the interfascicular regions in the ultrathin sections were observed under a transmission electron microscope.
(A) Interfascicular fiber cells of the wild type showing thick cell walls and small intracellular space.
(B) High-magnification image of the secondary wall of a wild-type fiber cell showing clear layers and smooth inner wall surface.
(C) Interfascicular fiber cells of *fra2* mutant showing much thinner cell walls and larger intracellular areas compared with the wild type (A).
(D) High-magnification image of the secondary wall of a *fra2* fiber cell showing no apparent layers and wavy inner wall surface (arrow).
En, endodermal cells; if, interfascicular fiber cells; ml, middle lamella; sw, secondary wall. Bars in (A) and (C) = 2.5 µm; bars in (B) and (D) = 1.1 µm.

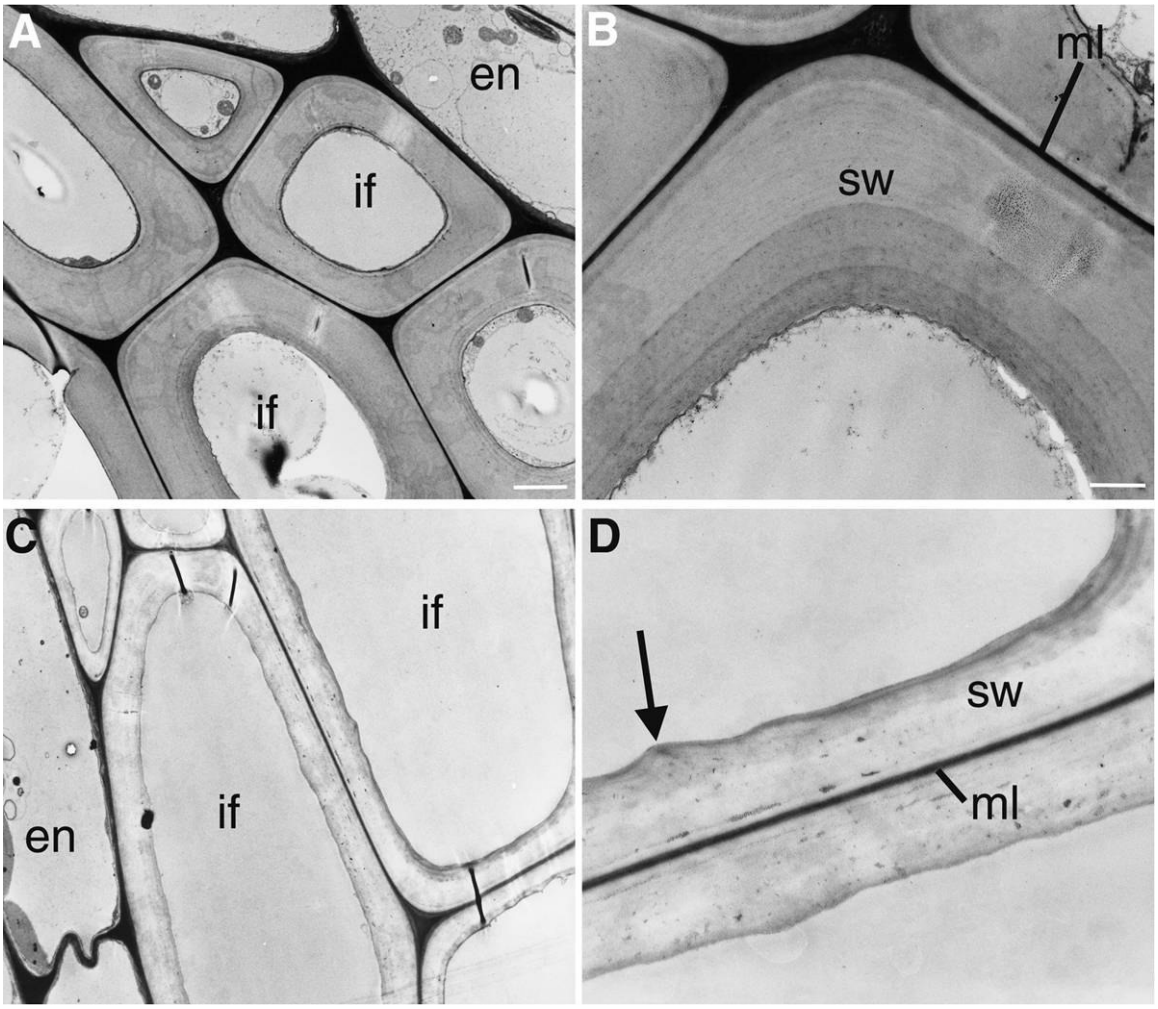
A
en
if
if
B
ml
sw
C
if
en
if
D
sw
ml

Figure 3.14. Structure of Pith Cell Walls in the Wild Type and the *fra2* Mutant.

Non-elongating regions of stems of 8-week-old plants were cross-sectioned, and the pith cells in the ultrathin sections were observed under a transmission electron microscope.

(A) Walls of wild-type pith cells. Note the dark line of the middle lamella.

(B) and (C) Walls of *fra2* pith cells showing thin walls and wavy inner wall surfaces.

ml, middle lamella; pw, primary wall. Bars = 0.21 µm.

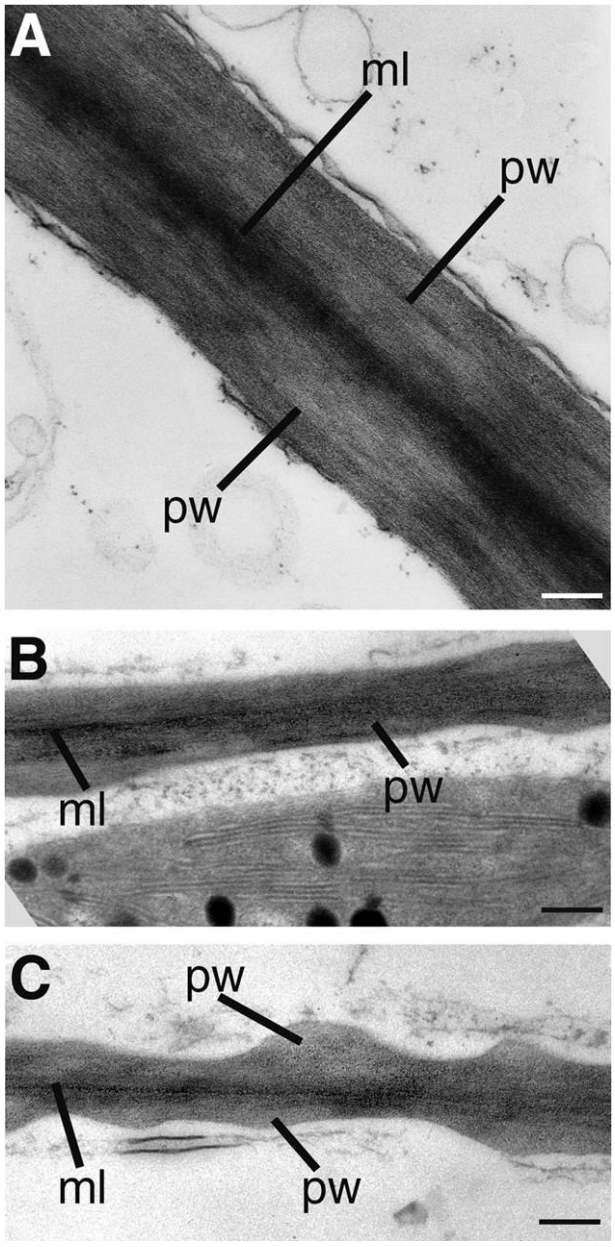
A
ml
pw
pw
B
ml
pw
C
pw
ml
pw

Figure 3.15. MT-Severing Activity of Recombinant Arabidopsis Katanin.

Recombinant Arabidopsis katanin was expressed in insect cells and purified for assay of MT-severing activity. The purified protein was incubated with taxol-stabilized, rhodamine-labeled MTs and the lengths of MTs were visualized under a confocal microscope. Typical fields of view are shown.

(A) MTs before incubation with recombinant katanin.

(B) MTs after incubation with recombinant katanin for 5 min. Note that MTs were cut into short fragments.

(C) MTs after incubation with recombinant katanin for 10 min. Note that some very short MTs (<2 μm) were still visible.

(D) MTs after incubation with a control protein for 10 min. Bar in (D) = 10 μm for (A) to (D).

(E) Distribution of MT lengths. The lengths of MTs were measured 5 min after treatment with a control protein (control) or recombinant Arabidopsis katanin (+AtKTN1). The distribution of MT lengths was expressed as percentage of total number of MTs measured (n = 150).

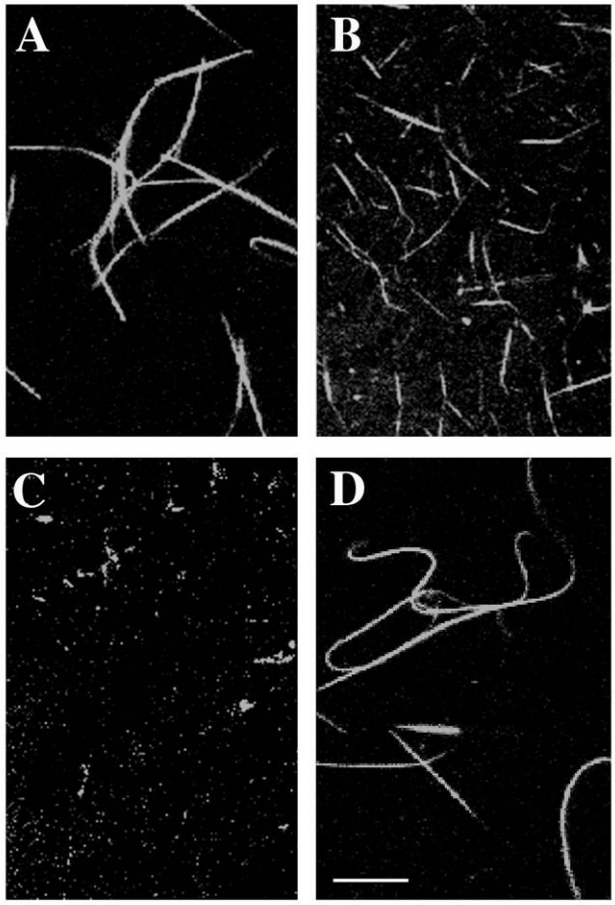
A
B
C
D

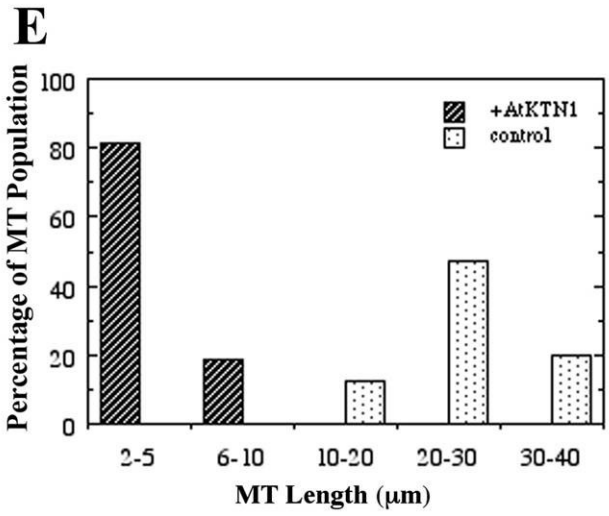
E
Percentage of MT Population
100
80
60
40
20
0
+AtKTN1
control
2-5
6-10
10-20
20-30
30-40
MT Length (μm)

Figure 3.16. Model of the Roles of Katanin (AtKTN1) in the Regulation of the Organization of Cortical MTs, Cellulose Microfibrils, and Directional Cell Elongation.
(A) In cells immediately after cytokinesis, AtKTN1 accelerates the formation of cortical MTs by disassembling perinuclear MTs from the nuclear envelope (a). During cell elongation (b), AtKTN1 mediates MT dynamic changes that are required for the transverse orientation of MTs along the elongation axis. The transversely oriented MTs regulate the parallel deposition of cellulose microfibrils, which determines the direction of cell elongation.
(B) Lack of AtKTN1 MT-severing activity in the *fra2* mutant causes a delay in the disassembly of perinuclear MTs and a concomitant delay of cortical MT formation (a). During cell elongation (b), a decrease in MT dynamics caused by lack of AtKTN1 MT-severing activity results in aberrant orientations of cortical MTs, which in turn leads to altered cellulose microfibril deposition and reduction in directional cell elongation.

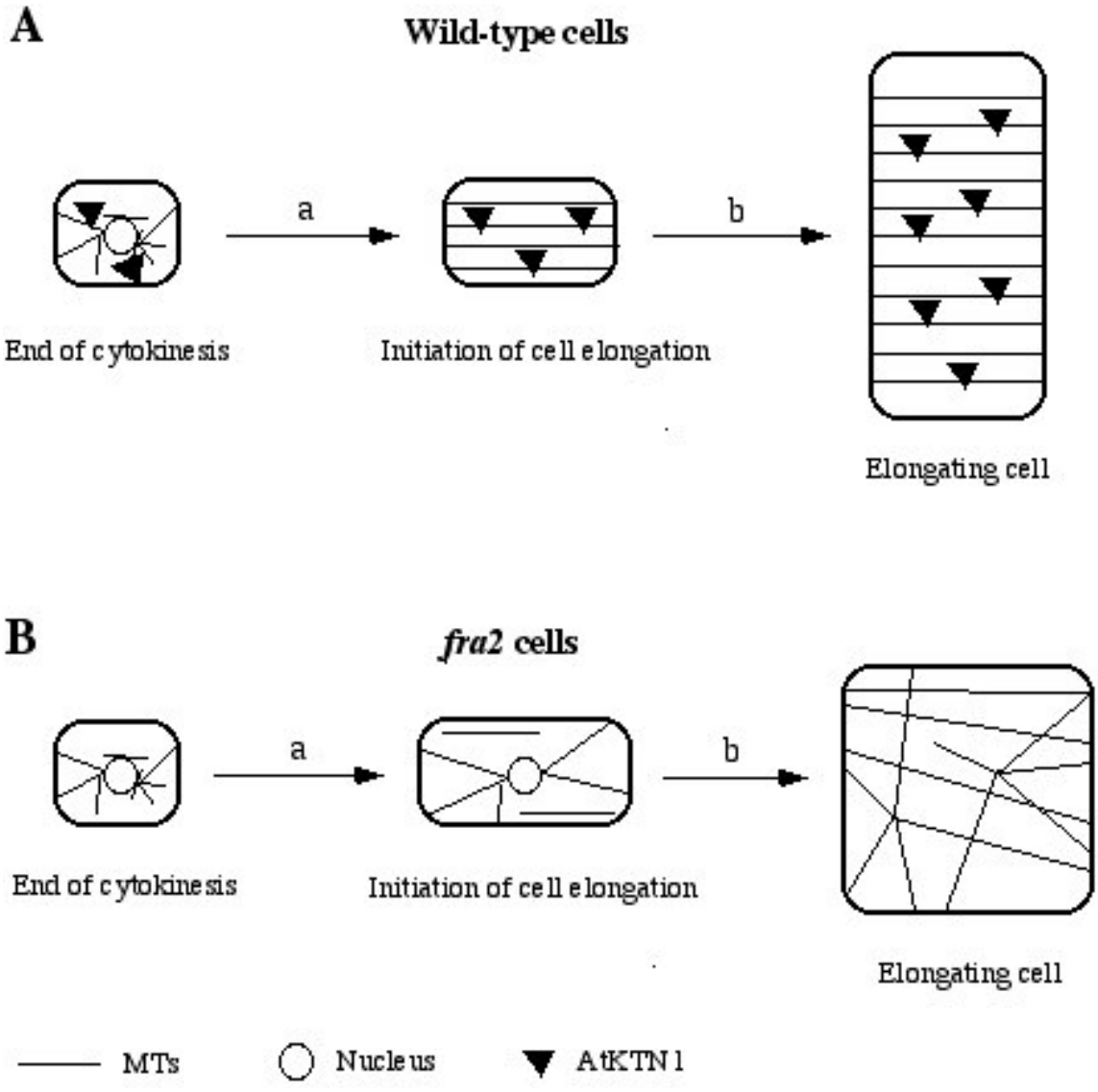
A
Wild-type cells
a
b
End of cytokinesis
Initiation of cell elongation
Elongating cell
B
fra2 cells
a
b
End of cytokinesis
Initiation of cell elongation
Elongating cell
MTs
Nucleus
AtKTN1

CHAPTER 4

OVEREXPRESSION OF THE *ATKTN1* CDNA AFFECTS PLANT CELL ELONGATION BUT DOES NOT CAUSE FRAGMENTATION OF THE CORTICAL MICROTUBULE ARRAY[1]

[1]Burk, D.H. 2003. To be submitted. Plant Physiology.

ABSTRACT

Plant cell elongation is believed to rely on the proper organization of the cortical microtubule (CMT) arrays beneath the plasma membrane. The ATP-dependent microtubule-severing protein, katanin, has been shown to play roles in regulating microtubule dynamics in animal systems. In vitro analysis of the plant katanin p60 subunit (AtKTN1) revealed that it does have microtubule severing activity; however the in vivo function of plant katanin p60 is still unclear. Using the wild type katanin cDNA, we created a 35S::*AtKTN* overexpression construct and analyzed its effects in transgenic plants overexpressing the *AtKTN1* cDNA (Fra2OE). Fra2OE plants had a phenotype similar to that of the original *fra2* mutants. The CMT arrays of overexpressing plants was disorganized in elongating cells except for those in roots and the CMFs from elongating stem and petiole cells showed aberrant deposition patterns of cellulose microfibrils. Interestingly, the overall lengths of microtubules in overexpressing plants were not apparently altered. Our results show that in vivo, AtKTN1 does not randomly sever the plant cortical microtubule array but affects the CMT organization.

INTRODUCTION

The anisotropic growth of plant cells is necessary for the plant to reap the maximum benefits from a survival and reproductive standpoint. The proper elongation of root hairs, cells of the hypocotyl and cells within roots, for example, give a plant the ability to reach nutrient and water-rich regions in the soil or to allow its photosynthetic machinery to bask in sunlight. In addition, the extent of filament cell elongation can mean the difference between successful self-pollination and sterility.

The turgor pressure generated within the vacuole is believed to be the driving force for plant cell expansion, and in conjunction with a constraining network of parallel cellulose microfibrils (CMFs) in the cell wall and proteins believed to loosen the wall matrix, plant cells are able to expand anisotropically (Cosgrove, 1997; Cosgrove, 2000; Kost and Chua, 2002). The plant cytoskeleton, made up of microtubules (MTs) and actin filaments, are also believed to play a large role in the organized expansion of cells although the precise method of action is still largely unknown (Cyr and Palevitz, 1995; Smith, 2003). The arrangement of cortical microtubules (CMTs) in cells undergoing rapid growth appears to mirror that of the CMFs in newly deposited cell wall. Disruption of the CMTs using MT depolymerizing drugs such as oryzalin and propyzamide can cause dramatic changes in cell expansion as well as disrupt the organized deposition of CMFs (Baskin, 2001).

Mutations which cause alterations to the CMT array or alter microtubule dynamics are ideal candidates for studying the roles MTs play in anisotropic growth processes. For example, the PILZ group including PORCINO, PFIFFERLING, HALLIMASCH, KIESEL (Kirik et al., 2002), are characterized by having mushroom shaped embryos and are defective in their ability to form microtubules in general (Mayer et al., 1999). Cloning of the genes responsible for these mutant phenotypes revealed that they encode tubulin-folding cofactors necessary for the proper formation of mature microtubule polymers (Mathur and Hülskamp, 2002; Kirik et al., 2002).

The *tangled1* mutant of maize and the Arabidopsis *tonneau2* mutant are similar in that both cause disruptions in the placement of the phragmoplast during cytokinesis and result in aberrant cell files. In *tan1* mutants all of the necessary cytoskeletal structures appear to be present and are structurally normal, however the preprophase band (PPB) and phragmoplast fail to orient properly. Cloning of the *Tangled1* gene showed that it encodes a highly basic protein that is distantly related to a basic MT-binding protein domain of vertebrate APC proteins. TANGLED1 is proposed to play a role in aiding in the orientation of the cytoskeletal structures involved in dividing cells perhaps by directing microtubules to proper positions at the cell cortex (Smith et al., 2001). Mutants of *ton2* appear to have properly aligned CMTs in hypocotyl epidermal cells but they are randomized in the interphase cells of roots. In addition, *ton2* mutant cells lack the PPB at the onset of mitosis. *Ton2* encodes a putative regulatory subunit of type 2A protein phosphatase (PP2A) and is proposed to play a direct role in organizing the CMT array (Camilleri et al., 2002).

The two SPIRAL loci appear to be involved in the organization of the CMT arrays in Arabidopsis. The *spiral1* and *spiral2* (*spr1* and *spr2*) mutants have defects in anisotropic growth of cells in the roots and hypocotyls and organs show right-handed twisting. Observation of the CMTs in these mutants show that they are either arranged in left-handed helices or are disorganized (roots and etiolated hypocotyls, respectively) when compared to wild type plants (Furutani et al., 2000). Mutation of the *Spike1* gene causes plants to assume a dwarf-like stature with narrow leaves and the epidermal cells of leaves appear to loose their normal 'lobed' appearance. In addition, trichomes of the mutant plants have fewer branches than wild type and trichome stalks are shorter than normal. Observation of the CMTs and actin microfilaments in epidermal pavement cells revealed that *spk1* mutants have defects in the spatial arrangement of these cytoskeletal elements. The SPK1 protein appears to share some similarity to the CDM-family of proteins that

have been implicated in reorganizing the cytoskeleton in animal cells in response to extracellular cues (Qiu et al., 2002).

Recently, the temperature-sensitive mutant *mor1* was characterized in Arabidopsis. Mutants in *mor1* grown under restrictive temperature exhibit left-handed twisting of organs, isotropic cell expansion, and impaired root hair polarity. Visualization of the CMT array in *mor1* plants revealed that after switching the growth conditions from permissive to restrictive temperature the CMTs were quickly disorganized and rapidly decreased in length. This disruption is completely reversible and resumption of growth at permissive temperature allows the CMTs to regain their wild type length and orientation (Whittington et al., 2001). A MOR1 homolog, TMBP200 exists in tobacco and has been shown to form inter-microtubule bridges about 10nm in length (Lloyd and Chan, 2002). MOR1 may function to bundle microtubules together and may act to stabilize them from rapid dissociation into tubulin heterodimers or may protect them from the action of other microtubule destabilizing proteins.

Another protein shown to have direct effects on the organization of the CMT array in Arabidopsis is the katanin-like protein, AtKTN1 (Bichet et al., 2001; Burk et al., 2001). Katanin is an ATP-dependent microtubule-severing protein first isolated from sea urchin eggs based on its ability to sever microtubules *in vitro* and has been shown to play a wide range of roles in animal systems. It has been determined that in animal systems katanin exists as a heterodimer of a p60 and p80 subunit. The p60 subunit has been shown to have ATP-dependant microtubule-severing activity and shares similarity to the AAA (ATPases associated with various cellular activities) family of ATPases. The p80 subunit of katanin seems to be involved in the subcellular targeting of the p60 subunit to the centrosome via WD40 repeats and can possibly regulate the MT-severing activity of p60 (McNally et al., 1996; Hartman et al., 1998; McNally et al., 2000). In addition, it is proposed that katanin is involved in the deflagellation process of *Chlamydomonas* based on studies in which katanin activity was diminished using anti-katanin antibodies as well

as by the localization of katanin to the specific site in which severing of the outer doublet occurs in this organism (Lohret et al., 1998; Lohret et al., 1999). Katanin has recently been implicated in the regulation of the size of the meiotic spindle apparatus in *C. elegans* through the isolation of mutations in the *Mei-1* and *Mei-2* genes which correspond to the p60 and p80 subunits, respectively, as well as the production of free microtubule ends at the mitotic spindle in human culture cells (Srayko et al., 2000; Buster et al., 2002). In neuronal cells, it appears that katanin may function in the release of microtubules from the centrosome as well as providing a pool of shorter MTs used in the elongation of neuronal outgrowths (Ahmad et al., 1999).

In vitro analysis of the Arabidopsis katanin, AtKTN1/AtKSS, has shown that it does have MT-severing ability in the presence of ATP (Burk and Ye, 2002; Stoppin-Mellet et al., 2002), but no conclusive evidence of its role in vivo is known. AtKTN1 protein appears to be localized around the perinuclear envelope during interphase in Arabidopsis root cells and around the spindle poles during mitosis and recently, a GFP::AtKSS fusion protein revealed that katanin protein appears to decorate cortical microtubules (McClinton et al., 2001; Bouquin et al., 2003). The allelic katanin mutants in Arabidopsis, FRAGILE FIBER 2/ECTOPIC ROOT HAIR 3/BOTERO/LUC SUPER EXPRESSING, cause a semi-dwarf phenotype with a reduction in the length of all organs of the plant (Bichet et al., 2001; Burk et al., 2001; Webb et al., 2002; Bouquin et al., 2003). Observation of the cellular phenotype in organs such as the roots, pith of stems, and hypocotyl revealed that the reduction in length and increase in width of these organs was due to a failure in anisotropic growth as cells are shorter than wild type and expand in the radial dimension. There appear to be no differences in the mitotic spindle between the wild type and *fra2* mutant; however there appears to be a delay in the disassembly of perinuclear MTs immediately after cytokinesis in mutant root cells (Burk et al., 2001). In rapidly elongating cells of root, stem, and petiole the CMT array is disorganized with respect to wild type. Instead of parallel arrays of CMTs oriented transversally to the axis

of cell elongation, the MTs of *fra2* cells are arranged almost randomly. In addition, the CMFs of *fra2* mutant plants in rapidly elongating cell types are disorganized when compared to wild type and this is believed to lead to the isotropic-like growth seen in cells of mutant plants (Burk and Ye, 2002).

Based on the observed phenotype of katanin mutants in plants, it appears that the function of the p60 subunit may differ somewhat from those in animal systems. Specifically, the mitotic spindle does not appear to be affected in mutants when compared to wild type. Instead, mutants show a disruption of the CMT array in interphase cells and a subsequent defect in polarized cell growth in almost all cell types possibly related to the disruption of MT dynamics immediately after cell division (Burk et al., 2001). Based on *in vitro* analysis, AtKTN1 is known to possess MT-severing activity but we wished to explore further the in vivo function of this protein. We hypothesized that if a mutation in katanin function can inhibit the severing of MTs from the perinuclear array and lead to a disorganization of the CMT array then overexpression of *AtKTN1* may cause a rapid disassembly of MTs or perhaps inhibit the proper formation of the CMTs. This hypothesis is based on both in vitro studies of AtKTN1 function as well as findings that transient overexpression of the human p60 katanin subunit in HeLa cells led to the disassembly of the interphase MT cytoskeleton (McNally et al., 2000). To this end, we produced Arabidopsis plants which overexpressed wild type *AtKTN1* cDNA using a constitutive 35S promoter and examined the overall plant phenotype as well as that of the cortical microtubules in cells undergoing rapid elongation. We show that the overexpression of *AtKTN1* cDNA causes a phenotype similar to *fra2* mutant plants with the exception that roots were not affected. Additionally, the CMT arrays of plants overexpressing AtKTN1 cDNA (Fra2OE) are disrupted in a similar manner as the *fra2* mutant but do not appear fragmented as was expected. Visual examination of the CMFs in cells of Fra2OE plants shows a concomitant disruption of the cellulose microfibrils in primary cell walls of rapidly elongating stem and petiole.

RESULTS

CORTICAL MICROTUBULES IN FRA2OE STEM AND PETIOLE PITH ARE DISORGANIZED BUT ARE NOT FRAGMENTED

In order to determine the potential in vivo function of AtKTN1 we utilized the pBI121 vector. Wild type *Fra2* cDNA encoding *AtKTN1* was introduced into the multiple cloning site under the control of the CaMV 35S promoter (Fig. 4.1) and transgenic Arabidopsis overexpressing wild type *Fra2* mRNA were isolated (R.Zhong, data not shown). As the *Fra2* gene product, AtKTN1, is known to possess ATP-dependent microtubule-severing activity (Burk and Ye, 2002; Stoppin-mellet et al., 2002), we hypothesized that overexpression of this protein may disrupt the formation of the CMT array through the continuous disassembly of long MTs. To test this hypothesis we observed CMTs directly in wild type and transgenic plants using immunofluorescence labeling of MTs in pith cells of rapidly elongating stem and petiole.

In wild type stems the CMTs were arranged transversely to the long axis of the cells and to the axis of organ elongation (Fig. 4.2A and 4.2B). The microtubules appeared to be intact for much of the length across the cell surface examined with occasional breaks seen in some MTs. Cells of Fra2OE stem, however, had CMT arrays that were arranged in an almost random manner (Fig 4.2C and 4.2D). The CMTs ran in different directions in most of the cells examined, however, some cells appeared to have local regions of CMTs arranged in parallel and transverse to the axis of organ elongation (Fig. 4.2C and 4.2D). The overall length of CMTs in Fra2OE cells did not appear to be affected by overexpression of *AtKTN1* as individual MTs appeared to be intact from one side of the visible cell cortex to the other (Fig. 4.2C to 4.2E). Examination of the CMT arrays in wild type and Fra2OE petiole cells were similar to stem (Fig. 4.3). Wild type CMTs were arranged in parallel perpendicular to the axis of cell elongation while those of transgenic plants were disorganized. Again, overexpression of katanin p60 did not appear to cause the random fragmentation of individual MTs in the cortical array. The

CMTs in cells of Fra2OE elongating roots were arranged similarly to wild type and were organized in parallel arrays perpendicular to the axis of cell elongation (data not shown).

THE ORIENTATION OF CELLULOSE MICROFIBRILS IN PRIMARY WALLS OF STEM AND PETIOLE CELLS IS DISRUPTED IN FRA2OE PLANTS

Previous research conducted on the *fra2* mutant in Arabidopsis revealed that a disruption in the CMT array led to aberrations in the organization of the cellulose microfibrils in primary and secondary cell walls (Burk and Ye, 2002). As the Fra2OE plants appeared to mimic the phenotype of the original *fra2* mutant in cell morphology we wished to determine if a similar disruption in the CMFs in transgenic plants also occurred. Such a correlation in the disorganization of the CMT and CMF may be the cause of the reduction in anisotropic growth seen in Fra2OE plant cells.

Using methods previously described by Sugimoto et al. (2000), we observed the orientation of CMFs of the primary walls of rapidly elongating stem and petiole parenchyma cells. Wild type petiole CMFs were seen to run parallel to each other and to be almost perfectly perpendicular to the axis of cell elongation with occasional variations in the pitch of the cellulose helices (Fig. 4.4A and 4.4B). In contrast, the rapidly expanding cells of Fra2OE petiole contained CMFs that were arranged in a disorderly manner with bundles of microfibrils that ran in different directions (Fig. 4.4C and 4.4D). Similarly, CMFs in the primary walls of wild type stem parenchyma cells were organized in parallel arrays transverse to the axis of cell elongation (Fig. 4.5A and 4.5B). The CMFs from Fra2OE stem cells, however, were not ordered in parallel arrays. There appeared to be some local ordering of the CMFs as bundles of as many as 15-20 individual fibrils traveled together in the same direction although the global order of CMFs was disrupted. Often bundles of cellulose microfibrils were seen to change direction in a small space and regions were apparent were bundles appeared to converge (Fig. 4.5C and 4.5D). These results show that the overexpression of *Fra2* cDNA can alter the deposition of CMFs in different organs.

STATISTICAL ANALYSIS OF CORTICAL MICROTUBULE AND CELLULOSE MICROFIBRIL ORIENTATION REVEAL CORRELATIONS

The above results clearly show that both the CMTs and CMFs of Fra2OE cells are disrupted in their orientation when compared to wild type cell walls (Figures 4.2 to 4.5). In order to quantify the degree of disruption of CMT and CMF orientation in Fra2OE cell walls we measured the angles of individual cortical microtubules and cellulose microfibrils in rapidly elongating cells of stem. Wild type CMTs were predominantly oriented perpendicular to the long axis of the cell with slight deviations of <20° from the transverse direction (Fig 4.6A). Measurements of individual CMFs from wild type cell walls revealed a similar distribution of angles with the majority of CMFs running in directions close to perpendicular to the axis of cell elongation (Fig. 4.6B). Both CMFs and CMTs of Fra2OE plant cells showed a broad distribution of angles when compared to wild type (Fig. 4.6A and 4.6B). These results clearly show that the overexpression of AtKTN1 in Arabidopsis affects the orientation of both cortical microtubules and cellulose microfibrils and mimics the results found in the original *fra2* mutant (Burk and Ye, 2002).

OVEREXPRESSION OF *ATKTN1* AFFECTS PLANT MORPHOLOGY

Interestingly, the overall phenotype of Fra2OE plants was strikingly similar to that of the original *fra2* mutant as well as other described katanin mutants in Arabidopsis. Examination of young plants before bolting revealed that the rosette was much more compact than wild type plants (Fig. 4.7A and 4.7B). This compact stature was the result of a large reduction in the length of Fra2OE petioles and leaf blades to 46% and 72% of wild type, respectively (Fig. 4.7D and Fig. 4.8). The width of Fra2OE leaves were also reduced to approximately 79% of wild type.

Upon reaching maturity, plants overexpressing the *Fra2* construct exhibited a dwarf phenotype with their total height reduced to 53% of wild type. This large reduction in the height of transgenic plants could be due to a decrease in the number of internodes

present; however examinations of 20 wild type and Fra2OE plants reveal that the total number of internodes is the same. Greenhouse grown plants also showed a marked increase in the width of the inflorescence stem that sometimes split lengthwise between the first and second internodes (Table 4.1 and Fig. 4.7E). The increase in stem diameter may be due to an apparent increase in the number of parenchyma cells found in Fra2OE stems (data not shown).

Table 4.1. Morphology of Inflorescence Stems and Trichomes of the Wild Type and the *Fra2* Overexpressing Lines

Morphology	Wild Type	Fra2OE
Main inflorescence stem[a]		
Total height (cm)	43.7 ± 5.0	23.0 ± 6.2
Height to last internode	13.0 ± 3.0	3.12 ± 1.7
Diameter (mm)[b]	1.8 ± 0.2	2.7 ± 0.4
Number of internodes	3.1 ± 0.9	3.3 ± 1.3
Trichome branch points (%)[c]		
No points	0	12.4
One point	1.8	75.7
Two points	82.7	11.8
Three points	15.4	0

[a] Data are mean values ±SE from 20 plants.
[b] The first internode was used for measurement of the stem diameter.
[c] A total of 110 (wild type) and 170 (*Fra2*OE) trichomes on rosette leaves were counted. The nomenclature of trichome branch points is according to Luo and Oppenheimer (1999).

ANATOMICAL EXAMINATION OF CELLULAR MORPHOLOGY REVEALS THAT REDUCTIONS IN ORGAN LENGTH IS DUE TO A DECREASE IN CELL LENGTH

The morphological differences seen in Fra2OE plants prompted us to examine the cellular anatomy of stems and petioles. Longitudinal sections of wild type and Fra2OE revealed differences in cellular anatomy. In wild type stems the parenchyma cells of pith appear almost rectangular and are arranged in regular files. Pith cells in overexpressing plants, however, appeared irregular in their shape and were shorter than wild type. In addition, the orderly cell files were occasionally disrupted by what seems to be misaligned cell walls in some cells (Fig 4.9A and 4.9B). This disruption of neat cell files is seen more clearly in pith cells from Fra2OE petioles. Wild type petiole parenchyma,

like stems, consists of regularly arranged rectangular cells. The transgenic petiole tissue appears to consist of irregularly shaped parenchyma and obvious alterations in the cell file arrangement (Fig. 4.9C and 4.9D).

Examination of cross sections of greenhouse-grown wild type and Fra2OE stem were conducted in order to determine if differences existed in the interfascicular fibers. No apparent differences were seen between wild type and Fra2OE plants in regard to the placement or organization of normal cell types seen in stems. The total number of cell layers in the cortex of transgenic plants was the same as wild type and the anatomy of vascular tissues were identical (Fig. 4.9E and 4.9F and data not shown). Differences were apparent in the number and size of interfascicular fibers present in the transgenic plants when compared to wild type. In addition, the thickness of the secondary cell walls in these cell types appeared to be dramatically reduced (Fig. 4.9G and 4.9H). To further characterize the apparent differences seen in the secondary cell walls of interfascicular fibers of Fra2OE stems we conducted transmission electron microscopic analysis of these tissues (Fig. 4.10). Wild type interfascicular fibers typically had secondary cell walls that were approximately 3.2 μm in thickness and had a smooth surface on the most recently deposited secondary wall layer (Fig. 4.10C and Table 4.2). The secondary walls of Fra2OE interfascicular fibers were approximately 46% the thickness of wild type and had inner wall surfaces that appeared bumpy in appearance (Fig. 4.10B, 4.10D, and Table 4.2).

SCANNING ELECTRON MICROSCOPY OF THE MORPHOLOGY OF CELLS AND ORGANS REVEAL DIFFERENCES IN THE SHAPES OF CERTAIN CELL TYPES

Our investigation of the differences in overall plant morphology led us to conduct more detailed examination of cells and organs of wild type and Fra2OE plants. One-week-old etiolated seedlings grown on agar plates were examined using field emission scanning electron microscopy (FESEM) as transgenic plants

Table 4.2. Wall thickness of Pith Cells and Fiber Cells in the Wild Type and the *Fra2* Overexpressing Plants

	Wall Thickness (μm)[a]	
Cell Type	Pith Cell[b]	Fiber Cell[c]
Wild type	0.36 ± 0.06	3.23 ± 0.67
*Fra2*OE	0.36 ± 0.04	1.50 ± 0.27

[a] Wall thickness was measured from transmission electron micrographs of cells. Data shown are means ±SE from 9 (for pith) to 24 (fiber) cells.
[b] Pith cells from nonelongating internodes of inflorescence stems were used for the measurement of wall thickness.
[c] Interfascicular fiber cells from nonelongating internodes of inflorescence stems were used for the measurement of wall thickness.

appeared to have differences in hypocotyl diameter. As seen in Figure 4.11, Fra2OE hypocotyls were wider than their corresponding wild type seedlings. This increase in diameter may be due to an increase in the size of hypocotyl cells as it appears that the epidermal cells of the hypocotyl in transgenic plants are wider than wild type (Fig. 4.11). The epidermal cells of adaxial and abaxial leaf surfaces were also altered in Fra2OE plants. Normally, wild type epidermal cells exhibit shapes that can be described as 'jigsaw-puzzle-shaped' with the adaxial cells showing a very sinuous margin consisting of lobes (Fig. 4.12A and 4.12C). The cells of transgenic plant leaf epidermis appeared to be swollen in the case of the adaxial leaf surface with a reduction in the number of lobes. Abaxial epidermal cells of the Fra2OE plants appeared to be reduced in their overall length and were less sinuous than wild type (Fig. 4.12B and 4.12D). In addition to changes in the shape of leaf epidermal cells, we also observed a reduction in the number of trichome branches in transgenic plants. Wild type Arabidopsis trichomes typically have 3 branches or 2 branch points (Luo and Oppenheimer, 1999), and our examination revealed that approximately 83% of wild type trichomes were three-branched. The majority (76%) of Fra2OE trichomes were two-branched with about 7.5% one-branched trichomes present (Table 4.1 and Fig. 4.12E and 4.12F).

Differences in the sizes of wild type and Fra2OE floral organs were also observed using FESEM. Typically, wild type filaments elongate such that the anthers come very

close to the stigma (Fig 4.13A). Transgenic flowers showed a dramatic difference in the overall size of flowers as well as a reduction in the length of filaments. This failure of filaments to elongate renders transgenic plants partially sterile as the pollen from anthers cannot reach the stigmatic surface of the carple. Closer examination of the cells of filaments show that Fra2OE cells are much shorter than wild type and can explain the reduction in this organ's length (Fig. 4.13C to 4.13F).

DISCUSSION

Based on studies of katanin in animal systems it is known that this microtubule-severing protein is involved in processes such as maintenance of the size of meiotic spindles in *C. elegans* and production of a pool of small microtubules for neuronal outgrowth (Ahmad et al., 1999; Srayko et al., 2000). Additionally, transient overexpression of the human p60 subunit in HeLa cells led to the disassembly of the MT array, confirming the role of p60 as a potent MT severing protein in animal systems (McNally et al., 2000). In plants, however, the exact function of the p60 katanin homologue is not so clear. Based on the phenotypes of the *fra2*, *botero*, and *erh3* mutants it appears that katanin function is closely associated with proper cell expansion and the organization of the cortical microtubule array (Burk et al., 2001; Burk and Ye, 2002; Bichet et al., 2001; Webb et al., 2002). In addition, in vitro analysis of AtKTN1 function has revealed that it does sever microtubules in the presence of ATP as animal katanin does (Hartman and Vale, 1999; Stoppin-Mellet et al., 2002). In order to better define the in vivo functions of AtKTN1 we wished to observe the phenotype of plants overexpressing AtKTN1 cDNA. Our findings reveal that an increased level of katanin cDNA does not cause the fragmentation of the CMT array but does affect the organization of the CMTs.

PLANTS OVEREXPRESSING *FRA2* HAVE DISORGANIZED CORTICAL MICROTUBULE ARRAYS

Based on the similarity of plant katanin to its animal homologue, it is feasible that plants overexpressing this MT-severing protein would have defects in MT dynamics due to a rapid severing of long MTs. Our observations of the CMT arrays in rapidly elongating pith cells of Fra2OE stem and petiole, however, reveal that AtKTN1 function in vivo may be tightly regulated by other factors. Wild type cells undergoing rapid elongation have CMTs typically arranged in parallel and perpendicular to the axis of cell and organ growth. In pith cells of plants overexpressing the *AtKTN1* transcript the CMT arrays are disorganized and appear almost random in their organization at the cortex (Figures 4.2, 4.3, and 4.13A). The appearances of the Fra2OE CMT arrays was similar to those seen in the *fra2* mutant pith cells and even share the characteristic star-like spots where several MTs appear to converge (See Burk and Ye, 2002, Figures 4 and 10). It was expected that the increased expression of a MT-severing protein would have led to an increase in the rate of MT disassembly in Fra2OE cells and cause the CMT arrays to appear fragmented as was seen in transient assays using HeLa cells (McNally et al., 2000) The results presented above, however, were unexpected as the apparent lengths of individual CMTs seem to be unaffected and bundles of MTs can be traced from one edge of a cell to the other (Figures 4.2 and 4.3). These results demonstrate that in vivo, AtKTN1 does not randomly sever MTs in the cell cortex. AtKTN1 activity may be tightly regulated during plant cell growth by other, yet uncharacterized, proteins. That this may be a possibility is strengthened by the recent finding that AtKTN1 interacts with other MT-associated proteins. Using full-length AtKTN1 as bait in a yeast two hybrid screen Bouquin et al. (2003) found several potential candidate proteins that interacted with AtKTN1. An Arabidopsis ortholog of the animal p80 subunit of katanin was abundantly represented in the clones obtained using the two-hybrid screen as well as KSN1, a putative kinesin motor protein. Co-immunoprecipitation assays conducted confirmed the association of

these proteins with AtKTN1 and database searches revealed the presence of four p80 homologues in the Arabidopsis genome. This finding is significant since it is known that the localization of MT-severing activity by the p60 subunit to centrosomes in animal cells is due to WD40 repeats within the C-terminal region of the p80 subunt and the activity of p60 appears to be stimulated by p80 (Hartman et al., 1998; Srayko et al., 2000; McNally et al., 2000).

The similarities between the Fra2OE CMT arrays and those of the *fra2* mutant may be due to several possibilities. Increased amounts of functional AtKTN1 protein may alter MT dynamics in a way not detectable in our examinations. If decreased MT severing in the *fra2* mutant can cause delays in the disassembly of the perinuclear array then perhaps increased severing at the perinuclear membrane after cytokinesis could affect the proper formation of the CMT array. Another possibility that could explain the CMT phenotype observed is that AtKTN1 cannot sever mature MTs in the cortex. In vitro studies utilize pure α- and β-tubulin subunits which form 'naked' microtubules. The polymerized MTs in vivo are known to be associated with a number of microtubule-associated proteins (MAPs) and some of these MAPs may protect the MTs from katanin severing. For example, the *mor1* mutant of Arabidopsis appears to have defects in the stability and organization of microtubules when grown under restrictive temperatures (Whittington et al., 2001). MOR1 may function as a MT stabilizing protein by protecting the MTs from disassembly by other proteins (Wasteneys, 2002). It is possible that MAPs exist which can stabilize the CMTs and prevent random severing of the long polymers by plant katanin.

Observations of purified sea urchin p60 and p80 subunits using rotary shadowed protein adsorbed onto mica chips revealed that p60 appears to form ring structures either alone or with equalmolar concentrations of purified p80 (Hartman et al., 1998). The exact nature of functional p60/p80 katanin heterodimers is not yet clear although it is known that katanin is made up of equalmolar amounts of each subunit and p60 function

does not rely on the presence of p80 (McNally and Vale, 1993). Excess p60 may induce the formation of non-functional aggregates that fail to associate properly with MTs. Inhibition of proper associations between AtKTN1 subunits, p80 subunits, and microtubules may lead to failure in the necessary and timely reorganization of MTs after cell division. We believe that the rapid severing of MTs at the perinuclear membrane and at cortical sites of MT nucleation are required for the proper orientation of the CMT array and a disruption in MT-severing leads to the random organization of CMTs seen in the Fra2OE plant cells. This inhibition of rapid MT severing in Fra2OE cells may result in the aster-like sites of MTs seen in the cell cortex in pith and petiole parenchyma (Figures 4.2 and 4.3). The finding that Fra2OE plants have roots that appear to elongate normally and have CMTs in wild type orientations (data not shown) may indicate that roots of Arabidopsis may have a higher level of the necessary p80 subunit to compensate for excess p60, may have mechanisms for removing excess AtKTN1 or may simply be less sensitive to increases in the level of AtKTN1.

DEFECTS IN THE CMT ARRAYS OF FRA2OE PITH CELLS ARE MIRRORED IN THE CMF ORGANIZATION IN PRIMARY WALLS

Disorganization of the CMT arrays in plant cells through the use of pharmacological drugs is known to alter normal cell expansion and leads to isotropic growth (Mathur and Hülskamp, 2002). This alteration of CMTs is believed to affect the deposition of nascent cellulose microfibrils in the cell wall and results in aberrations in cell growth due to the loss of a structured microfibrillar arrangement (Giddings and Staehelin, 1991; Baskin, 2000) although exceptions to this MT/CMF parallelism hypothesis exist (See Wasteneys, 2000). Visualization of the CMT array and the CMFs of rapidly elongating cells in the *fra2* mutant revealed a distinct correlation between these two components and is believed to be the basis for the loss of proper diffuse growth in these plants (Burk and Ye, 2002). We wished to examine the possibility that overexpression of AtKTN1 may cause a similar disruption of the cellulose microfibrils in cell walls of petiole and stem pith cells

and, therefore, possibly explain the failure of these cells to expand properly. Using field emission scanning electron microscopy, we were able to discern differences in the CMFs of Fra2OE plant cell walls when compared to wild type (Figures 4.4 and 4.5). Wild type microfibrils at the innermost layer of elongating cell walls were arranged in parallel and perpendicular to the axis of cell elongation and this arrangement was statistically different from that of Fra2OE CMFs (Fig. 4.6B). The arrangement of the CMFs in transgenic plant cells from elongating pith and petiole were found to vary widely in their orientation and bundles of five to 15 individual microfibrils could be seen running in different directions. These bundles sometimes appeared to travel together for long distances before dramatically altering their orientation, sometimes completely reversing their original course (Figures 4.4D and 4.5D, arrowheads). Additionally, we occasionally found sites at the innermost layer of cell walls where multiple bundles of CMFs appeared to cross each other forming aster-like structures (Figure 4.5C, arrow). Our analyses of the CMF arrangements in conjunction with statistical analysis of the orientation of CMTs in wild type and Fra2OE elongating cells reveal a very tight correlation between the two (Figure 4.6A and 4.6B). We propose that the overexpression of *Fra2* cDNA in Arabidopsis somehow affects the MT-severing activity of AtKTN1 protein in all tissues except roots and this inhibition leads to a failure in the proper organization of the CMT array. This leads to defects in the organized deposition of CMFs in transgenic plant cell walls and allows more isotropic-like growth of cells to occur.

OVEREXPRESSION OF *ATKTN1* CDNA AFFECTS PLANT MORPHOLOGY

Fra2OE plants shared characteristics of the original *fra2* mutants. Specifically the plants appeared dwarfed when compared to wild type and had reductions in the length of organs such as petioles, leaves, and stems (Figures 4.7 and 4.8 and Table 4.1). The effects of *AtKTN1* overexpression were also noted in dark-grown hypocotyls, floral organs, epidermal cells of leaves, and trichomes (Figures 4.11 to 4.13). Surprisingly, the roots of Fra2OE plants were not affected by the increased levels of *Fra2* even though northern

analysis clearly shows a marked increase of this transcript in roots. Recently, another allele of *AtKTN1*, *lue1*, was isolated in a screen for mutants with altered expression patters of a gibberellin-response gene fusion. In attempts to identify the putative location of the LUE1 protein using a GFP fusion approach it was found that ectopic expression of this fusion protein in Arabidopsis phenocopies the original lue1 mutant phenotype. The morphology of the GFP::LUE1 transgenic plants was proposed to be due to the creation of a dominant negative form of AtKTN1 which lacks wild type katanin activity (Bouquin et al., 2003). Based on our research, however, it appears that increases in the wild-type levels of *AtKTN1* somehow disrupt the normal MT dynamics in plant cells and lead to the overall dwarf phenotype through reductions in cell elongation.

Analysis of the cellular anatomy of Fra2OE plants revealed that the reduction in organ length we observed was due to a decrease in cell length. In addition, pith parenchyma cells of stems and petiole appeared to have disruptions in the orderly arrangement of cell files (Figure 4.9). This cellular phenotype has also been noted in the *botero*, *fra2*, and *erh3* mutants that are known to have mutations in the gene encoding AtKTN1 (Burk et al., 2001; Bichet et al., 2001; Webb et al., 2002).

METHODS

MATERIALS

Wild type and Fra2OE *Arabidopsis thaliana* seeds were germinated on Murashige and Skoog (1962) medium on vertically placed plates and grown in a growth chamber at 24°C under a 16-h-light/8-h-dark photoperiod. For analysis of 5-day-old dark grown hypocotyls, Petri dishes were covered with aluminum foil. Stems and petioles used for the visualization of cellulose microfibrils were from plants grown in soil in a growth room at 22°C under a 12-h-light/12-h-dark photoperiod. The first emerging elongating internodes of inflorescence stems were used for the examination of MT and cellulose microfibrils in pith cells. For examination of secondary cell wall structure of

interfascicular fibers, plants were grown under greenhouse conditions and the second internode from the base of the inflorescence stem was used.

HISTOLOGY

Tissues were fixed in 2% glutaraldehyde in PBS (33 mM Na_2HPO_4, 1.8 mM NaH_2PO_4, and 140 mM NaCl, pH 7.3) at 4°C overnight. After fixation, segments were dehydrated through a gradient of ethanol, cleared in propylene oxide, and embedded in Araldite resin (Electron Microscopy Sciences, Fort Washington, PA). One-micrometer-thick sections were cut with a microtome and stained with toluidine blue for observation of anatomy.

FIELD EMISSION SCANNING ELECTRON MICROSCOPY

For observation of surface features of wild type and Fra2OE plants, fresh tissue was flash-frozen in liquid N_2 slush under low pressure and quickly transferred to the cryo-preparation chamber of a Gatan Alto 2500 Cryotransfer attachment (Gatan Incorporated, Pleasanton, CA). Tissues were then warmed for a short time to sublimate ice crystals before being coated with gold and moved to the Gatan Alto 2500 cryostage for examination using a LEO 982 FE scanning electron microscope (LEO, Thornwood, NY) at an excitation voltage of 4 to 5.00 kV at a working distance of 10-11 mm.

Cellulose microfibrils at the innermost layer of cell walls were visualized using field emission scanning electron microscopy according to Sugimoto et al. (2000). Elongating stems and petioles were cut longitudinally using a vibratome after fixation. Tissues were dried using a Samdri critical point dryer (Tousimis, Rockville, MD) before being mounted on stubs with carbon paste. Samples were coated with platinum using an Edwards 306 vacuum evaporator (Edwards high Vacuum International, Wilmington, MA) and viewed using a LEO 982 FE scanning electron microscope at an excitation voltage of 1.00 kV at a working distance of 3-4 mm utilizing the SE inlens.

IMMUNOLOCALIZATION OF MTS

MTs were visualized by immunolabeling α-tubulins according to Sugimoto et al. (2000). Young elongating stems and petioles were used for MT localization. Samples were probed first with mouse monoclonal antibody against chicken α-bubulin (1:800 dilution; Sigma) and then incubated with fluorescein isothiocyanate-conjugated goat antibody against mouse IgG (1:800 dilution; Sigma). MTs were visualized using a Leica TCS SP2 spectral confocal microscope (Leica Microsystems, Heidelberg, Germany). Images were saved and processed with Adobe Photoshop version 5.0 software (Adobe, San Jose, CA).

TRANSMISSION ELECTRON MICROSCOPY

Tissues were fixed in 2% (v/v) glutaraldehyde in phosphate buffer (50 mM, pH 7.2) at 4°C overnight. After fixation, tissues were postfixed in 2% (v/v) OsO_4 for 2 h. After being washed in phosphate buffer, tissues were dehydrated in ethanol, infiltrated with Araldite/Embed 812 resin (Electron Microscopy Sciences, Fort Washington, PA), and finally polymerized in Araldite/Embed resin. For electron microscopy, 90-nm-thick sections were cut with a Reichert-Jung ultrathin microtome (C. Reichert Optische Werke AG, Vienna, Austria), mounted on formvar-coated copper grids, and poststained with uranyl acetate and lead citrate. Cell wall structure was visualized with a Zeiss EM 902A electron microscope (Jena, Germany).

QUANTATIVE ANALYSIS

Statistical analysis of CMT and CMF angles were determined as described by Burk and Ye (2002). Briefly, five or six representative images of wild type and Fra2OE cell walls or CMTs from different cells were reduced to a fixed size, and a grid was overlaid on the image so that approximately 200 evenly spaced grid points were available for analysis. At each grid point, the angle of the single microtubule or microfibril that passed through or was closest to the point was measured using the ruler tool of Adobe Photoshop 5.0.

The MT or CMF was traced along its length for a fixed distance from the grid point, and the angle noted. If at any grid point the MT or CMF was not resolved sufficiently for

tracing, that point was discarded. All angles were measured relative to the axis perpendicular to the long axis of the cell. This perpendicular axis was arbitrarily assigned an angle of 0°. Using this method, CMTs and CMFs can approach angles of ≈90° and correspond to fibrils approaching a longitudinal orientation in a left- or right-handed helix.

ACKNOWLEDGEMENTS

I thank R. Zhong for her expert assistance in generation of the AtKTN1 fusion construct and transgenic plants as well as for conducting RT-PCR analysis of AtKTN1 expression, Z.-H. Ye for his help throughout my work on this experiment as well as critical advice on my writing, and J. Shields and M. Farmer for their training and help with the cryo-SEM and confocal microscopy. I was supported by a Plant Evolution Training Grant from the National Science Foundation.

REFERENCES

Ahmad, F.J., Yu, W., McNally, F.J., and Baas, P.W. (1999). An essential role for katanin in severing microtubules in the neuron. J Cell Biology 145, 305-315.

Baskin, T.I. (2000). The cytoskeleton. In Biochemistry and Molecular Biology of Plants, B.B. Buchanan, W. Gruissem, and R.L. Jones, eds (Rockville, MD: American Society of Plant Physiologists), pp. 202-258.

Baskin, T.I. (2001). On the alignment of cellulose microfibrils by cortical microtubules: a review and a model. Protoplasma 215, 150-171.

Bichet, A., Desnos, T., Turner, S., Grandjean, O., and Höfte, H. (2001). *BOTERO1* is required for normal orientation of cortical microtubules and anisotropic cell expansion in Arabidopsis. Plant J 25, 137-148.

Bouquin, T., Mattsson, O., Næsted H., Foster, R., and Mundy, J. (2003). The Arabidopsis *lue1* mutant defines a katanin p60 ortholog involved in hormonal control of microtubule orientation during cell growth. Journal of Cell Science 116, 791-801.

Burk, D.H., and Ye, Z.-H. (2002). Alteration of oriented deposition of cellulose microfibrils by mutation of a katanin-like microtubule-severing protein. Plant Cell 14, 2145-2160.

Burk, D.H., Liu, B., Zhong, R., Morrison, W.H., and Ye, Z.-H. (2001). A katanin-like protein regulates normal cell wall biosynthesis and cell elongation. Plant Cell 13, 807-827.

Buster, D., McNally, K., and McNally, F.J. (2002). Katanin inhibition prevents the redistribution of γ-tubulin at mitosis. Journal of Cell Science 115, 1083-1092.

Camilleri, C., Azimzadeh, J., Pastuglia, M., Bellini, C., Grandjean, O., and Bouchez, D. (2002). The Arabidopsis TONNEAU2 gene encodes a putative novel protein phosphatase 2A regulatory subunit essential for the control of the cortical cytoskeleton. Plant Cell 14, 833-345.

Cosgrove, D.J. (1997). Relaxation in a high-stress environment: the molecular basis of extensible cell walls and enlargement. Plant Cell 9, 1031, 1041.

Cosgrove, D.J. (2000). New genes and new biological roles for expansins. Current Opinion in Plant Biology 3, 73-78.

Cyr, R.J., and Palevitz, B.A. (1995). Organization of cortical microtubules in plant cells. Current Opinion in Cell Biology 7, 65-71.

Furutani, I., Watanabe, Y., Prieto, R., Masukawa, M., Suzuki, K., Naoi, K., Thitamadee, S., Shikanai, T., and Hashimoto, T. (2000). The *SPIRAL* genes are required for directional control of cell elongation in Arabidopsis thaliana. Development 127, 4443-4453.

Giddings, T.H. Jr., and Staehelin, L.A. (1991). Microtubule-mediated control of microfibril deposition: a re-examination of the hypothesis. In *The Cytoskeletal*

Basis of Plant Growth and Form. Edited by Lloyd C.W. London: Academic Press; 85-99.

Hartman, J.J., Mahr, J., McNally, K., Okawa, K., Iwamatsu, A., Thomas, S., Cheesman, S., Heuser, J., Vale, R.D., and McNally, F.J. (1998). Katanin, a microtubule-severing protein, is a novel AAA ATPase that targets to the centrosome using a WD40-containing subunit. Cell 93, 277-287.

Kirik, V., Grini, P.E., Mathur, J., Klinkhammer, I., Adler, K., Bechtold, N., Herzog, M., Bonneville, J.-M., and Hülskamp, M. (2002). The Arabidopsis *TUBULIN-FOLDING COFACTOR A* gene is involved in the control of the α/β-tubulin monomer balance. Plant Cell 14, 2265-2276.

Kost, B., and Chua, N.-H. (2002). The plant cytoskeleton: vacuoles and cell walls make a difference. Cell 108, 9-12.

Lloyd, C., and Chan, J. (2002). Helical microtubule arrays and spiral growth. Plant Cell 14, 2319-2324.

Lohret, T.A., McNally, F.J., and Quarmby, L.M. (1998). A role for katanin-mediated axonemal severing during *Chlamydomonas* deflagellation. Mol. Biol. Cell 9, 1195-1207.

Lohret, T.A., Zhao, L., and Quarmby, L.M. (1999). Cloning of Chlamydomonas p60 katanin and localization to the site of outer doublet severing during deflagellation. Cell Motility and the Cytoskeleton 43, 221-231.

Luo, D., and Oppenheimer, D.G. (1999). Genetic control of trichome branch number in Arabidopsis: The roles of the *FURCA* loci. Development 126, 5547-5557.

Mathur, J., and Hülskamp, M. (2002). Microtubules and microfilaments in cell morphogenesis in higher plants. Current Biology 12, R669-R676.

Mayer, U., Herzog, U., Berger, F., Inzé, D., and Jürgens, G. (1999). Mutations in the PILZ group genes disrupt the microtubule cytoskeleton and uncouple cell cycle

progression from cell division in Arabidopsis embryo and endosperm. European Journal of Cell Biology 78, 100-108.

McClinton, R.S., Chandler, J.S., and Callis, J. (2001). cDNA isolation, characterization, and protein intracellular localization of a katanin-like p60 subunit from *Arabidopsis thaliana*. Protoplasma 216, 181-190.

McNally, F.J., and Vale, R.D. (1993). Identification of katanin, an ATPase that severs and disassembles stable microtubules. Cell 75, 419-429.

McNally, F.J., Okawa, K., Iwamatsu, A., and Vale, R.D. (1996). Katanin, the microtubule-severing ATPase, is concentrated at centrosomes. J Cell Science 109, 561-567.

McNally, K.P., Bazirgan, O.A., and McNally, F.J. (2000). Two domains of p80 katanin regulate microtubule severing and spindle pole targeting by p60 katanin. J Cell Science 113, 1623-1633.

Murashige, T., and Skoog, F. (1962). A revised medium for rapid growth and bioassays with tobacco tissue culture. Physiol. Plant. 15, 473-497.

Qiu, J.-L., Jilk, R., Marks, M.D., and Szymanski, D.B. (2002). The Arabidopsis *SPIKE1* gene is required for normal cell shape control and tissue development. Plant Cell 14, 101-118.

Shibaoka, H. (1994). Plant hormone-induced changes in the orientation of cortical microtubules: alterations in the cross-linking between microtubules and the plasma membrane. Annu Rev Plant Physiol Plant Mol Biol *45*, 527-544.

Smith, L.G. (2003). Cytoskeletal control of plant cell shape: getting the fine points. Current Opinion in Plant Biology 6, 63-73.

Smith, L.G., Gerttula, S.M., Han, S., and Levy, J. (2001). TANGLED1: A microtubule binding protein required for the spatial control of cytokinesis in maize. Journal of Cell Biology 152, 231-236.

Srayko, M., Buster, D.W., Bazirgan, O.A., McNally, F.J., and Mains, P.E. (2000). MEI-1/MEI-2 katanin-like microtubule severing activity is required for Caenorhabditis elegans meiosis. Genes Development 14, 1072-1084.

Stoppin-Mellet, V., Gaillard, J., and Vantard, M. (2002). Functional evidence for *in vitro* microtubule severing by the plant katanin homologue. Biochem J 365, 337-342.

Sugimoto, K., Williamson, R.E., and Wasteneys, G.O. (2000). New techniques enable comparative analysis of microtubule orientation, wall texture, and growth rate in intact roots of Arabidopsis. Plant Physiol. 124, 1493-1506.

Wasteneys, G.O. (2000). The cytoskeleton and growth polarity. Current Opinion in Plant Biology 3, 503-511.

Wasteneys, G.O. (2002). Microtubule organization in the green kingdom: chaos or self-order? Journal of Cell Science 115, 1345-1354.

Webb, M., Jouannic, S., Foreman, J., Linstead, P., and Dolan, L. (2002). Cell specification in the Arabidopsis root epidermis requires the activity of *ECTOPIC ROOT HAIR 3* – a katanin-p60 protein. Development 129, 123-131.

Whittington, A.T., Vugrek, O., Wei, K.J., hasenbein, N.G., Sugimoto, K., Rashbrooke, M.C., and Wasteneys, G.O. (2001). MOR1 is essential for organizing cortical microtubules in plants. Nature 411, 610-613.

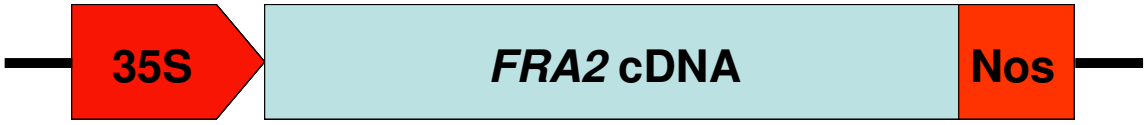

Figure 4.1. Diagram of the AtKTN1 construct.

The full length cDNA of the *Fra2* (*AtKTN1*) gene was inserted in the multiple cloning site of the vector pBI121 and its expression is dictated by the constitutive 35S promoter.

Figure 4.2. Visualization of CMTs in Pith Cells of Stems.

Pith cells from elongating internodes were used for MT labeling with a monoclonal antibody against α-tubulin. Antibody-labeled MTs were detected with fluorescein isothiocyanate-conjugated secondary antibodies, and the signals of fluorescent MTs were visualized with a confocal microscope.

(A) and (B) Wild type pith cells showing transversely oriented CMTs.

(C) Pith cells of Fra2OE plants showing the random organization of CMTs in most cells. Note that in some cells, the CMTs appear to have a transverse alignment (arrowheads).

(D) Higher magnification of a Fra2OE pith cell showing the aberrantly arranged CMTs.

(E) High magnification of a transgenic pith cell showing the disorganized arrangement of CMTs as well as multiple sites of MT convergence.

Bars in (A) to (C) = 20 μm; bars in (D) and (E) = 10 μm.

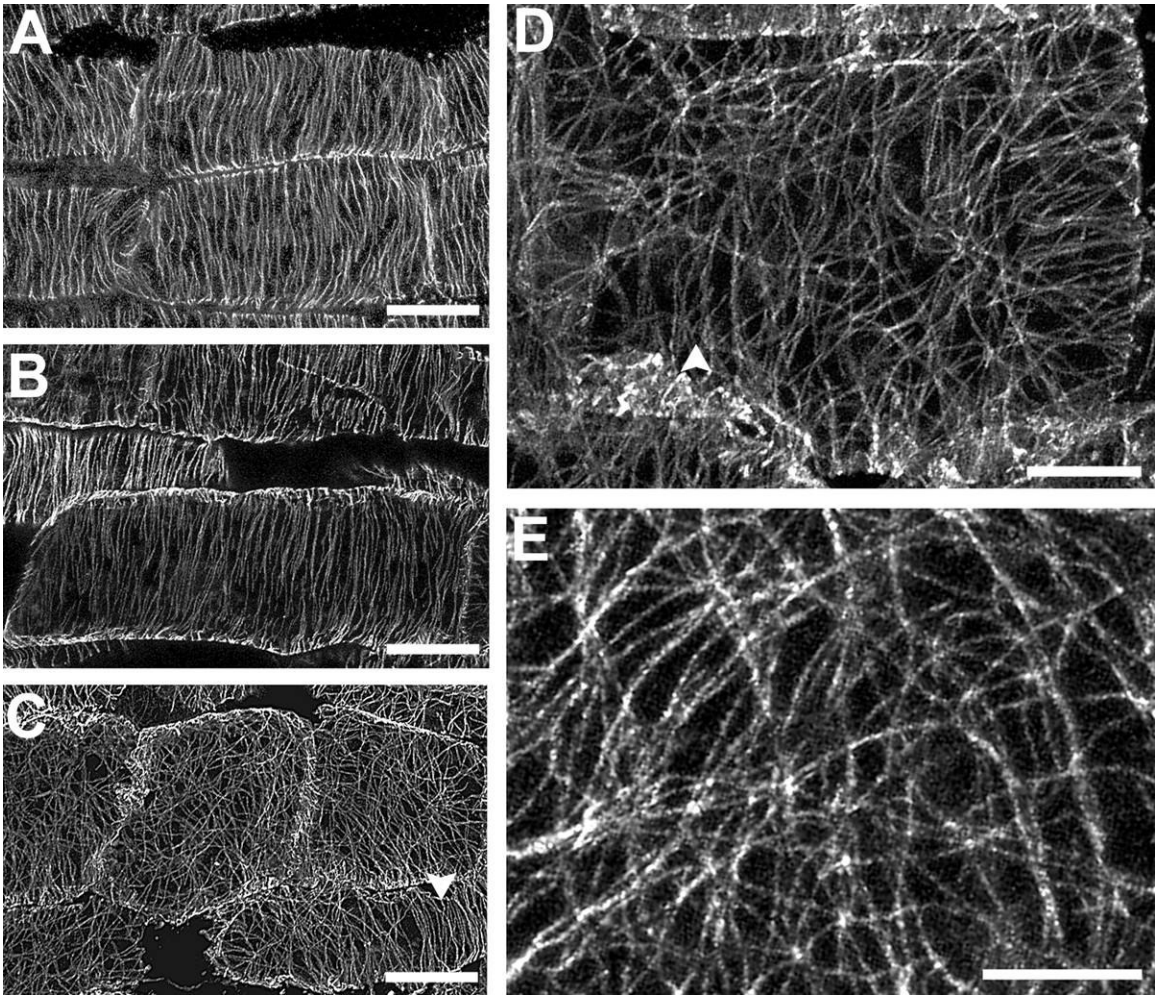
A
B
C
D
E

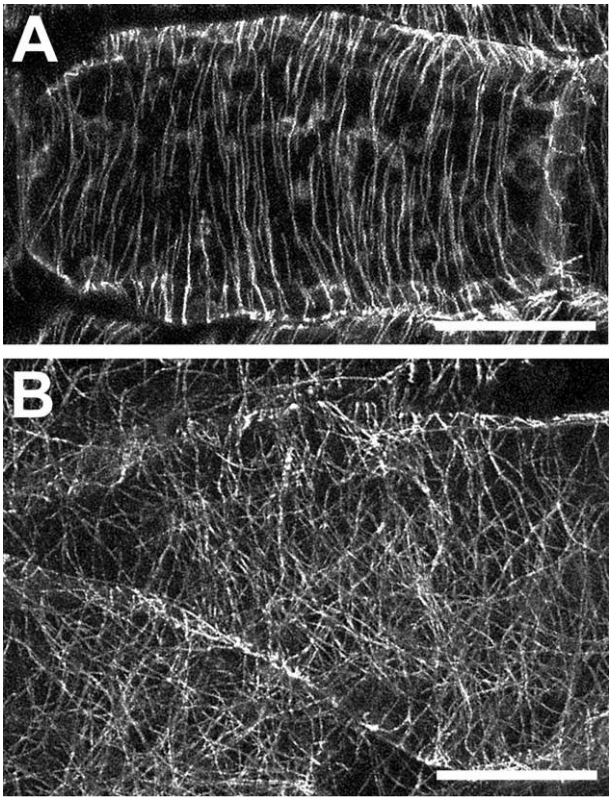

Figure 4.3. Visualization of Cortical Microtubules in Elongating Petiole Cells.

Parenchyma cells from elongating petioles were used for immunofluorescent labeling of CMTs.

(A) Wild type petiole parenchyma cell showing the transverse orientation of CMTs.

(B) A Fra2OE petiole parenchyma cell showing the aberrant organization of CMTs.

Bars = 20 μm.

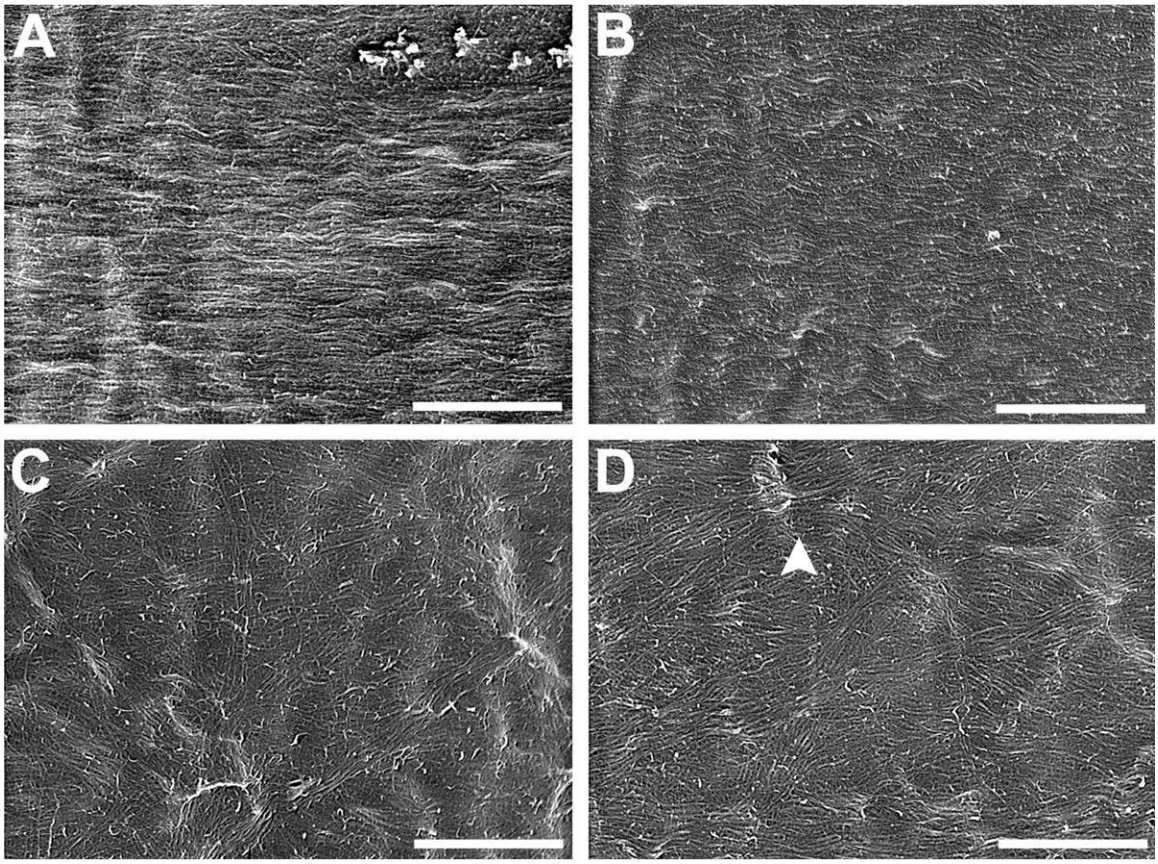

Figure 4.4. Visualization of CMFs in the Innermost Layer of Elongating Petiole Cell Walls.

(A) and (B) CMFs in wild type elongating petiole showing the parallel and transverse arrangement.

(C) and (D) CMFs in Fra2OE parenchyma cell walls showing a distorted pattern. Note the bundle of CMFs which appear to change direction by almost 90° (arrowhead).

Bars = 1 μm.

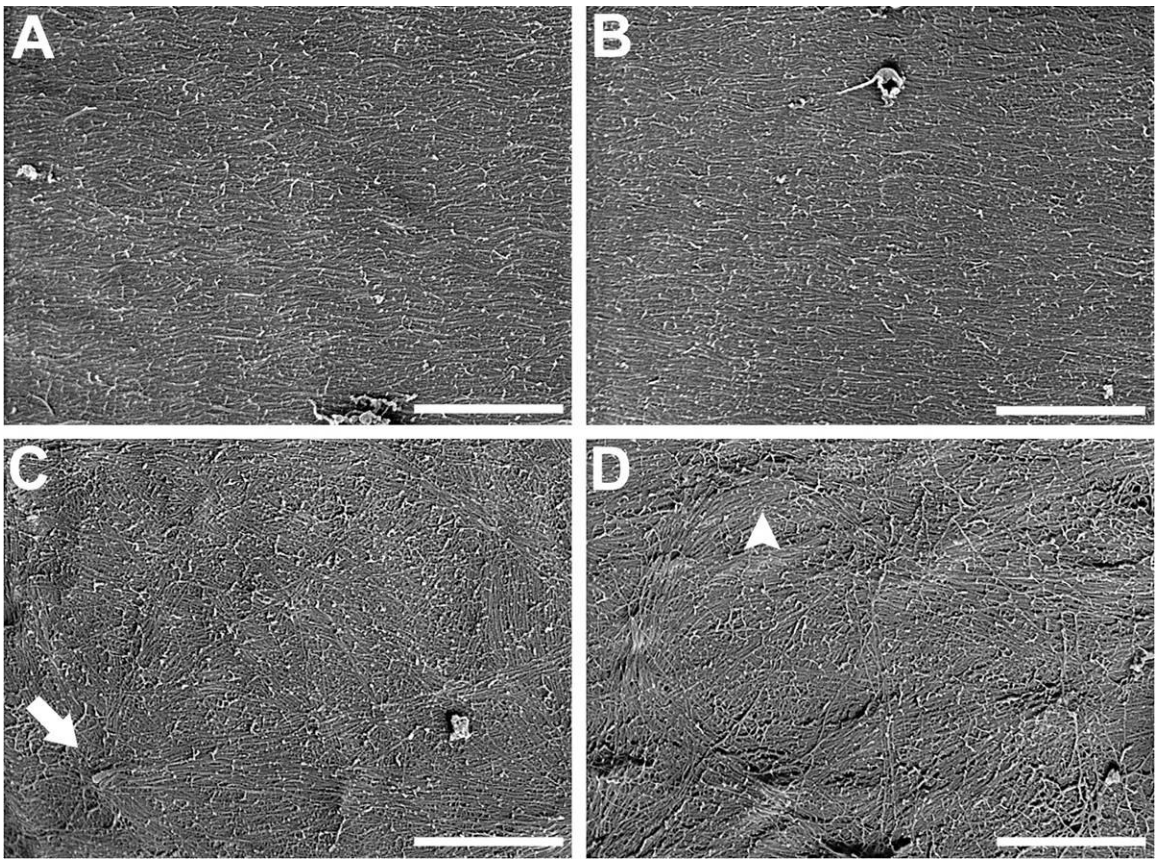

Figure 4.5. Visualization of CMFs in the Innermost Layer of Elongating Pith Cell Walls.

(A) and (B) Cellulose microfibrils in wild type pith cell walls showing their transverse orientation.

(C) and (D) Cellulose microfibrils in transgenic cell walls showing disorganization of the microfibrils. Notice the CMFs appear to radiate from a particular area in (C) (arrow) and make a dramatic change in their orientation in (D) (arrowhead).

Bars = 1 μm.

Figure 4.6. Quantative Measurements of CMT and CMF Angles in Elongating Pith Cells of Stem.

Angles of 493 wild type and 437 Fra2OE CMTs from confocal images were measured for (A) and are represented in angles of 10° increments. Angles of 491 wild type and 571 Fra2OE CMFs from field emission scanning electron micrograps of the innermost layer of cell walls were measured for (B). CMTs and CMFs at different angles were calculated as a percentage of the total examined. The transverse direction relative to the elongation axis was arbitrarily defined as 0°, and angles deviating from the transverse orientation are represented by positive or negative numbers of degrees. Insets (a), (b), and (c) show the directions of microtubules (A) or microfibrils (B) corresponding to the defined angles.

(A) Cortical microtubules of pith cells. CMTs in wild type cells show a prominent transverse orientation with <20° deviation, while the angles of CMTs in Fra2OE cells had a much higher distribution.

(B) CMFs in wild type cell walls are arranged predominantly in the transverse orientation with <20° deviation from the transverse, whereas cellulose microfibrils in Fra2OE cell walls show a much broader distribution of angles.

A

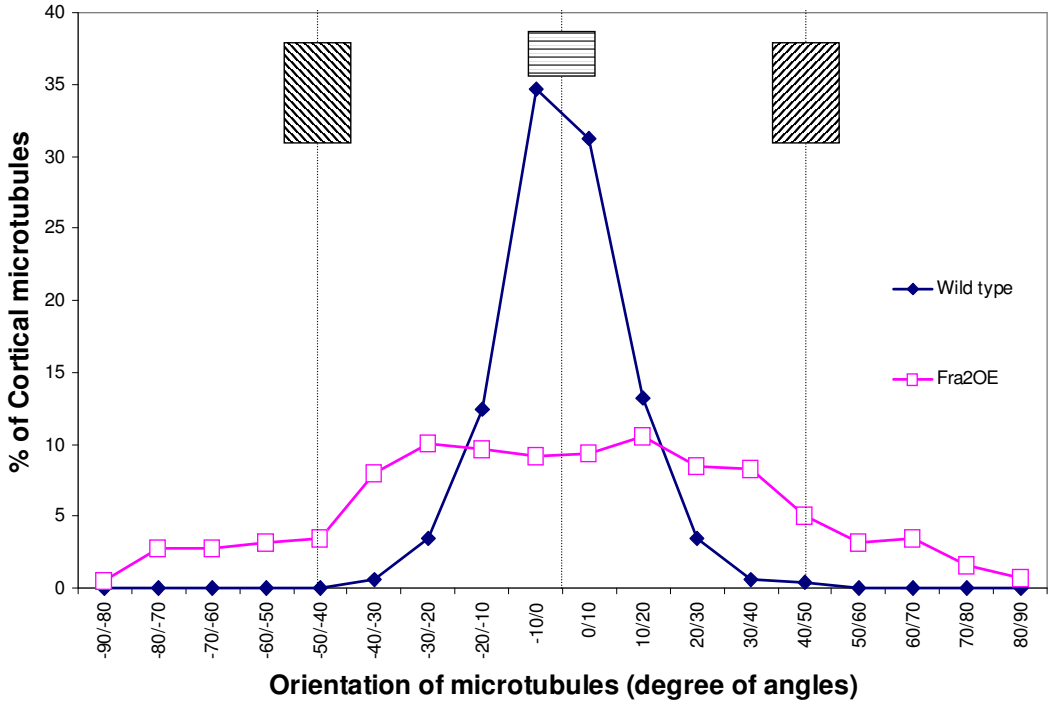
% of Cortical microtubules
40
35
30
25
20
15
10
5
0
Wild type
Fra2OE
-90/-80
-80/-70
-70/-60
-60/-50
-50/-40
-40/-30
-30/-20
-20/-10
-10/0
0/10
10/20
20/30
30/40
40/50
50/60
60/70
70/80
80/90
Orientation of microtubules (degree of angles)

B

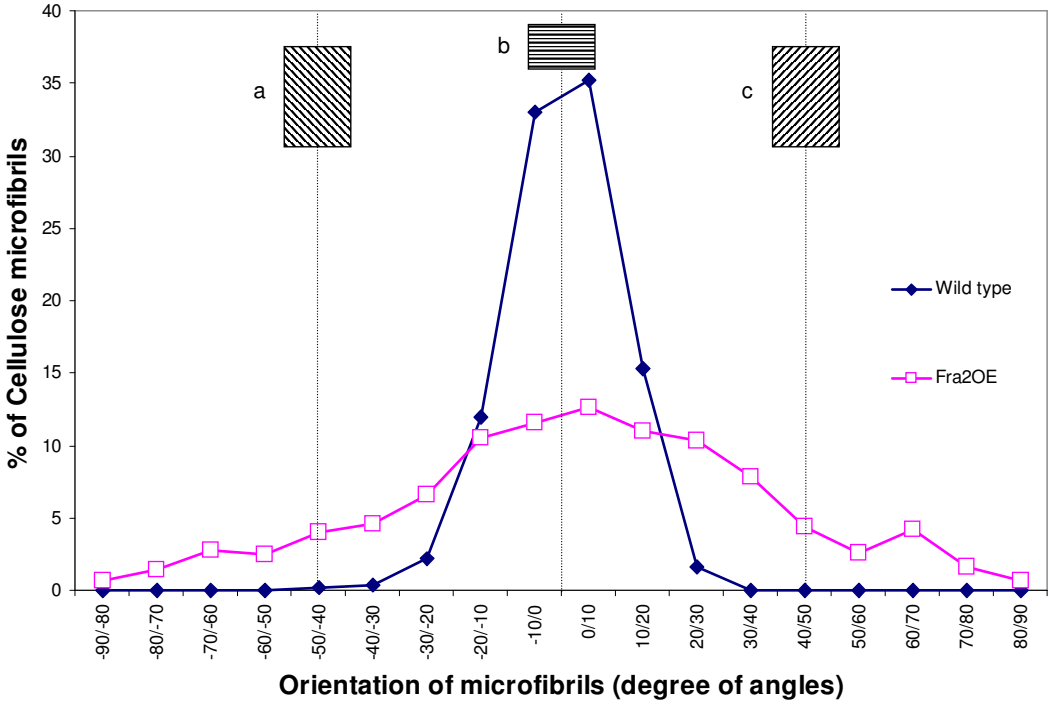
% of Cellulose microfibrils
a
b
c
40
35
30
25
20
15
10
5
0
Wild type
Fra2OE
-90/-80
-80/-70
-70/-60
-60/-50
-50/-40
-40/-30
-30/-20
-20/-10
-10/0
0/10
10/20
20/30
30/40
40/50
50/60
60/70
70/80
80/90
Orientation of microfibrils (degree of angles)

Figure 4.7. Morphology of Wild type and Fra2OE Plants.

(A) and (B) The rosette leaves of a 5-week-old Fra2OE plant (B) are more compact than those of a wild type plant (A).

(C) Morphology of 8-week-old plants. The main inflorescence stem of a Fra2OE plant (left) is much shorter than that of a wild type plant (right).

(D) The seventh rosette leaf from a wild type (left) and Fra2OE (right) plant. The length of the petiole and blade of the Fra2OE (right) are reduced when compared to wild type (left).

(E) Close-up of a Fra2OE greenhouse grown inflorescence stem showing that it has split lengthwise between the first and third internodes (arrow).


A
1 cm
B
1 cm
C
D
E

Figure 4.8. Measurement of the Length and Width of Leaves.

The fifth to seventh leaves of 5-week-old plants were measured for their length and width. Data are means ±SE of 10 leaves.

(A) Length of leaf blades, showing a reduction in Fra2OE compared with wild type.

(B) Width of leaf blades, showing an approximately 79% reduction of wild type width.

(C) Length of petioles, showing a dramatic reduction in Fra2OE compared to wild type.

A

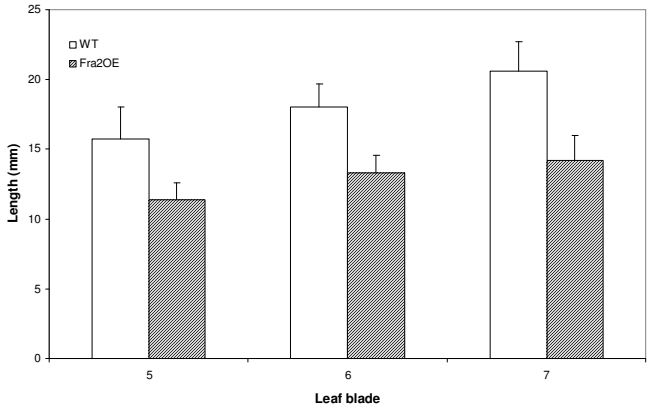
WT
Fra2OE
Length (mm)
25
20
15
10
5
0
5
6
7
Leaf blade

B

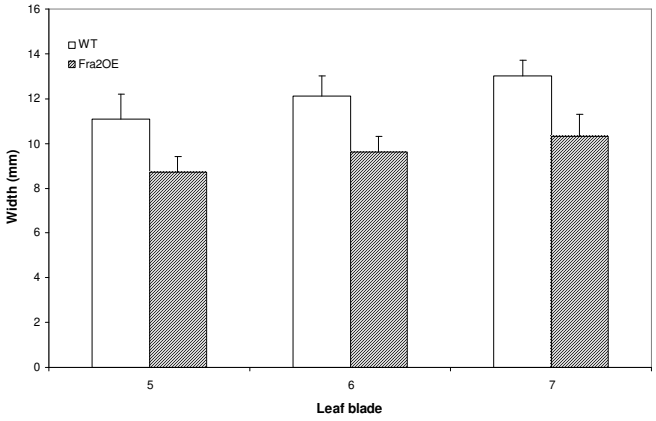
WT
Fra2OE
Width (mm)
16
14
12
10
8
6
4
2
0
5
6
7
Leaf blade

C

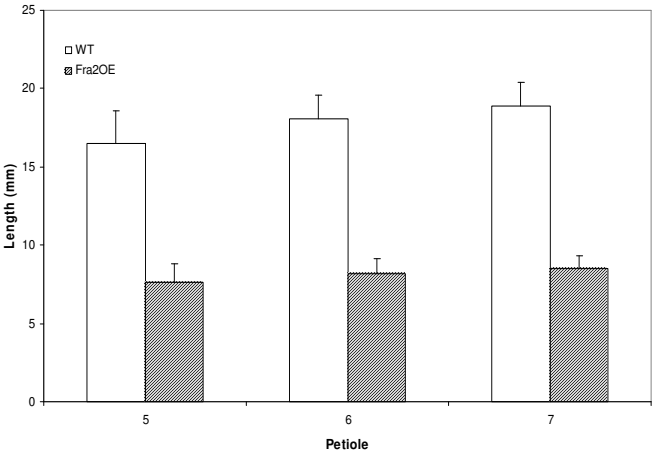
WT
Fra2OE
Length (mm)
25
20
15
10
5
0
5
6
7
Petiole

Figure 4.9. Anatomy of Pith Cells in Wild Type and Fra2OE Stem and Petiole and Interfascicular Fibers in Stems.

(A) and (B) Longitudinal sections of the stems of wild type (A) and Fra2OE (B) plants.

(C) and (D) Longitudinal sections of wild type (C) and Fra2OE (D) petiole. Notice the aberrant cell files in Fra2OE pith (D).

(E) and (F) Cross-sections of greenhouse grown stems of the wild type (E) and Fra2OE (F).

(G) and (H) Higher magnification of the interfascicular region of wild type (G) and Fra2OE (H) stems showing the reduction in secondary cell wall thickening in the transgenic plants as well as an increase in their radial dimensions.

C, cortex; e, epidermis; if, interfascicular fiber; pi, pith. Bars in (A) to (F) = 82 μm; bars in (G) and (H) = 40 μm.

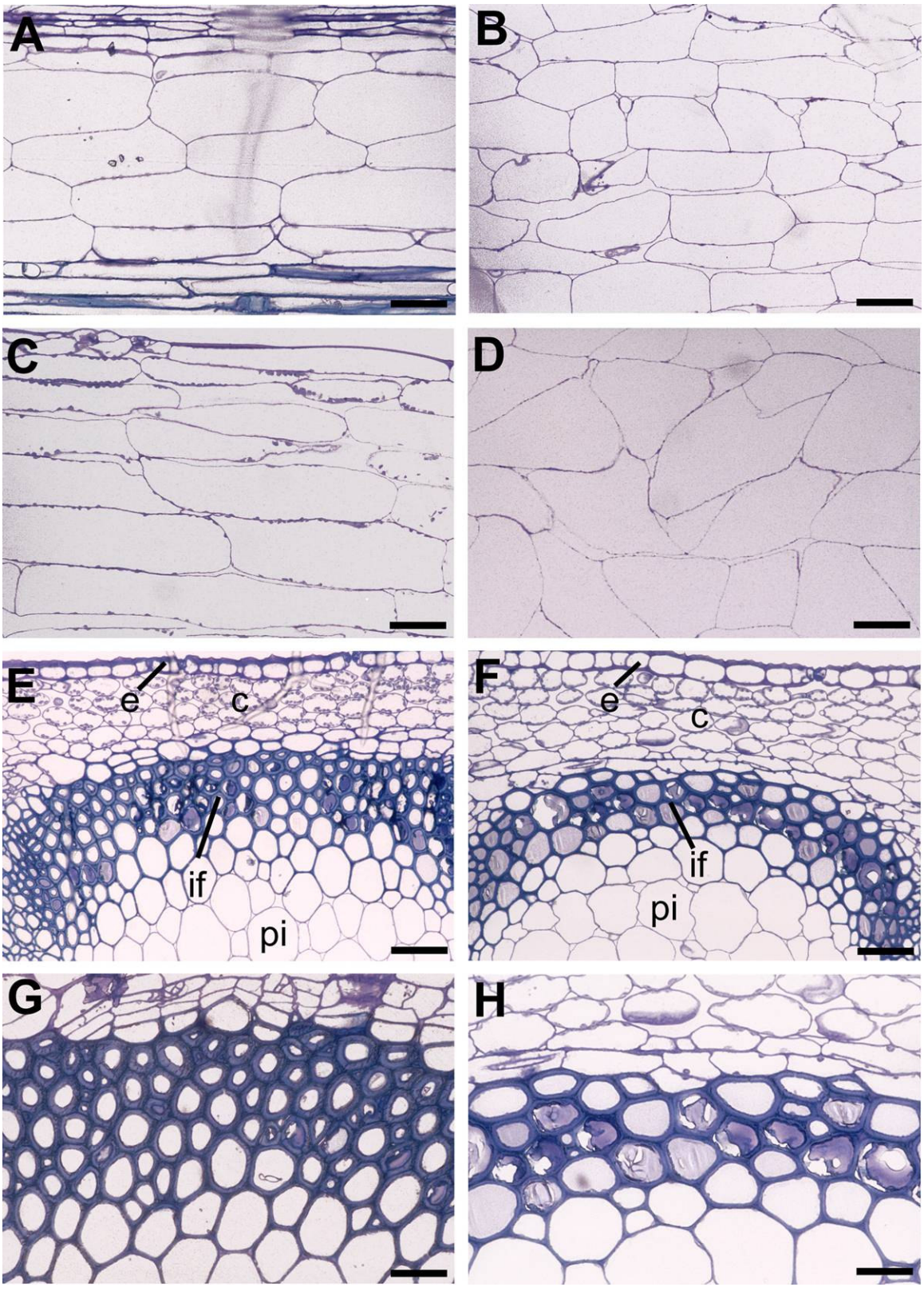
A
B
C
D
E
e
c
if
pi
F
e
c
if
pi
G
H

Figure 4.10. Structure of Fiber Cell Walls in the Wild Type and Fra2OE Plants.

(A) Interfascicular fiber cells of the wild type showing thick secondary cell walls.

(B) Interfascicular fiber cells of a Fra2OE plant showing much thinner secondary wall.

(C) Higher magnification image of the secondary cell wall of the wild type fiber cell showing a smooth inner wall surface.

(D) Higher magnification of a Fra2OE fiber wall showing less secondary wall thickening and a rough or wavy inner wall surface.

En, endodermal cells; if, interfascicular fiber cells; ml, middle lamella; sw, secondary wall. Bars in (A) and (B) = 2.5 μm; bars in (C) and (D) = 1.1 μm.

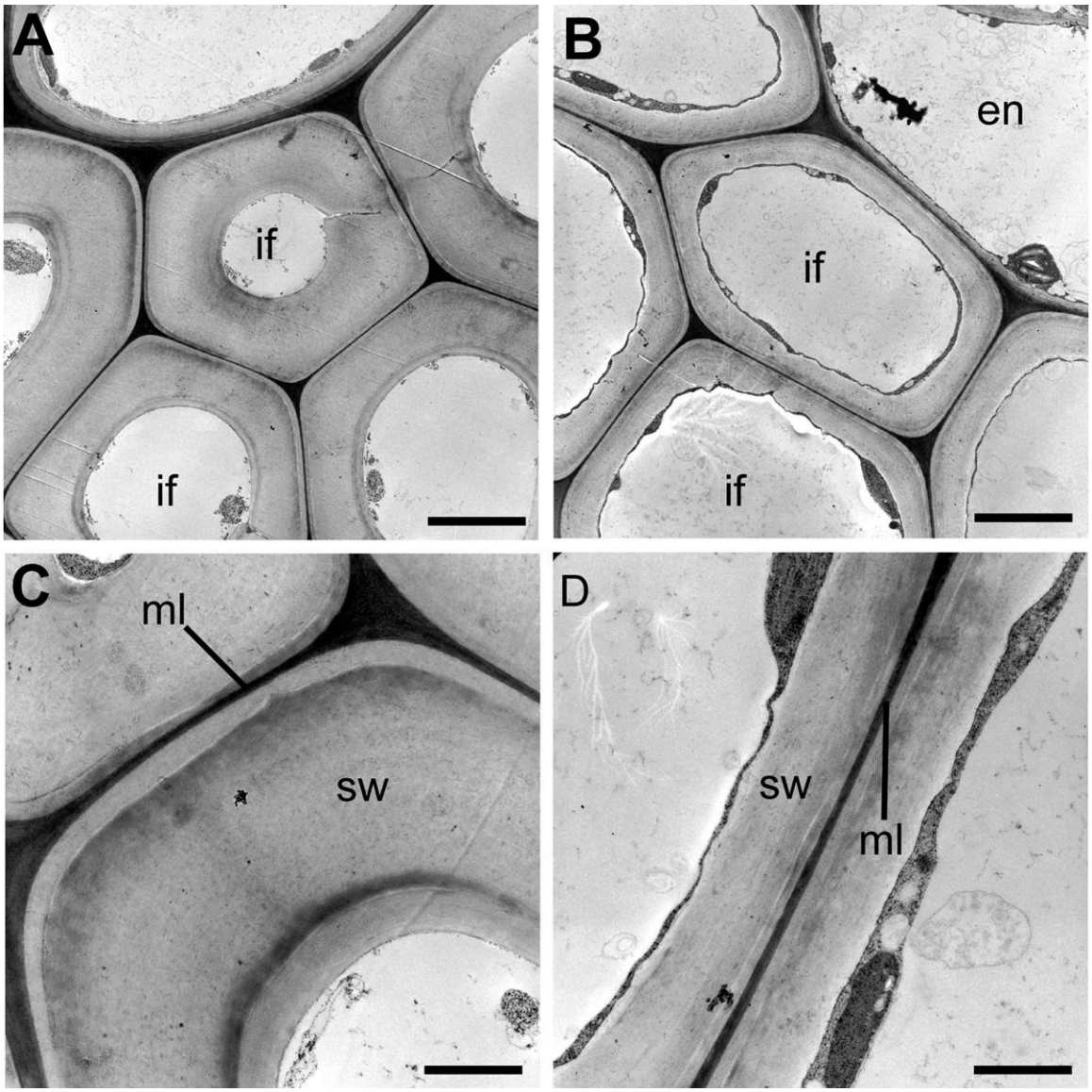
A
if
if
B
en
if
if
C
ml
sw
D
sw
ml

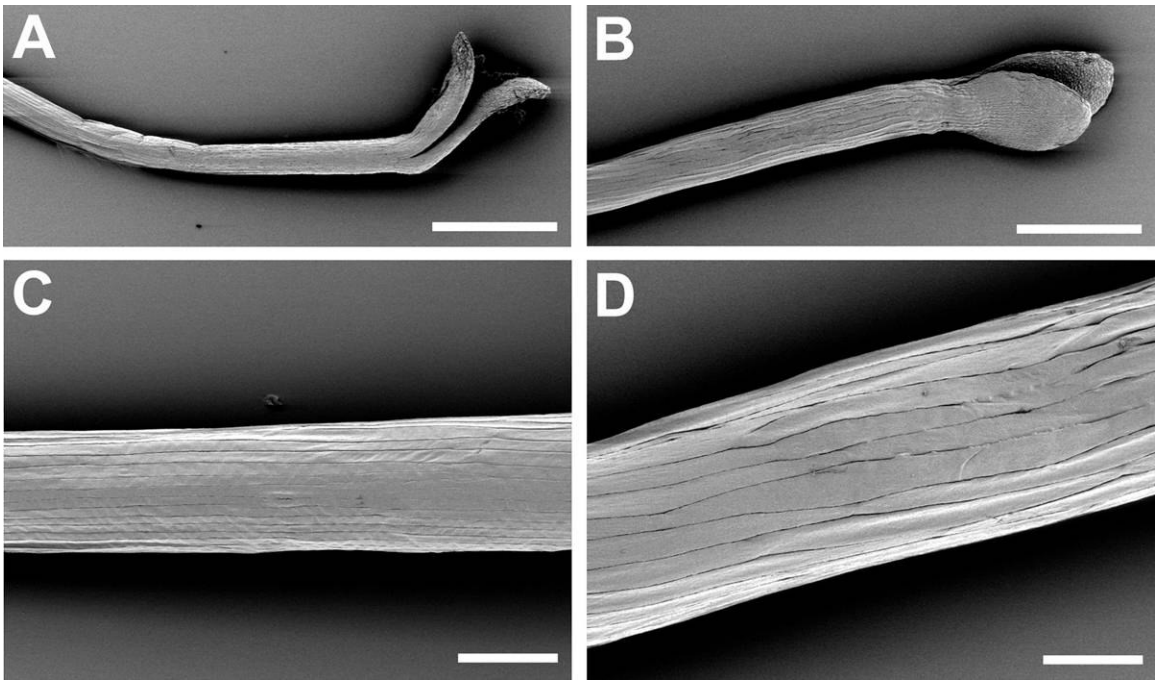

Figure 4.11. Scanning Electron Micrographs of Dark-grown Hypocotyl.

(A) and (B) Five-day-old dark-grown seedlings showing that the Fra2OE (B) hypocotyl is wider than the wild type (A).

(C) and (D) Higher magnification of the wild type (C) and Fra2OE (D) hypocotyl. Note the increased width of the transgenic hypocotyl as well as the individual epidermal cells (D).

Bars in (A) and (B) = 500 μm; bars in (C) and (D) = 100 μm.

Figure 4.12. Scanning Electron Micrographs of Wild Type and Fra2OE Leaf Surfaces.

(A) and (B) Adaxial epidermal cells of the Fra2OE (B) plants are swollen and not as lobed as the wild type (A).

(C) and (D) Abaxial epidermal cells of the transgenic plants (D) appear more compact than wild type (C) with smaller lobes.

(E) and (F) Trichomes showing that the wild type (E) has two branch points and Fra2OE plants (F) have one branch point.

Bars in (A), (B), (E), and (F) = 100 μm; bars in (C) and (D) = 50 μm.

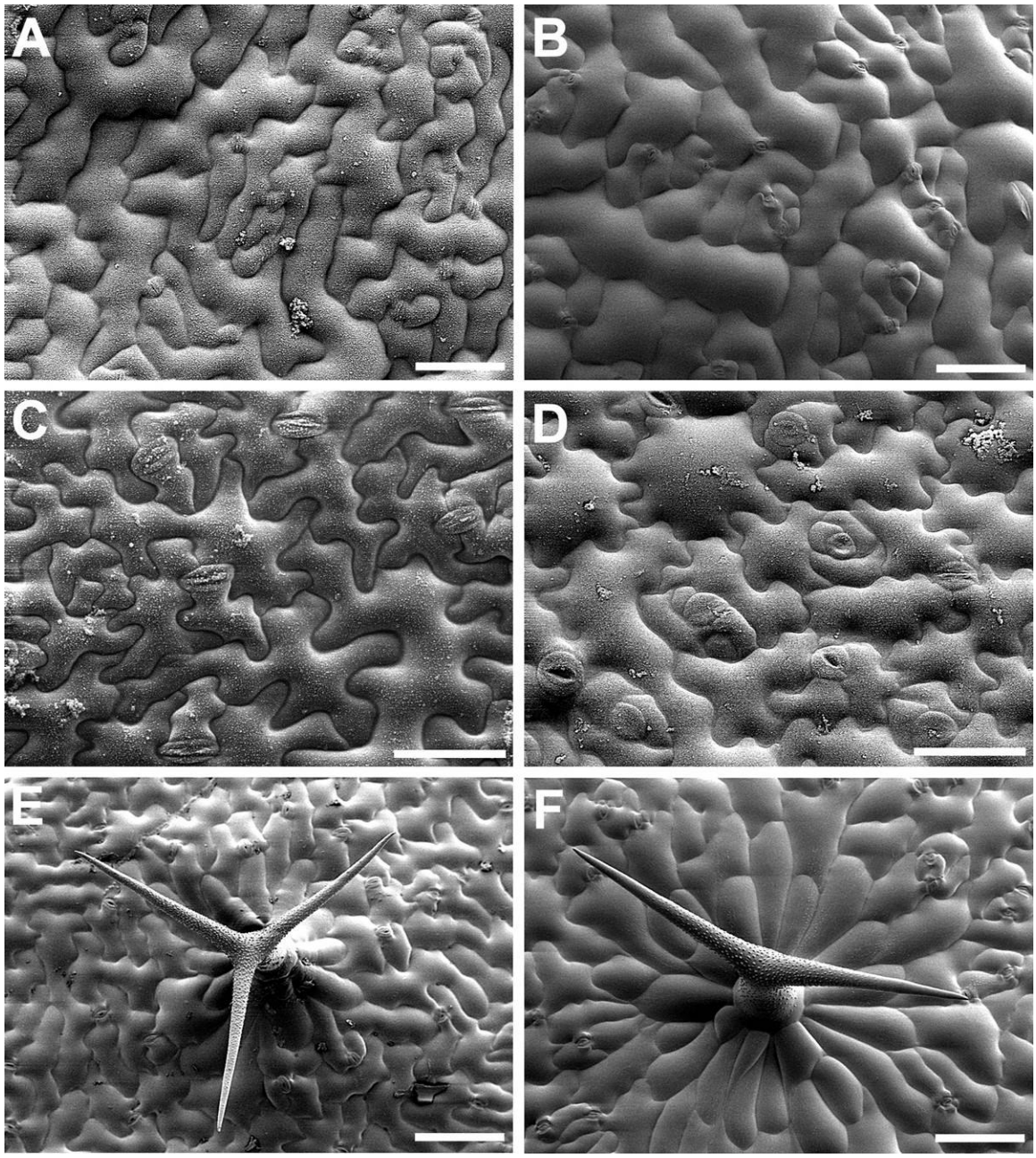
A
B
C
D
E
F

Figure 4.13. Scanning Electron Micrographs of Floral Organs.

(A) and (B) Wild type flowers (A) have longer organs than Fra2OE (B). Also, notice how much shorter the filaments of the transgenic plants are (B).

(C) and (D) Higher magnification of the wild type (C) and Fra2OE (D) anther.

(E) and (F) High magnification of wild type (E) and Fra2OE (F) filament cells showing a reduction in the length of transgenic plant cells (F).

Bars in (A) and (B) = 500 μm; bars in (C) and (D) = 100 μm; bars in (E) and (F) = 50 μm.

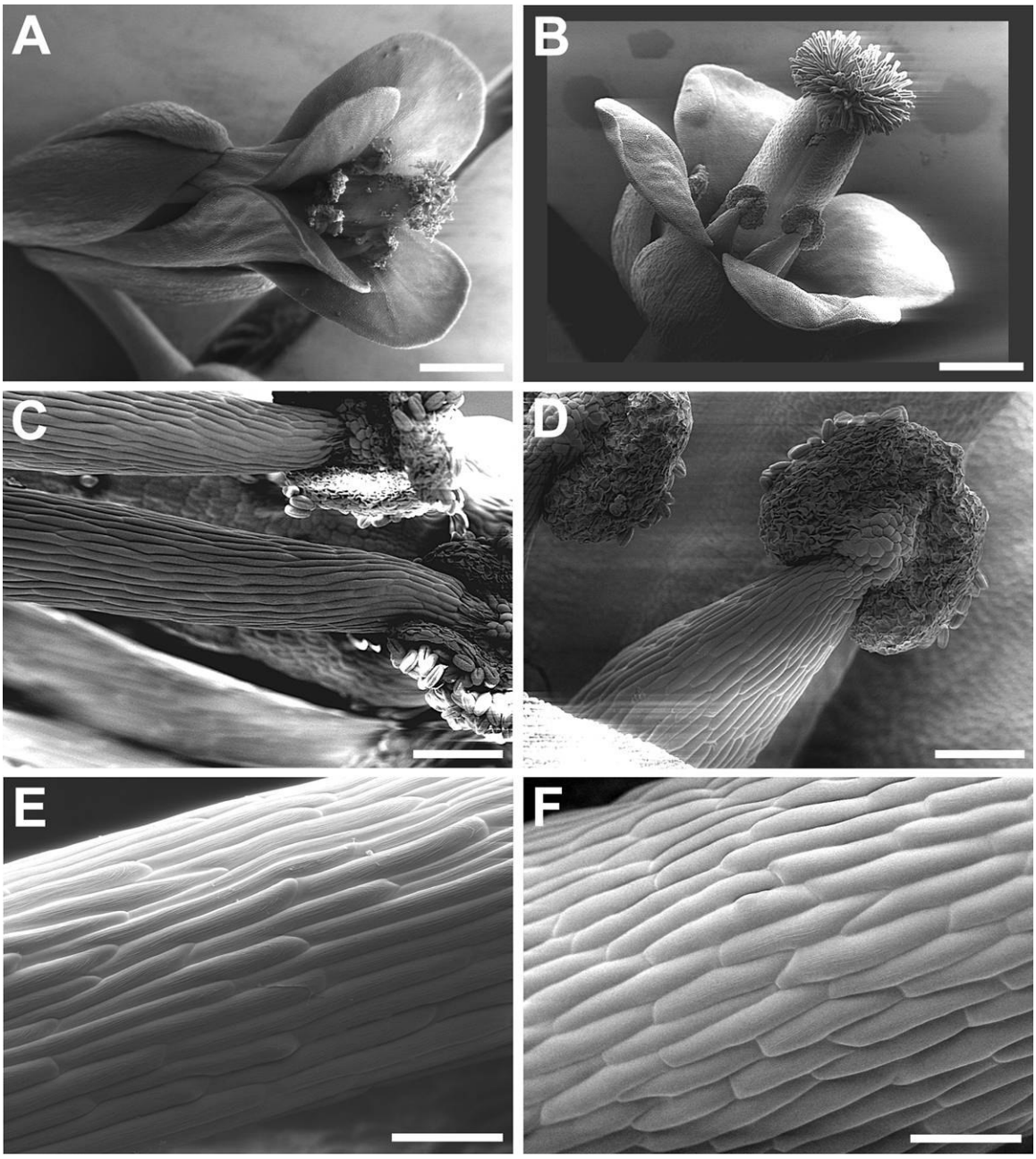
A
B
C
D
E
F

CHAPTER 5

CONCLUSIONS

KATANIN FUNCTION IS NECESSARY FOR PROPER CELL ELONGATION IN ARABIDOPSIS

Characterization of mutants of the FRAGILE FIBER 2 (FRA2) locus has revealed that lack of proper FRA2 function leads to dwarfism in mature plants and reductions in the lengths of all organs that rely on diffuse cell growth for their proper extension. Our findings that mutation of the *fra2* gene causes a disruption in the proper anisotropic growth in cells of petioles, stems, and roots with an apparent increase in the number of improperly placed cell walls in pith parenchyma were confirmed by other researchers working on allelic mutations in this organism (Bichet et al., 2001; Webb et al., 2002; Bouquin et al., 2003). Fine scale mapping of the *fra2* gene led to the discovery that it encoded the plant ortholog of animal p60 katanin subunit, an ATP-dependent MT-severing protein that shares similarity with the AAA (ATPases associated with various cellular activities) family of ATPases. It is apparent then, that FRA2 (renamed AtKTN1) is a necessary component of plant cell elongation. It should be noted, however, that *fra2* mutant plants were, in a sense, normal in that they were able to properly form roots, leaves, the proper number or internodes, and flowers with no gross morphological aberrations such as lack of stomata, improper floral organ organization, disorganized vascular tissue or an increase in number or loss of particular cell files in stems or roots. This finding reveals that although cell elongation and, in the case of pith cells, proper cell plate formation, is impaired in *fra2* mutants, Arabidopisis must contain other proteins that regulate cell expansion, differentiation, and organization patterns that operate

independently or can function in a redundant manner compensating for a loss of AtKTN1 activity.

MUTATION OF THE FRA2 GENE AFFECTS THE ORGANIZATION OF THE CORTICAL MICROTUBULE ARRAY IN ELONGATING INTERPHASE CELLS OF STEMS, ROOTS, AND PETIOLES

Based on the findings of one of our colleagues, Bo Liu (see Chapter 2), in which it was shown that *fra2* mutant root cells had delays in the disassembly of the perinuclear MT array, we wished to determine if the CMT array was also affected in *AtKTN1* mutants. It is known that the timely depolymerization of the perinuclear array is a specific step in the formation of the CMT array (see Hasezawa and Kumagai, 2002); therefore, we hypothesized that the defect in the perinuclear MT array disassembly may lead to a concomitant disruption of the CMTs. Our findings confirmed this hypothesis as comparison of *fra2* mutant cells from stems, petioles, and roots that were undergoing rapid elongation to wild-type cells showed that the CMT was organized in an almost random manner. Wild type cells typically had CMTs in parallel arrays that were arranged perpendicular to the axis of cell elongation while *fra2* cells' CMT arrays appeared to have no local or global organization with the exception that a few cells had MTs that appeared relatively normal in their organization. These findings were significant in that they showed that a mutation in a MT-severing protein, AtKTN1, was sufficient for the disruption of normal CMT array organization in elongating pith parenchyma cells of stems and petioles and epidermal cells of roots. We believe that katanin activity is necessary after cytokinesis for the timely disassembly of the perinuclear array which is itself required for the proper formation of the CMT array. Additionally, visualization of the CMTs of mutant cells revealed regions of the cortex in which several MTs appeared to radiate, forming aster-like structures. We believe that these structures may represent cortical areas that contain MTOC-like activity and that, in wild type cells with functional AtKTN1, these clusters are not seen due to the rapid

dissociation of MT fragments or tubulin dimers from the cortical MTOC and incorporation into parallel CMT arrays. Unfortunately, we were unable to confirm the subcellular localization of AtKTN1 in Arabidopsis cells as we lacked antibodies to this protein. Work done by other researchers, however, has shown that AtKTN1 appeared to localize at or around the perinuclear envelope as well as at sites in the cytoplasm and in a punctate pattern along cortical microtubules in interphase cells (McClinton et al., 2001; Bouquin et al., 2003). These findings lend support to our hypothesis that katanin function is required at the perinuclear array as well as within the cell cortex. This concept of MTOC activity in the cell cortex as well as katanin localization within the CMT array is not new (see Wasteneys, 2002) but lacks definite confirmation.

DEFECTS IN ATKTN1 FUNCTION CAUSE THE DISORGANIZED DEPOSITION OF CELLULOSE MICROFIBRILS IN PRIMARY AND SECONDARY CELL WALLS

Our findings that the CMT array in *fra2* mutant cells was disorganized prompted us to examine the patterns of CMF deposition patterns in rapidly elongating cells. Current models dealing with cellulose deposition patterns place specific importance on the organization of the CMT array as it is believed that CMTs directly or indirectly influence the organization of CMFs in the cell wall. We hypothesized that the inhibition of anisotropic growth seen in *AtKTN1* mutants may be due to changes in the pattern of CMFs in the walls of mutant cells which would alter the expansive properties of the cell wall and, therefore, inhibit proper elongation. Our hypothesis was confirmed via direct visualization of the CMFs in mutant walls which revealed a dramatic difference between the organizations of CMFs in *fra2* walls when compared to those of wild-type cells. The pattern of CMFs in wild-type cell walls mirrored that of the underlying CMTs; both were arranged in parallel arrays that traveled almost perpendicular to the axis of cell elongation. Mutant CMFs, like the CMTs, displayed a broad range of angles that varied widely from perpendicular to the elongation axis. In addition, bundles of CMFs were seen to travel together in all cell types examined and these bundles sometimes changed

their orientation drastically in a small area. Statistical analysis revealed a close correlation between the pattern of CMTs in *fra2* cells and that of the CMFs. These findings, we believe, show that disruption of katanin function which leads to aberrations in the CMT array organization, leads to a disruption of the deposition of CMFs and results in defects in anisotropic growth. Unlike previous experiments which attempted to show a correlation between the CMT array and CMF deposition patterns by using pharmacological drugs, we were able to show that a specific mutation in a MT-severing protein was sufficient for the alteration of CMF deposition patterns.

OVEREXPRESSION OF *AtKTN1* ALTERS PLANT MORPHOLOGY, CELL ELONGATION, CMT ORGANIZATION, AND CMF DEPOSITION PATTERNS BUT DOES NOT CAUSE THE FRAGMENTATION OF THE CMT ARRAY

Based on the MT-severing activity of AtKTN1 in vitro (R. Zhong, Chapter 3; Stoppin-Mellet et al., 2002) we thought that the overexpression of this protein would cause the rapid disassembly of CMTs in transgenic plants and thereby alter cell growth polarity. Examination of plants which overexpressed *AtKTN1* cDNA (Fra2OE plants) however, revealed that the CMT arrays in interphase cells of stem and petiole parenchyma were not fragmented and appeared much like those seen in the *fra2* mutant. In addition, although the overall plant morphology was similar to *fra2* mutant plants, the roots of transgenic Arabidopsis which overexpressed katanin were phenotypically wild-type and their CMT arrays appeared normal. Our results were surprising in that transient overexpression of the human p60 subunit of katanin in HeLa cells has been shown to cause the disassembly of the MT cytoskeleton (McNally et al., 2000). Obviously differences exist between the MT arrays of plants and animals; plants lack centrosomes and animal cells do not have a cortical microtubule array. Due to the large evolutionary distances between higher plants and animals it is conceivable that katanin function in plants may be somewhat different from that of animal cells even though both possess MT-severing activity in vitro. The finding that Fra2OE roots were phenotypically normal was another interesting discovery

from our research. It appears that even though high levels of *AtKTN1* transcript exist in overexpressing root cells, they can somehow compensate for this. Perhaps excess katanin is eliminated via the ubiquitin-mediated degradation pathway or it may be that surplus katanin in root cells can be tolerated and does not affect the dynamic MT reorganization processes during cell elongation.

PROSPECTS FOR FUTURE ANLYSIS

To date, only one mutation in the p60 subunit of katanin has been isolated in animal systems, the *mei-1* mutant in *Caenorhabditis elegans*, and it was determined that MEI-1 function in this organism was necessary for the proper formation of the meiotic spindle (Srayko et al., 2000). Other research in animal systems such as sea urchin, *Xenopus*, CV-1 cells (monkey kidney), human fibroblast cells, and sympathetic neurons from mice have shown that katanin is localized to mitotic spindle poles and the centrosome which are animal microtubule organizing centers (MTOCs) (McNally et al., 1996; Hartman et al., 1998; Ahmad et al., 1999; McNally et al., 2000; Buster et al., 2002; McNally, et al., 2002;). In addition, McNally et al. (2000) determined that increased levels of human p60 katanin subunit in interphase HeLa cells could cause the disruption of the MT cytoskeleton and further strengthened the in vivo role of katanin as a MT-severing protein. Plants lack definite sites of MTOC activity such as centrosomes and instead seem to rely on diffuse regions on the perinuclear membrane and possibly the cell cortex and endoplasmic reticulum for the nucleation of MTs. In addition, the mutation of *AtKTN1* in Arabidopsis does not appear to affect mitotic or meiotic events. Based on our research using the *fragile fiber 2* mutant as well as examination of plants overexpressing the *AtKTN1* gene we have shown that katanin plays a role in (1) the disassembly of the perinuclear MT array (2) the proper organization of the CMT array in interphase cells undergoing rapid elongation (3) the ordered deposition pattern of CMFs in primary and secondary cell walls and (4) proper anisotropic growth of diffusely growing cells. Of course, most of these effects are probably not primary effects of aberrant katanin function

but are secondary and based on the uncoupling of the timing of MT dynamics and cell growth.

It appears that shortly after cytokinesis the MTs of the perinuclear array must be severed by katanin. In addition, cells that are just entering a rapid elongation phase may require katanin activity in the cortical region for the proper reorientation of the CMTs to form parallel arrays transverse to the axis of cell elongation. The use of GFP-fusion constructs should enable us to better define the spatial and temporal patterns of katanin function through the use of live imaging coupled with confocal microscopic technology. Unfortunately, the visualization of the MTs in cells just exiting from the meristematic zone of root-tips is difficult at best and may hinder attempts to examine microtubule dynamics and katanin localization in living whole-root cells immediately after cytokinesis. The use of tobacco BY-2 cells grown in culture may be a more viable option in this regard as they have routinely been used in visualizing the changes in MT organization that occur during and immediately after mitotic events.

It is known that deeitolated hypocotyl cells have their CMTs arranged transverse to the cell elongation axis and that exposure to light causes the reorientation of the CMTs to a more longitudinal formation. A comparison of the events that occur in hypocotyl cells exposed to light after growth in darkness using wild-type and mutants of *AtKTN1* could help us better understand the processes necessary for MT orientation changes in the cell cortex. Possible approach would make use of Arabidopsis *AtKTN1* mutants that can conditionally express wild-type katanin. The examination of the reorganization of the CMT arrays in certain cell types after induction of katanin transcription may help reveal the specific sites of katanin action and could be used if other microscopic analyses fail especially if the katanin construct was fused with GFP.

Our findings that mutation of the AtKTN1 gene result in aberrantly organized CMFs could potentially expand our understanding of the processes by which MTs influence CMF deposition. Several models which attempt to explain the correlation between

CMTs and the organization of CMFs in cell walls rely on the direct association of MTs and the terminal complexes in the plasma membrane through as yet unidentified linking proteins. In contrast, models exist which attempt to explain the orderly deposition of CMFs without MT involvement. It would be interesting to determine if the bands of CMFs seen in mutant cell walls align with CMTs. Perhaps the rapid changes in the direction of the bundles of CMFs seen in *fra2* mutant cell walls are due to clusters of terminal rosettes, which may be traveling beneath or adjacent to underlying CMTs, colliding with a CMT oriented at some angle to the original MT. The use of both transmission and scanning electron microscopic techniques could be used to confirm or discredit this hypothesis. Research currently being conducted and not included in this work will make use of immunocytological techniques to determine the spatial relationship between the plasma membrane and the CMTs of cells of wild-type, *fra2* mutants, and plants overexpressing a tubulin gene. We believe that in some cases the disorganization of the CMT array may not lead to the complete disruption of the CMF deposition patterns and may be due to the dissociation of CMTs from the plasma membrane. In such cases, a geometrical model proposed by Emons et al. (2002) may explain the helical arrangement of CMFs in cells which have disorganized CMT arrays.

Our understanding of the components involved in plant cell elongation is constantly growing and we believe that our analyses of the *fra2* mutant and Fra2OE plants have helped advance this field. It appears that the anisotropic growth of cells in plants require 1) turgor pressure, 2) properly organized CMT arrays, 3) properly organized CMFs in the cell walls, and 4) proteins either within cell walls (expansins, XETs) or between MTs and CMFs for the regulation of cell wall expansion and directed cellulose synthase movement in the plasma membrane. There are undoubtedly more proteins involved than what we have found so far that assist in the regulation of cell elongation and other factors such as biophysical forces within cell walls may also play important roles in how cells expand. The recent finding that a kinesin-like protein (FRA1) is involved in the ordered

deposition of CMFs in secondary cell walls yet does not alter the organization of CMT arrays (Zhong et al., 2002) is evidence that there are proteins yet to be discovered that work between CMTs and cellulose deposition steps. It is strange that more proteins such as FRA1 have not been characterized, but perhaps mutation of genes that ultimately assist in the "communication" between CMTs and cellulose synthases causes lethality during embryogenesis. We must also discover why it is possible to disrupt the CMT array in plant cells yet allow them to retain a relatively normal CMF deposition pattern. This researcher believes that the final frontier of cell elongation research and the only way to discover which model in the MT/CMF paradigm debate is correct is to focus attention to the interface between the CMTs and the CMFs. This will undoubtedly be hard work as the use of advanced microscopic techniques will be required as well as brute-force biochemical methods to attempt to isolate the proteins that link MTs to the plasma membrane and cellulose synthesizing machinery. The fruits of this hard work, though, should more than pay for the costs as we would then have a detailed picture of how the CMTs organization affects CMF deposition and the directed localization of cellulose modifying enzymes.

In summary, we have shown the importance of a katanin-like MT-severing protein in the proper elongation of Arabidopsis cells. Disruption of the katanin gene, *AtKTN1*, results in aberrant anisotropic growth through the disruption of the CMT array and the subsequent disruption of the ordered deposition of CMFs in cell walls. We have also shown that increased levels of *AtKTN1* transcript also affect CMT arrangements and cell growth but do not cause the fragmentation of CMTs. This is the first genetic evidence of a direct correlation between proper MT dynamics and cell expansion and, hopefully, further analysis of katanin function will lead to an understanding of the events necessary for the initial formation of the parallel CMT arrays seen in elongating cells as well as shed light on the relationship between CMTs and cellulose deposition patterns.

REFERENCES

Ahmad, F.J., Yu, W., McNally, F.J., and Baas, P.W. (1999). An essential role for katanin in severing microtubules in the neuron. J Cell Biology 145, 305-315.

Bichet, A., Desnos, T., Turner, S., Grandjean, O., and Höfte, H. (2001). BOTERO1 is required for normal orientation of cortical microtubules and anisotropic cell expansion in Arabidopsis. Plant J 25, 137-148.

Bouquin, T., Mattsson, O., Næsted H., Foster, R., and Mundy, J. (2003). The Arabidopsis *lue1* mutant defines a katanin p60 ortholog involved in hormonal control of microtubule orientation during cell growth. Journal of Cell Science 116, 791-801.

Buster, D., McNally, K., and McNally, F.J. (2002). Katanin inhibition prevents the redistribution of γ-tubulin at mitosis. Journal of Cell Science 115, 1083-1092.

Emons, A.M.C., Schel, J.H.N., and Mulder, B.M. (2002). The geometrical model for microfibril deposition and the influence of the cell wall matrix. Plant Biol 4, 22-26.

Hartman, J.J., Mahr, J., McNally, K., Okawa, K., Iwamatsu, A., Thomas, S., Cheesman, S., Heuser, J., Vale, R.D., and McNally, F.J. (1998). Katanin, a microtubule-severing protein, is a novel AAA ATPase that targets to the centrosome using a WD40-containing subunit. Cell 93, 277-287.

Hasezawa, S., and Kumagai, F. (2002). Dynamic changes and the role of the cytoskeleton during the cell cycle in higher plant cells. International Rev Cytology 214, 161-191.

McClinton, R.S., Chandler, J.S., and Callis, J. (2001). cDNA isolation, characterization, and protein intracellular localization of a katanin-like p60 subunit from Arabidopsis thaliana. Protoplasma 216, 181-190.

McNally, F.J., Okawa, K., Iwamatsu, A., and Vale, R.D. (1996). Katanin, the microtubule-severing ATPase, is concentrated at centrosomes. J Cell Science 109, 561-567.

McNally, K.P., Bazirgan, O.A., and McNally, F.J. (2000). Two domains of p80 katanin regulate microtubule severing and spindle pole targeting by p60 katanin. J Cell Science 113, 1623-1633.

McNally, K.P., Buster, D., and McNally, F.J. (2002). Katanin-mediated microtubule severing can be regulated by multiple mechanisms. Cell Motility and the Cytoskeleton 53, 337-349.

Srayko, M., Buster, D.W., Bazirgan, O.A., McNally, F.J., and Mains, P.E. (2000). MEI-1/MEI-2 katanin-like microtubule severing activity is required for Caenorhabditis elegans meiosis. Genes Development 14, 1072-1084.

Stoppin-Mellet, V., Gaillard, J., and Vantard, M. (2002). Functional evidence for in vitro microtubule severing by the plant katanin homologue. Biochem J 365, 337-342.

Wasteneys, G.O. (2002). Microtubule organization in the green kingdom: chaos or self-order? Journal of Cell Science 115, 1345-1354.

Webb, M., Jouannic, S., Foreman, J., Linstead, P., and Dolan, L. (2002). Cell specification in the Arabidopsis root epidermis requires the activity of ECTOPIC ROOT HAIR 3-a katanin-p60 protein. Development 129, 123-131.